DCU

Development of Novel Gas Sensors

By

Brendan Duffy B. Sc.

Thesis for the degree of

Doctor of Philosophy

Submitted to

Dublin City University

School of Chemical Sciences

September 2002

For Maura

To infinity and beyond……….plus 1!

Acknowledgement

Before I started I was warned that a PhD would be an endurance test. Looking back I have to agree, but one which I would gladly take again. J207 will always remind me of Quake for reasons Aogan, Fran, Shane, and Darren will be familiar with. The switch over to X150 didn't upset things too much either, except for more players in John and Liam! Sometimes the "girls" were invited to play, but usually they had more sense.

Starting in DCU also meant making plenty of new friends, and there are plenty of people that I would like to mention but it would look just like a mailing list, so to one and all….cheers!

One of the people I'd like to thank has to be my supervisor Prof. D, who kept me going when I was running around in circles! I'd also especially like to thank Kim, who without doubt kept me on the right track!

I'd also like to say a big thank you to all the staff, both academic and technical, in the school and all the gang in the BEST Centre office. I threw plenty of questions and requests their way and they always had time for me.

To my family it may have seemed that I'd remain the eternal student, but eventually I got to the end! They have been with me all the way and I know that they are proud of me!

Of course there is the other side to a postgrad, and I would have been lost had it not been for Maura. They say that behind every great man there is an even greater woman, how true! You and me babe……we did it!

Elvis has left the building, and left all the chemicals behind!

<u>Declaration</u>

I hereby certify that this material, which I now submit for assessment on the programme of study leading to the award of PhD is entirely my own work and has not been taken from the work of others save and to the extent that such work has been cited and acknowledged within the text of my work.

Signed: _____ ID No.: <u>97970158</u>

          Candidate

Date: _____

Table of Contents

Chapter 1: Introduction

Chapter 2: Bulk Acoustic Wave Coatings

Chapter 3: Experimental

Chapter 4: Gas Chromatography Phases as BAW Coatings

Chapter 5: Polypyrrole Coatings

Chapter 6: Calixarenes as BAW Sensor Coatings

Chapter 7: Conclusions and Future Work

Appendix 1

Chapter 1

1 Introduction

1.1 Gas Sensing Principles:

1.1.1 The Human Sense of Smell

Of all human senses our ability to detect odours may be the least appreciated and certainly the least understood [1], and yet is one of the most powerful. Humans can only *see* a narrow region of the light spectrum (300-700 *nm*), *hear* a small range in the frequency spectrum (20-20KHz), *touch* objects that are close. The smell and taste of substances however can give us much more information about an objects nature. However quantifying these senses is difficult. The taste of substances has been provisionally classed as being Sour, Bitter, Sweet or Salty. Smells have been classed as being camphoraceous, ethereal, floral, minty, musky, pungent or putrid [2], but this has been described as being over simplistic [3]. Therefore to mimic the nose it is necessary to understand how the nose functions.

The human nose contains about 10^7 receptors located in a $6cm^2$ area of mucosa at its internal apex [4]. When one "sniffs" something they alter the natural direction of the air in nasal breathing. With this change in direction the air passes by these receptors, which are then stimulated. The mode of stimulation has been the subject of debate and two schools of thought have emerged:

➢ The "lock and key" hypothesis suggests that an odourous molecule or part of such molecule fits into an area on the protein receptor thereby changing its conductance. Historically this kind of theory has existed since the time of Epicurus in the 4th century BC, and more recently has been studied in depth [2].

➢ The "vibrational energy" hypothesis suggests the receptors are stimulated by vibrational energies inherent to the chemical bonds of the molecule, thereby failed to describe the actual method of signal transduction.

When the transduction method occurs a conductance change in the olfactory membrane, or epithelium, is seen as a signal from the branches of the olfactory nerve to the olfactory bulb, situated on the underside of the anterior lobe of the brain, where it then passes back to the olfactory cortex [4].

The number of different types of receptor proteins is debatable but it is believed that there are up to 100 with overlapping selectivities and sensitivities for volatile odour chemicals [5]. The human nose is very sensitive and can detect concentrations to down as far as parts per trillion in some cases. The size of the epithelium is a good indicator of the acuity of an animal's sense of smell. For example, the surface area of a human epithelium is 10 cm^2, whereas the surface area of a dog's epithelium is 170 cm^2. Dogs also have 100 times more receptors per cm^2 than humans, so, needless to say, dogs have a much better sense of smell!

1.1.2 Chemical Sensors for Gas Sensing

Currently there is an increasing level of research and development being dedicated to the area of gas detection. The impetus of this research is to develop gas sensors and sensor arrays that will help: [6]
- compliment analytical chemistry techniques (*e.g.* GC) in order to classify gas mixtures, odours, air quality
- correlate electronic signals of such sensor arrays with human odour perception
- develop cheap and reliable instruments for "imaging" such gases with high spatial and temporal resolution and
- develop new materials for odour detection, that act in a similar fashion to the human nose.

The area of olfaction, or smelling, is very complex in comparison to the international referenced measurements of light, sound and pressure. Odours tend to be a mixture of a multitude of chemical compounds, and as such are difficult to characterise.

Up until about ten years ago, the area of smell and gas detection using sensors was restricted to very specialised applications such as humidity levels. Then with the combination of the emerging topic of chemometrics, interest in the use of sparingly selective sensors in sensor arrays, multichannel data loggers combined with faster computers and improved software, research in the area increased dramatically. With this increased research came the inevitable push towards commercial devices. Several devices came onto the market, which had previously relied solely on test panels of highly trained humans. Developed by companies such as AromaScan, Alpha-MOS and Neotronics Technology, these devices were marketed as "Electronic Noses", and were seen as pioneering tools in this, as yet unexplored, field. Products, such as the Fox2000 (Alpha-MOS), offer a wide set of interchangeable sensors to meet various customer needs. Unfortunately the drive to produce a marketable tool was greater than the development of adequate research, and various problems were encountered. Overcoming problems such as humidity and contamination has proven difficult, and a re-think of the area has since begun. Several companies experienced difficulties as a result (*e.g.* Bloodhound Ltd., Leeds, U.K.)

The most common types of gas sensors can be classified according to their mode of signal transduction. The most important sensors are based on piezoelectric, calorimetric, electrochemical, and optical phenomenon. A comprehensive review of these modes of detection has been published [7] but it is piezoelectric sensors that this thesis shall deal with.

1.2 Piezoelectricity

1.2.1 History

Probably the first piezoelectric material ever to be used for this unusual property was flint. With sufficient force a spark would be generated when two pieces of flint came into contact. However Alder *et al.* detailed a history of piezoelectricity in an interesting review paper [8], which stated that Coulomb was the first person to propose the possibility of producing electricity by the application of pressure on a suitable material [9]. Hauy further investigated the field and as did Bequerel [10],

3

who carried out experiments on certain crystals that showed electrical conductivity when compressed. However some of the crystals used were not piezoelectric and as a result the phenomenon was attributed as being "contact electricity". In 1880 Jacques and Pierre Curie [11] showed that when some crystals were compressed in particular directions the electrical potential was produced between the deformed surfaces and this potential was found to be proportional to the force applied. Lippmann [12] predicted that the converse effect would also be possible and in 1881 the Curies verified this.

It wasn't until the start of the First World War, however, that the first practical uses of this type of crystal were made. Quartz plates were used to serve as emitters and receivers of high frequency waves under water by Langevin [13], which in turn led to the development of Sonar. Crystal controlled devices with high frequency stability were used for radios and communication lines by Cady [14], Pierce [15] and others.

1.2.2 Theory

Piezoelectricity is a reversible effect whereby application of a force across one direction of certain anisotropic materials (quartz, Rochelle salt, lithium sulphate, barium titanate *etc.*) produces polarisation of the material in that direction or an orthogonal direction; the charge produced being proportional to the force. A substance is anisotropic when any of its physical properties (*e.g.* thermal or electrical conductivity) are different in different principal directions. This occurs in crystals that do not posses a centre of symmetry. The majority of crystal types, of which there are 32, do not contain a centre of symmetry. When pressure is applied to a dielectric material deformities are created in the crystal lattice, thereby causing a separation in the centre of gravity of the oppositely charged species, which in turn gives rise to a dipole moment in each molecule. The reverse effect to applying a force to generate a voltage is to apply a current across the crystal thereby inducing a force.

When an alternating electric field is applied to a crystal a potential difference (p.d.) is generated between the two electrodes. This p.d. causes a change of position

4

within the crystal lattice that then is seen as a standing shear wave, whose frequency matches that of the natural frequency of the crystal. The lattice determines the direction of this oscillation, which in turn is dependent on the cut of the crystal with respect to its geometric axes. When a crystal oscillates in the thickness shear mode (TSM) a displacement is caused parallel to the surface. As the potential is only seen between the electrodes it is only this region that is said to be piezoelectrically active. The natural frequency of the crystal is dependent on several parameters such as size, cut density *etc*., but the most important parameter for our purposes is the relation ship with the mass of the crystal.

There are two crystal orientations that vibrate exclusively in the TSM, and they are the AT and BT cuts. The AT-cut refers to the crystals cut at +35°15″ angle to the z-axis. AT is the desired type due to its favourable temperature properties such as a low temperature coefficient that guarantees stable frequencies across a wide range. There are two ways to monitor the frequency of a quartz crystal [16]:

a: Incorporation of the crystal into an oscillator circuit where the crystal vibrates at its natural frequency

b: Connection of a crystal to an external instrument which applies an alternating current at various frequencies

Therefore when a suitably cut crystal is incorporated into an oscillator circuit, the crystal will resonate at a its natural frequency, which is dependant on the mass of the body [17]. AT-cut crystals oscillate in the thickness shear mode (TSM) as illustrated in Figure 1-1.
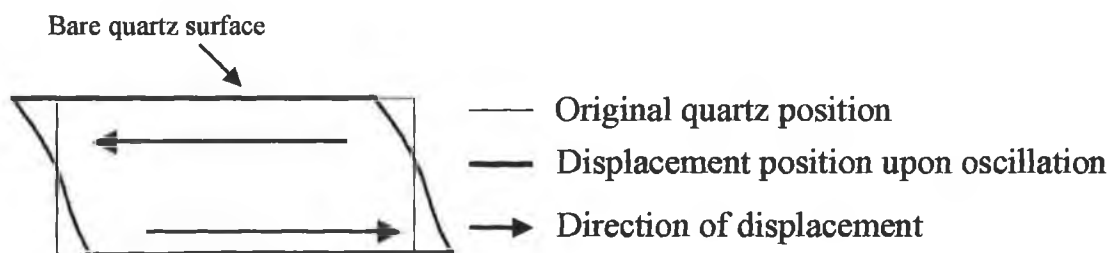
Figure 1-1: Thickness Shear Mode Oscillation of an AT-cut quartz crystal

As the TSM causes a displacement on the surface, any change in the surface will cause a change in the oscillations. Should a layer be attached to the bare quartz

surface, there will be a change in the oscillation. This change will be dependant on the rigidity of the layer.

(A)   Rigidly coupled layer

Should the layer applied to the surface be rigid, it will move synchronously with the quartz crystal surface, without any change in its physical form. Therefore the transverse shear wave will pass through this layer and suffer no energy loss.

Rigidly coupled film
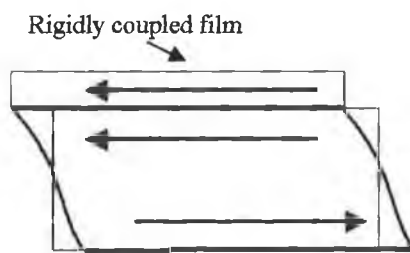
Figure 1-2: Thickness Shear Mode Oscillation of an AT-cut quartz crystal with a rigidly coupled film

(B)   Non-rigidly coupled layer

However, should the layer applied to the surface be non-rigid, it will not move synchronously with the quartz crystal surface. This lack of cohesive movement will cause changes in the transverse shear wave, and will reduce its amplitude/energy. The implications of this kind of layer will be discussed later in Sec.1.3.6.

Non-rigidly coupled film
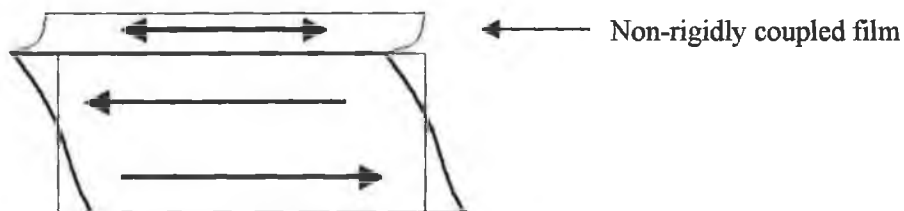
Figure 1-3: Thickness Shear Mode Oscillation of an AT-cut quartz crystal with a non-rigidly coupled film

6

1.2.3 Common Applications

Quartz crystals have become integral parts of most everyday electronic tools, from radios, watches, thermostats, gas-lighters to advanced machinery such as sonar, radar, interferometers *etc.*

1.3 Quartz Crystal Microbalance Devices

1.3.1 Design

The Quartz Crystal Microbalance, or QCM, is a thin wafer of quartz onto which gold electrodes have been attached. The resonant frequency of the crystal was monitored as the gold electrodes were sputtered onto the surface until the frequency of the crystal changed to the desired level. Before the gold is sputtered on the surface of the quartz however, the surface is coated with chromium that acts as a binder between the gold and quartz. The thickness of this layer is less than $5\mu m$. The electrodes are then polished, using non-abrasive solvents, to give a clean surface. The crystal is then held in place by two holders and is fixed using non-conducting glues. The configuration of the QCM can be varied depending on crystal shape, but the QCM used in this thesis will be the HC49 model. The quartz disk in this configuration is about 10mm in diameter, and about $50\mu m$ in thickness at it's thickest. When supplied the crystals are sealed by a metal cap, to protect it from contamination.
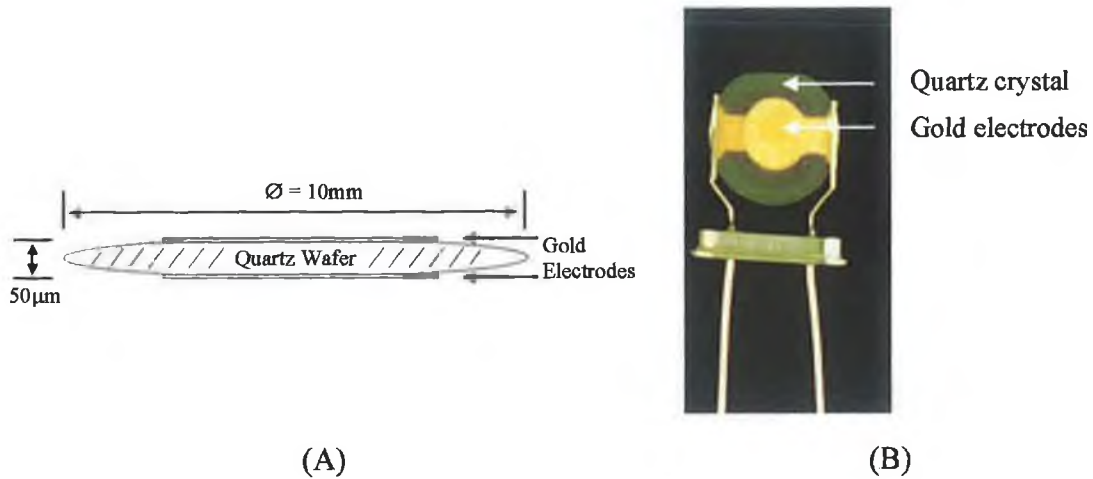
Figure 1-4: (A) Schematic of QCM (B) Photo of bare QCM

1.3.2 Crystal Choice

Quartz crystal in its perfect natural form is shown in Figure 1-5, along with its respective orthogonal axes. For a QCM to operate harmonically, the acoustic wave must propagate in a direction perpendicular to the crystal surface. For this to happen the crystal must be cut to a specific orientation with respect to the crystal axes [18]. The type of cut required belongs to the rotated Y-cut family, and the AT- and BT-cuts are the only useful representatives of this family.
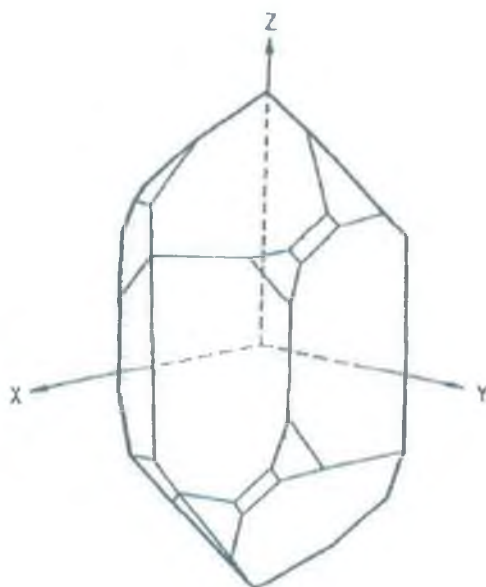
Figure 1-5: A perfect quartz crystal and its assigned axes [18]
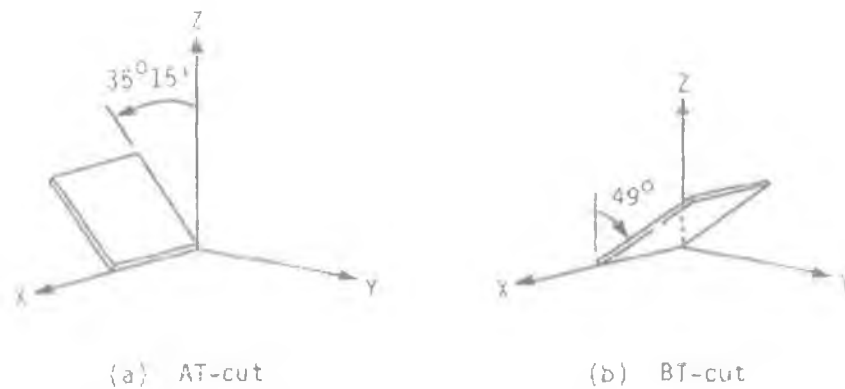
Figure 1-6: AT- and BT-cuts quartz crystals [18]

The AT- and BT-cuts are high frequency mode plates and have low or zero temperature coefficients [19]. The AT has superior temperature coefficient and mass sensitivity and is the preferred choice.

Acoustic waves normally propagate vectorally in an x, y, z direction. For the AT-cut quartz only one direction of propagation is piezoelectrically supported, due to zero coupling factors for the two other orthogonal modes [20]. Having one mode of oscillation means only one fundamental frequency and consequently only one fundamental anti-resonant frequency. This eliminates the possibility of interference from other spurious modes.

3 modes exist for each orientation of an acoustic wave (a, b, and c) and are ranked in descending order of their velocity. a being the largest component is in the direction of the propagation, and is called the "quasi-longitudinal mode". The other two orthogonal modes are referred to as being the "fast quasi-thickness shear" and the "slow quasi-thickness shear", as they're dominated by shear components. Certain orientations exist where either a, b, or c are purely longitudinal or transverse. For AT-cut crystals the only mode is c and as is a purely transverse wave, meaning that energy is not easily radiated away from the device, resulting in a high Q-factor (see Sec. 1.3.4).

1.3.3 QCM Equivalent Circuit

An electrical equivalent circuit as shown in Figure 1-7 can be used to describe the mechanical behaviour of a quartz crystal. This circuit involves a capacitor (C_1) in parallel with an inductance-capacitor-resistor (LCR) series. In this equivalent circuit the resonant resistance (R) reflects the mechanical resistance of the quartz crystal, the capacitance (C_2) reflects the mechanical elasticity and the inductance (L) reflects the total mass of the quartz crystal and the contact material on it. C_1 is related to the disk capacitance formed by the disk electrodes and the dielectric quartz substrate. As C_1 is large in comparison to the other components of the circuit, its effect on the circuit is negligible, due to the inverse nature of its impedance, *i.e.* $Z_{capacitor} = (j\omega C)^{-1}$.
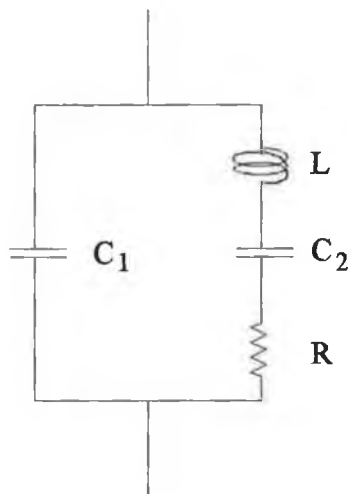
The resonant frequency, f_0, is given by the following expression:

$$f_0 = \frac{1}{2\pi\sqrt{LC_2}}$$

Equation 1-1

Figure 1-7: QCM equivalent circuit

When the sensor is exposed to an analyte vapour the value of L will increase and so the fundamental frequency of the sensor will drop. This new frequency is then compared to an uncoated sealed reference crystal, independently incorporated into the circuitry and a relative frequency change is obtained [21]. Correspondingly a change in the elastic properties of the coating will change C_2, thereby changing the frequency.

10

1.3.4 Physical Properties of Quartz Crystals

Any sensor being designed for rigorous use must be physically strong and stable under varying conditions. Quartz crystals will now be examined under the following headings;

1.3.4.1 Stability

The main influences on the stability of a QCM are time, operating temperature, and external circuitry.

Time

Time influences can be short-term (phase noise), intermediate-term (temperature fluctuations) and long-term (aging).

(a)   Short-Term (Noise)

Noise is unavoidable in any measurement system, but can be minimised. The most common noise in QCM's is thermal noise, or Johnson noise, and arises due to the quartz's motional resistance. The second source is the scattering of phonons within the crystal lattice due to defects and scattering at the crystal/electrode interface. A phonon is a pocket of sound-wave energy, and has energy of hf where h is Planck's constant and f is the resonant frequency within the crystal. This loss of energy decreases the Q-factor or Quality factor. The Q-factor is given by Equation 1-2, where E_{max} is the maximum energy stored in the crystal, and E_L is the energy lost per cycle of oscillation. Typical Q values for quartz are of the order of 100,000.

$$Q = 2\pi \left[\frac{E_{max}}{E_L} \right]$$ **Equation 1-2**

(b)   Intermediate Term (Drift)

Should the environment temperature vary over the course of an analysis then there may be a change in the resonant frequency of the circuit. This will be commonly

seen as a drift in the signal, and may be positive or negative. Compensation techniques are then necessary to allow for such dynamic baselines.

(c) Long-term (Aging)

Aging is seen as a gradual significant change in the crystals resonant frequency over a period of weeks, but is negligible over the course of one working day. The main causes [22] are mass transfer on the surface due to contamination, and stress relief in the crystal bonding. Due to the nature of the crystal use mass-transfer cannot be avoided, and must be always considered to be present. Stress relief again cannot be avoided but can be minimised by using crystals of high quality and smaller contacts. The oscillating circuitry can also have an effect but this can be minimised by using larger load capacitances, thereby reducing any frequency changes, and properly sealed components.

Operating Temperature

Depending on the cut of the crystal the temperature coefficient may vary, and consequently the effect of temperature will vary. AT-cut crystals are supposed to have a zero temperature coefficient, but this can often not be the case due to the quality of the quartz wafer. For higher frequencies the effects of temperature are more pronounced (Figure 1-8) and a change of 1K can change the resonant frequency of a 30MHz QCM by 5Hz [23]. For practical applications such a change is small and can be compensated for using a reference crystal in the sustaining circuitry.

12
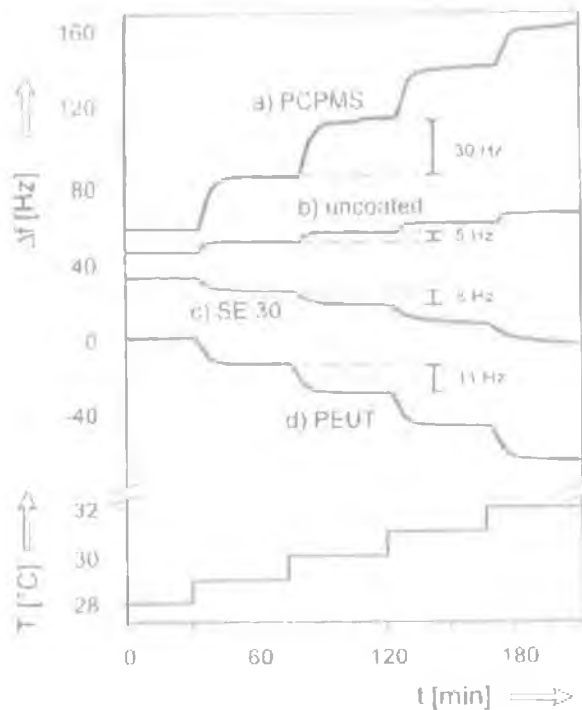
Figure 1-8: Resonant frequency shifts of (a) Poly (cyanopropyl)methylsiloxane, (c) Polydimethylsiloxane, (d) poly(ethereurethane) coated, and (b) uncoated 30MHz QCM sensors due to temperature changes [23]

External Circuitry

Many oscillators use tuned circuits, such as matching circuits and filters, to hinder unwanted modes. Small changes in temperature can affect these circuitry inductances and capacitances can cause a change in the phase oscillations. These changes then can disrupt the harmonic oscillations within the crystal. These disruptions take on the form of non-harmonic oscillations causing destructive interference that in turn reduce the energy of the harmonic wave. This change in energy, and subsequent Q-factor decrease, is seen as a decrease in the oscillating current.

1.3.4.2 Temperature ranges

Ideal operating temperatures for AT-cut crystals are considered to be between −20 and +60°C. Within this range the temperature coefficient is considered to be zero.

13

This however has shown not to be the case [23], but it is still negligible. The relationship between frequency and temperature is cubic, outside of this range for AT-cut crystals and quadratic for BT-cuts

1.3.4.3 Operating Frequency

QCM's are supplied at a variety of frequencies ranging from 5MHz up to 1 GHz. As the frequency is an inverse function of thickness, lower frequency crystals tend to physically thicker and hence stronger towards physical loadings on the surface. For this reason 10 MHz and 30MHz tend to be very popular. These frequencies are for the fundamental resonance frequencies, however improved sensitivities can be achieved by operating the crystals at higher overtones, but the extra work on the circuitry can introduce increased levels of noise.

With a coupling factor of just 8.8% AT-cut quartz can be easily excited using low voltages.

1.3.4.4 Radial Sensitivity

As the potential difference of a QCM is applied between the two electrodes, only this area can be piezoelectrically excited. Therefore this is most sensitive region and it has been experimentally found that the sensitivity decreases quite rapidly outside this region [24]. Therefore care should be taken to ensure that the coating, in this area is as uniform as possible.
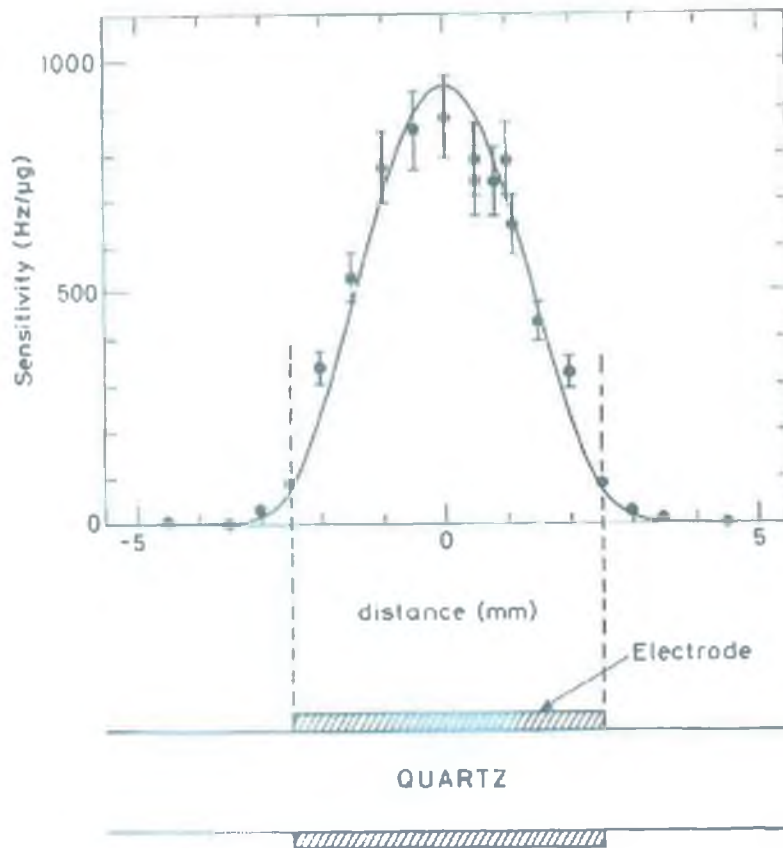
Figure 1-9: Sensitivity Profile of a QCM [24]

1.3.4.5 Mass Loading

When QCM devices are being used for sensing applications, the properties of the measurand are determined by the change in the resonant frequency of the crystal. When this measurand is a thin rigid layer on the surface of the crystal, it changes the frequency according to an equation derived by Sauerbrey in 1959 [25].

1.3.5 Sauerbrey Equation

This equation applies only to AT-cut crystals vibrating in the thickness shear mode, where the electric field is applied along the y-axis. The frequency (F) can be expressed as:

$$F = \frac{V_{tr}}{2t} = \frac{N}{t}$$

Equation 1-3

where V_{tr} is the velocity of propagation of the transverse wave in the plane of the crystal, t is the thickness and N is the frequency constant ($N = V_{tr} / 2$). On algebraic manipulation of Equation 1-3 a frequency change, Δf, is obtained on a change of the quartz thickness, t, by the amount Δt:

$$\frac{\Delta F}{F} = \frac{\Delta t}{t}$$

Equation 1-4

The thickness of the quartz wafer can be expressed in terms of the density of the quartz (ρ), the surface area (A), and the mass of the quartz plate (M):

$$t = \frac{M}{A\rho}$$

Equation 1-5

Substitution of the differential form of Equation 1-5 into Equation 1-4 yields Equation 1-6.

$$\frac{\Delta F}{F} = -\frac{M}{tA\rho}$$

Equation 1-6

For pure shear mode vibrations, the strains are all zero at the principal faces as earlier discussed. Sauerbrey assumed that if the plate were divided into an infinite number of parallel planes along the x-z axis, only the planes close to the surface would affect the frequency through their mass and not through their elastic character. Therefore the frequency change resulting from the deposition of a thin uniform film of any foreign substance is equivalent to that of a thin layer of quartz of same mass. Combining Equation 1-3 and Equation 1-6 Sauerbrey developed the more general form of the relationship to give Equation 1-7;

16

$$\frac{\Delta F}{F} = -\frac{\Delta m_s F}{A\rho N}$$

Where ΔM_s is the mass of the deposited material.

Substituting for the various constants for quartz gives Equation 1-8.

$$\Delta F = -2.3x10^6 F^2 \left(\frac{\Delta M_s}{A}\right)$$

The assumptions made in the derivation of this equation are important and are as follows:

- The change in the fundamental frequency is caused by an infinitesimally small change in crystal thickness.

- The film is of uniform thickness and density

- The density of the film is equivalent to that of the quartz.

- The shear velocity in the film is identical to that in the crystal.

A rigid coating, such as a sputtered layer of gold, can easily satisfy these conditions but should the crystal be coated with a viscoelastic coating such as a polymer (or come into contact with a liquid) the Equation 1-8 requires some modification. The redefined version in this case is

$$\Delta f = -f^{3/2}(\frac{\rho_L \eta_L}{\pi \rho_Q \mu})^{1/2}$$

Where ρ_L is the density of the coating / liquid, η_L is the viscosity of the coating / liquid, ρ_Q is the density of the quartz, and μ is the shear modulus of the quartz [26].

Strictly speaking the QCM should be referred to as a Bulk Acoustic Wave device (BAW), as its resonant frequency is affected not only by the mass of any applied layers but also by the elastic nature.

1.3.6 Physical Conditions of Coatings

Acoustic waves in BAW's are heavily influenced by the boundary conditions imposed by the physical dimensions of the device, and the physical properties of the attached material through which the wave passes [21]. Piezoelectric crystals are passive solid-state electronic devices that can respond to changes in temperature, pressure, and most importantly, to changes in the physical properties at the interface between the device surface and a foreign solid or fluid. Examples of such physical changes would be variations in interfacial mass density, elasticity, viscosity, and layer thickness.

1.3.6.1 Viscoelastic Effects

As already mentioned in Sec. 1.3.3, the resonant frequency of a BAW is dependant on the elasticity of the film attached to the crystal surface. There are three common models that now apply for the quartz crystal in contact with; (a) an elastic film (b) liquid (c) a viscoelastic film, and the shear vibrating mode is displayed for each of these models in Figure 1-10.

(a) Rigid Film

For an elastic film coated quartz crystal there is no energy loss, as the shear mode will propagate in the film identically to that in the quartz. This implies that there is no resonant resistance (R), no mechanical resistance (C), and so the resonant frequency will only change due to the additional mass of the film (L) according to Equation 1-1.

(b) Liquid

When in contact with a liquid, the frequency change reflects the mass effect of the liquid, which moves with the shear vibrating quartz plate. The shear wave has been experimentally found to decrease further out into the liquid [27]. The change in effective mass of the crystal has been determined to be a linear function dependant on the viscous penetration depth of the liquid.

(c) Viscoelastic Film

The viscoelastic model can be viewed as a hybrid of (a) and (b) above. If the film has a high enough viscosity then the shear wave does not disappear into the film, but is sustained, albeit at a higher frequency. The magnitude of this change is dependant on the thickness of the film and will be a competing effect to that of the mass change. Therefore when using non-rigid films the thickness has to be restricted to avoid these problems.
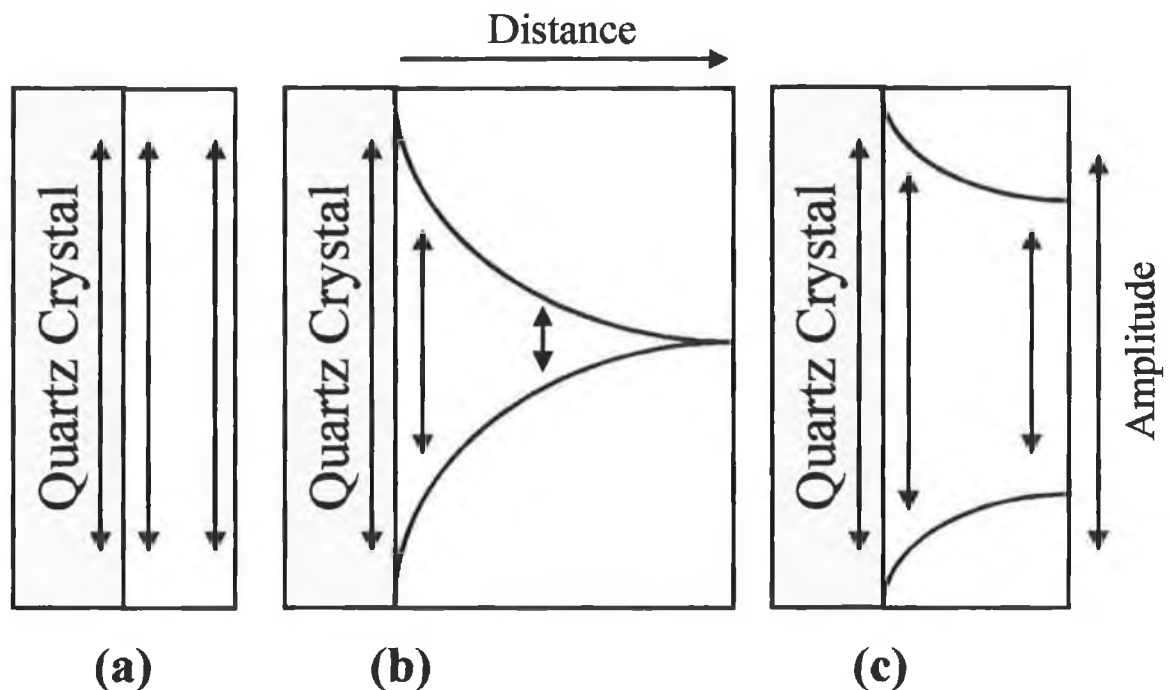
Figure 1-10: Schematic models of shear vibration modes of quartz, as a function of distance and amplitude, in contact with; (a) an elastic film (b) liquid (c) a viscoelastic film

1.3.6.2 Thickness

The thickness of coatings that can be applied to 10 MHz BAW's has been reported as being from 300-600nm [23], before any quenching of the resonant oscillation is observed. As the fundamental frequency of the sensor increases this limiting thickness decreases. For lower frequency sensors, greater film thickness' increase viscoelastic effects. These effects can give misleading information about the adsorbed mass, where different concentrations of analyte give the same response.

The sensitive coating must be evenly applied over the electrodes, as this is the most sensitive region (Sec. 1.3.4). It has been seen that the sensitivity decreases rapidly in a radial manner away from the electrodes to a virtually negligible value at the bare crystal [28].

1.3.6.3 S/N ratio

The signal to noise ratio (S/N) is the best indicator of the merit of a sensor and can be used to characterise its quality. This ratio is important as it relates to (a) the precision, expressed as standard deviation, (b) the limit of detection, which is defined as the concentration of an analyte when the S/N = 3, (c) the partial sensitivity, or slope of the calibration curve.

1.3.6.4 Swelling

Absorption of a gas into a BAW coating changes some of its physical properties. The first is the mass of the coating, followed by its density, thickness, rigidity *etc*. At low concentrations the mass of the gas that can be dissolved in the solvent (BAW coating) is proportional to the pressure of the gas, according to Henry's Law. Therefore at higher concentrations this relationship is no longer linear. At these elevated concentrations swelling can occur, where the solute reduces the rigidity of the solvent (coating). This swelling can change a rigidly coupled elastic film into a non-rigid viscoelastic film, and hence upset the shear wave oscillations. The swelling can also affect the binding of the coating to the gold surface and so creep

can result. Creep will be seen as an intermediate-term time effect, or even a short-term effect, and will be seen as an increase in the resonant frequency of the sensor.

1.3.6.5 Ideal coating

There are conditions that the ideal coating for a BAW sensor must satisfy; stability, sensitivity, selectivity (3 S's), reversible, repeatability, responsivity, and reproducibility (4 R's)

Stability

The most important feature of a good sensor coating has to be stability. The coating must not evaporate and must be well adhered, physically, to the electrode surface. To this end it is important that when the sensors are being prepared, the coating solvent is allowed to evaporate fully. Real-time monitoring of the crystal resonance frequency during, and after, coating can follow this. When the frequency has reached steady state (Figure 1-11), it can be assumed that all the solvent that will evaporate has done so. The evaporation process has been described as being in two parts.

1.   Rapid evaporation of the saturated solvent
2.   Formation of shell when saturated conditions are no longer maintained, thus decreasing the rate of solvent loss. This second period has been termed the falling period [29].

After being coated, the stability of the crystal coating can then be monitored over a period of weeks, to determine if it is stable.
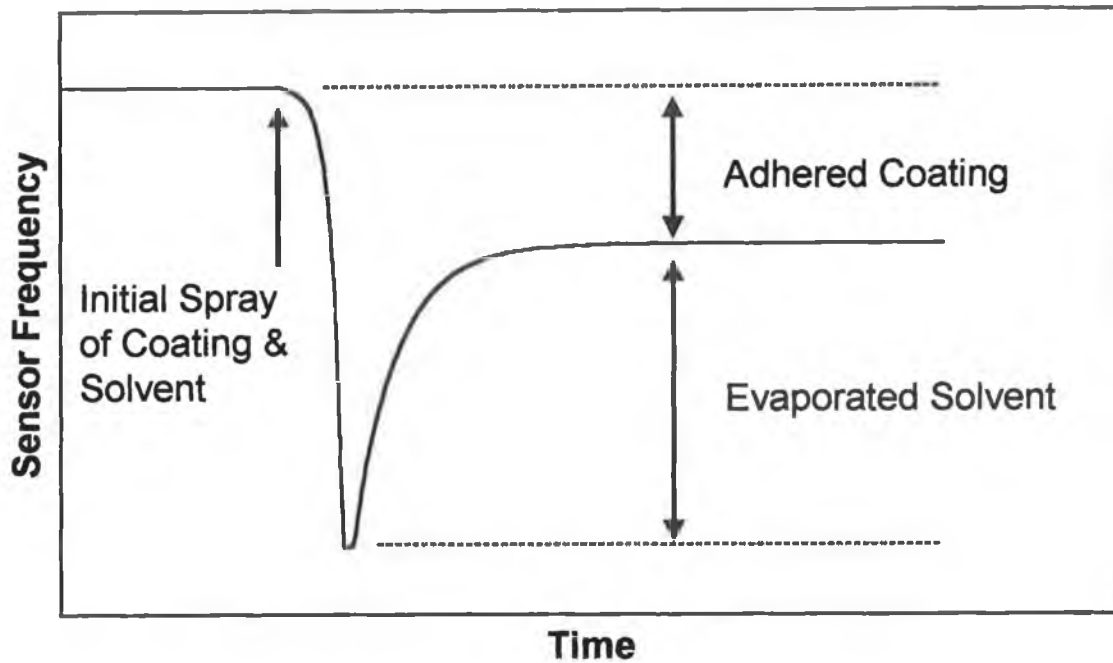
Figure 1-11: Frequency profile of BAW before, during and after coating

Sensitivity

The sensitivity of sensors in the array will vary for different analytes, so when comparisons are being made it is essential that the same concentrations of analyte are used. However the response of a sensor is also dependant on the level of coating, which will vary from one sensor to another. Therefore it is useful to quote the response as the frequency change per unit mass of coating material. It may sometimes be found that the response of a sensor to an analyte varies over extended periods of time. Should the period of time be significantly greater than the period of sampling then the change in response can be acceptable. However should this nature of this drift in response be comparable to the sampling time then compensation techniques may be required. These techniques however can only be used if the nature of the drift is consistent and not random. Therefore sensor validation before and after use is an important part of the sampling process.

Selectivity

The selectivity of a coating is dependant of its chemical affinities. To this end a sensor may be tailored for specific applications. However such sensors are difficult to produce and can suffer from reversibility problems. Consequently arrays have become popular for reasons outlined in Sec. 1.4, in combination with chemometric techniques (Sec. 1.5.)

Reversibility

The BAW sensors being considered can be employed in continuous monitoring, or multiple use modes. Therefore the nature of the chemistries involved must be weak and reversible, and so ionic and covalent bonding, with bond energies of several hundred KJmol^{-1}, are undesirable. Weaker interactions, such as hydrogen bonding and Van der Waals forces are more favourable, and will be discussed in more detail in Chapter 2.

Response Time

For practical purposes, continuous (recirculating) flow systems have to compete with established instrumental methods such as gas chromatography. Therefore the system must have sensors that have a rapid sample turnover. BAW systems satisfy this criteria with sampling times determined by the equilibrium time of sample headspaces, which can sometimes be of the order of seconds! BAW sensors are stable over short thermal ranges, and by using thin film coatings, can reach equilibrium with headspaces quickly. The coating materials used, allow for rapid diffusion into, and out of, the thin film (thickness < 100nm). Materials with low Tg, or glass-transition temperature (where the coating changes from a rigid lattice structure to an amorphous liquid) are therefore avoided in preference to more open amorphous coatings.

23

Repeatability

Gas flow systems are designed to create saturated headspaces, which allow sensors to have the best chance of giving repeatable responses. There are conditions that such sensors must satisfy; they must respond consistently, they must not age or react with the sample and they must return to their original state. BAW sensors satisfy these criteria, with relative standard deviations as low as 1-2%.

Reproducibility

Reproducible sensors must have good stability properties. The method of coating application must also be reproducible, to give sensors with similar morphologies. Therefore various methods of application must be investigated for repeatability, uniformity, ease of use, and control over the mass loading.

1.4 Arrays

Optimising a single sensor for an analyte of interest represents the first step in any detector development [30]. In some cases this might be easily achievable but some environments may be quite complex, and difficult to interpret using just one sensor with a specific selectivity. In certain environments the concentration of an analyte might be much lower than that of competing interferences. In such circumstances where selectivity is not sufficient, chemometric techniques become important. There is no such thing as a perfectly ideal chemical sensor. However, through careful selection, BAW sensors offer reversible, fast responses with satisfactory selectivity. Integrating such sensors into an array offers certain advantages, by increasing sensitivity through a combination of varying moderate selectivities. To optimise such an array it is necessary to include sensors that would be particularly selective to different classes of analytes. Then, through this combination of sensors, a pattern or fingerprint could be generated (Figure 1-12). This fingerprint could be assigned to a particular analyte and a library of such responses could be built up, provided the responses are consistently repeatable.
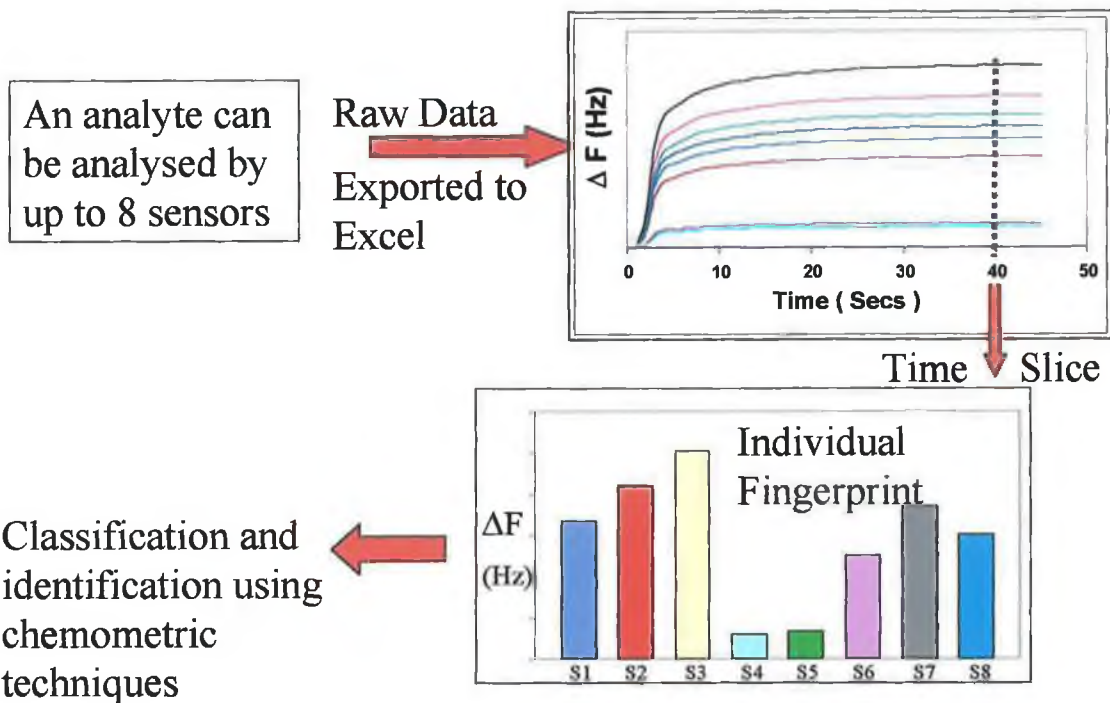
Figure 1-12: Typical analysis procedure using an array of sensors, from data acquisition to interpretation

1.5 Chemometrics

With the increase in the complexity of instruments, vast data sets are regularly generated and need to be interpreted. The data first has to be reduced, clearly represented graphically and then information extracted. With this increase in instrumentation complexity has been the ready availability of computers with continually increasing processing power to process this data. Together these two rapidly expanding areas led to the creation of a new discipline known as chemometrics. Svante Wold, who worked extensively with Bruce R. Kowalski, created the name for this area in 1971 and together they formed the International Chemometrics Society in 1974.

The actual definition of chemometrics has been accepted as: [31]

~ the chemical discipline that uses mathematical and statistical methods, to design or select optimal measurement procedures and experiments, and provide maximum chemical information by analysing chemical data.

Consequently chemometrics has made complicated mathematical methods practicable and the use of such techniques is becoming increasingly regular.

1.5.1 Chemometric Methods

Analytical processes usually start with a definition or selection of matter to be investigated [32]. Therefore it is important to note that every object being dealt with has a history that may cause systematic errors in our process evaluation. Therefore unless the complete history of an object is known for certain, one should be careful drawing conclusions from any chemometric results.

Currently there are four components to an analytical process [32]:
Sampling, **sample pre-treatment**, **measurement**, and **interpretation** of the results. *Procedure* is the term that covers the process from sample definition to the extraction of information by interpretation. The term *method* describes the processes carried out between sample pre-treatment and interpretation of the results, while *principle* relates to how the analyte matter produces a signal and how it is treated (Figure 1-13).

Procedure

Principle

Sampling → Sample Pretreatment → Measurement → Interpretation
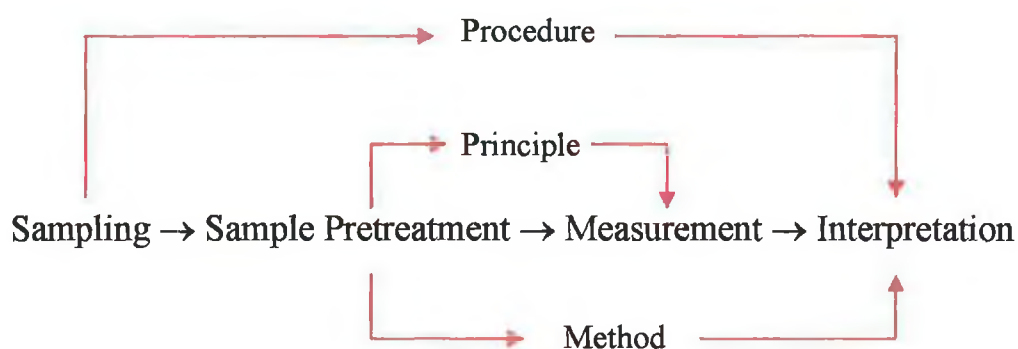
Method

Figure 1-13: Components of an analytical process

When data is derived from measurements it can sometimes be helpful to use advanced chemometric methods to extract information that would otherwise not be recognisable. Such techniques can find structures or similarities, such as groups or

classes, within the data while possibly also providing a quantitative relationship between the properties of such classes and relevant variables or descriptors.

$$Measurement \xrightarrow{\text{Data Evaluation}} Interpretation$$

Figure 1-14: Advanced method of chemometric data evaluation

1.5.1.1 Typical Chemometric Model

Our aim in chemometrics is to try to describe a chemical system as a mathematical model based on several *controllable* and *uncontrollable factors*. A factor is any aspect of the experimental conditions that can have an effect on the desired value to be attained from the experiment. Therefore an example of a controllable factor would be the temperature, reagent concentration *etc.* An uncontrollable factor would be one over which the experimenter would have no control over, such as the site location of a test sample.

It is also important to keep in mind that there is a difference between macromodels and micromodels. Where temperature and pressure are primary factors on a macro scale, molecular conformations or charge distributions might be more prevalent on a microscale [33].

Most models, **M**, are based on the following parameters (Figure 1-15):

X: A set of controllable variables or factors, on which the system is based *e.g.* Temperature, concentration *etc.*.

E: Random uncontrollable factors, to facilitate the deviations between the model and the real situation.

27

X Controllable Factors e.g. Temp	+	E Uncontrollable Factors e.g. Location	=	M Model

Domain
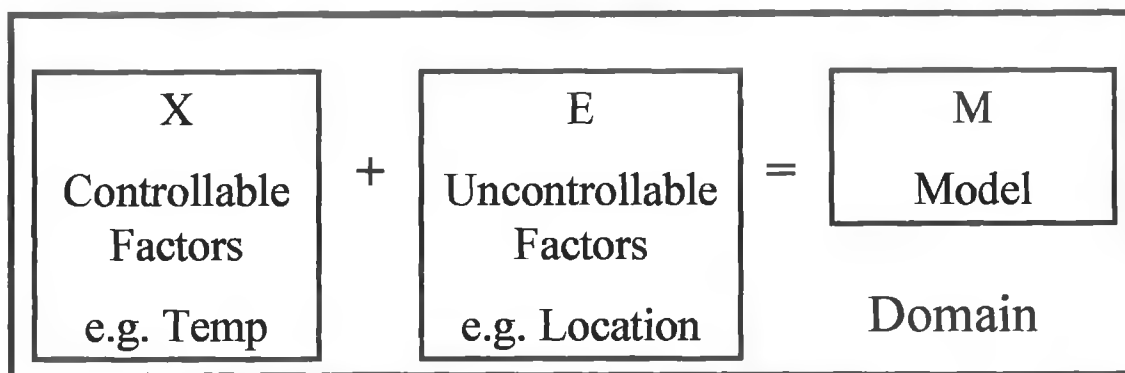
Figure 1-15: Schematic of a typical chemometric model

E could also be called the residual or the error and is necessary, as we can never achieve ideal situations, which unfortunately most models or theories are based upon.

Within any experiment there are parameters within which our model is limited and hence forms a domain. This domain has a maximum efficiency for a particular mode of analysis. To find this point we need to examine each variable with respect to the outcome, to determine the optimum conditions. Sometimes these variables might be independent whereupon the problem becomes very simple and fast to solve. However, sometimes the factors are intrinsically linked and so a compromise, or balance, must be reached.

1.5.1.2 Types of Model Error

Any measurement has an intrinsic error or noise associated with it, which is unavoidable. Random noise in a continuous flow system cannot be avoided but can be minimised through the use of a properly sealed system, stable sensors, and controlled laboratory temperatures. Other types of noise that can be seen are systematic, examples of which would be the heat given of by a component of an instrument which might be time dependant therefore changing through out the course of an experiment. Gross operator errors are assumed not to happen but cannot be ruled out from consideration. These errors, if not tackled early on in an experiment can nullify any results, thus resulting in significant losses of time and efficiency.

1.6 References

1   A. Newman, Electronic Noses, *Anal. Chem.*, **63(10)** (1991) 585A-588A

2   J.E. Amoore, Molecular Basis of Odours, Charles C. Thomas, Springfield, IL, 1970

3   J.W. Gardner, P.N. Bartlett, Performance definition and standardisation of electronic noses, *Sensors and Actuators B*, **33** (1996) 60-67

4   J. Greenwood, B. Crawley, K. Dunn, Something smells good in Manchester, *European Hospital Management Journal*, **4(3)** (1997) 58-60

5   Gibson, T.D. et al, Detection and simultaneous identification of microorganisms from headspace samples using an electronic nose, *Sensors and Actuators B*, **44** (1997) 413

6   W. Göpel, Chemical imaging: I. Concepts and visions for electronic and bioelectronic noses, *Sensors and Actuators*, **52** (1998) 125-142

7   J. Janata, *Principles of Chemical Sensors*, Plenum, New York, 1989

8   J.F. Alder, J.J. McCallum, Piezoelectric crystals for mass and chemical measurements, *Analyst*, **108** (1983) 1169

9   W.G. Cady, "Piezoelectricity", First Edition, McGraw-Hill, New York and London, 1946

10   A.C. Becquerel, *Bull. Soc. Philomath.*, Paris, **7** (1820) 149 (Series 3)

11   J. Curie, P. Curie, *Bull. Soc. Min. Paris*, **3** (1880) 90

12   G. Lipmann, *An. Chim. Phys., Ser.* **5(24)** (1881) 145.

13   A. Langevin, "Piezoelectricity", First Edition, McGraw-Hill, New York and London, 1946 p. 5

14   W.G. Cady, *Proc. Inst. Radio Eng.*, **12** (1924) 805

15   G.W. Pierce, *Proc. Am. Acad. Arts Sci.*, **59** (1923) 81

16   R.L. Bundee, E.J. Jarvi, J.J. Rosentreter, Piezoelectric Quartz Crystal Biosensors, *Talanta*, **46** (1998) 1223-1236

17   A.R. Hillman, H.L. Bandley, M. Gonsalves, The electrochemical quartz crystal microbalance as an analytical tool: Problems and solutions, *Annali di Chimica*, **81** (1991) 177-186

18   C.K. Sullivan, G.G. Guilbault, Commercial quartz crystal microbalances – theory and applications, *Biosensors and Bioelectronics*, **14** (1999) 663-670

19   J. Hlavay, G.G. Guilbault, Applications of the piezoelectric crystal detector in analytical chemistry, *Anal. Chem.*, **49(13)** (1977) 1890-1899

20   R.F. Schmitt, J.W. Allen, J.F. Vetelino, J. Parks, C. Zhang, Bulk acoustic wave modes in quartz for sensing measurand-induced mechanical and electrical property changes, *Sensors and Actuators B*, **76** (2001) 95-102

21   S-M. Chang, H. Muramatsu, C. Nakamura, J. Miyake, The principle and applications of piezoelectric crystal sensors, *Mat. Sci and Eng. C*, **12** (2000) 113

22   F.L. Walls, J.R. Vig, Fundamental limits on the frequency stabilities of crystal oscillators, *IEEE Trans. Ultrason., Ferroelec., and Freq. Cont.*, **42(4)** (1995) 576-588

23   K. Bodenhöfer, A. Hierlemann, G. Noetzel, U. Weimar, W. Göpel, Performance of mass-sensitive devices for gas sensing: thickness shear mode and surface acoustic wave transducers, *Anal. Chem.*, **68** (1996) 2210-2218

24   P.J. Cumpson, Quartz crystal microbalance; a new design eliminates sensitivity outside the electrodes, often wrongly attributed to electric fringing field, J. Vac. Sci. Technol. A., **15(4)** (1997) 2407-2412

25   G.Z. Sauerbrey, Z. Phys., **155** (1959) 206

26   K.K. Kanazawa, J.G. Jordan, *Anal. Chim. Acta.*, **175** (1985) 99

27   A.P.M. Glassford, *J. Vac. Sci. Technol.*, **15** (1978) 1839

28   D.M. Ullevig, J.F. Evans, M.G. Albrecht, Effects of stressed materials on the radial sensitivity function of a quartz crystal microbalance, *Anal. Chem.*, **54** (1982) 2341

29   M.T.S.R. Gomes, A.C. Duartes, J.A.B.P. Oliveira, Critical assessment of the parameters that affect the selection of coating compounds for piezoelectric quartz crystal microbalances, *Talanta*, **48** (1999) 81-89

30   J.W. Grate, M. Abraham, Solubility interactions and the design of chemically selective sorbent coatings for chemical sensors and arrays, *Sensors and Actuators B*, **3** (1991) 85-111

31   D.L. Massart, Chemometrics : a textbook, Amsterdam; New York : Elsevier, 1988

32   M. Otto, Chemometrics: Statistical and Computer Application in Analytical Chemistry, Wiley-VCH, 1999

33   S. Wold, Chemometrics and Intelligent Laboratory Systems, **30** (1995) 109-115

Chapter 2

2   Bulk Acoustic Wave Coatings

2.1   Application of Coating

The conversion of a blank BAW into a BAW sensor is quite simple and just requires the coating to be placed on the surface. The application of the coating however is important and the merits of various methods will be discussed in the following chapter. However it is quite easy to estimate the level of coating once it has been applied, as it will be measured as the change in the resonant frequency of the BAW. This frequency can then be converted into its mass equivalent using the Sauerbrey equation (Chapter 1), assuming that it satisfies the necessary criteria. Figure 2-1 illustrates the change in the fundamental resonant frequency (ΔF), i.e. F_A-F_B, after the application of the coating.
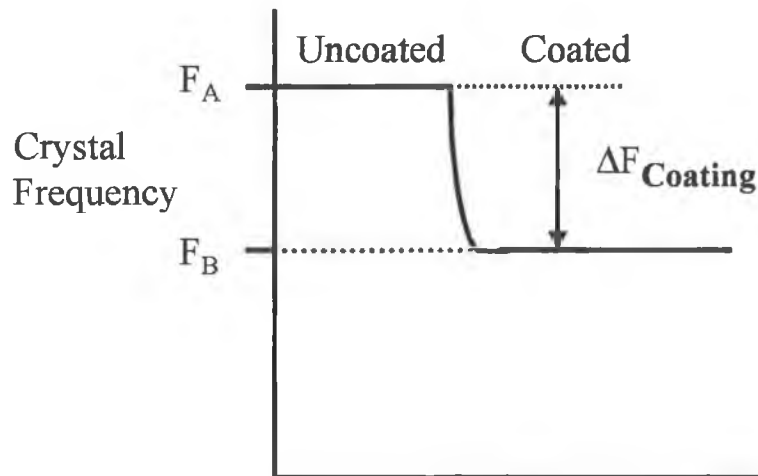
Figure 2-1:   Frequency profile of BAW before and after coating application

The issue now arises of what to use as our sensing layer. The concept of an ideal sensor coating has been introduced in the previous chapter, in terms of its physical attributes, and will be discussed in this chapter in terms of its chemical attributes.

2.2 Sensitivity

The sensitivity of a sensor to a particular analyte of interest is dependant on the interactions with the sensor coating. For BAW sensors it is dependant on the partition of the analyte vapour into the sensor coating. This partition is now considered.

2.2.1 Vapour/Coating Partition

When a coating comes into contact with a vapour a partition of the vapour between the gas phase and the coating takes place (Figure 2-2). The affinity of the vapour for the coating may be interpreted in terms of solvent interactions, *i.e.* the extent to which the vapour dissolves in to the coating.

Numerically this affinity is quantified in terms of K, the partition coefficient (Equation 2-1).

$$K = \frac{C_C}{C_G}$$

Equation 2-1

Where C_G is the concentration of the analyte is the gas phase, and C_c is the concentration of the analyte in the polymer coating. The gas phase concentrations are determined using a variation of the Ideal Gas Law (Equation 2-2)

$$C_G = \frac{M_r.P.V}{R.T}$$

Equation 2-2

where M_r is the molecular mass ($gmol^{-1}$), P is the solvent vapour pressure (Pa), V represents volume (dm^{-3}), R is the universal gas constant ($8.314 JK^{-1}mol^{-1}$), and T represents temperature (298K).

Therefore the partition coefficient is also dependant on the operating temperature of the system and increases with increasing temperature.
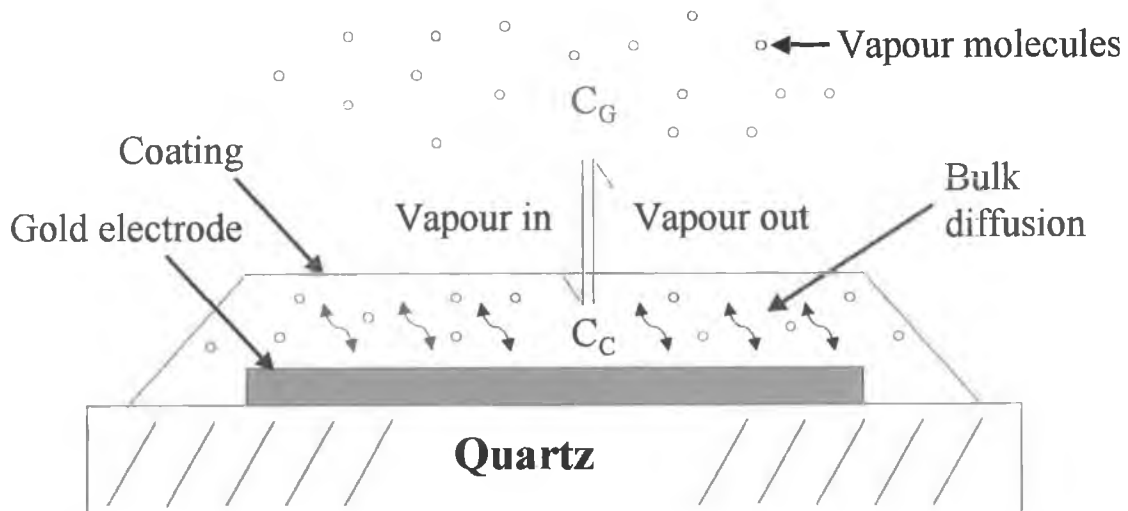
Figure 2-2: Interfacial partition of vapour at a sensor coating

To consider this partition, the stages through which a bare BAW must pass before it becomes a working sensor must be addressed. There are four states that the BAW crystal experiences in this process, and a graphically presented in Figure 2-3:

(A)   Uncoated Crystal:

Bulk acoustic wave devices are purchased in their bare form with a gold electrode on the quartz surface. Their oscillating frequency has been adjusted to F_A (Figure 2-3) through careful sputtering of the required amount of gold onto the surface.

(B)   Coated Crystal

When a suitable coating material has been chosen, it is applied to the gold surface using a selected coating method. The additional mass on the surface will change the resonant frequency of the BAW to F_B. The drop in frequency, ΔF, will be almost entirely directly related to the mass adsorbed onto the electrode area, as this is the most sensitive region (as explained in Chapter 1).

(C)   Absorption of Vapour

When a coating is exposed to a vapour, their interaction will be dependant on their respective chemistries. A concentration gradient arises where the vapour concentration in the headspace is much higher than that in the coating. Absorption of the vapour by the coating the progresses through a two-stage process (see Sec. 2.2.1.1). In the first stage the vapour will be adsorbed onto the surface of the polymer. This stage is very quick and happens in the as soon as the vapour "reaches" the coating. The second stage, the rate-determining step, involves the adsorbed vapour diffusing into the bulk coating. The rate of this diffusion is dependant on certain factors such as the size and chemistry of the vapour molecules. For example the smaller the molecule, the easier and faster it will diffuse in. The general rule of thumb for solute-solvent interactions applies, "like dissolves like". A polar coating will "dissolve" alcohol vapours more readily than aliphatic hydrocarbon vapours. The time for vapour concentration in the coating to match that in the headspace is called the equilibrium time, and is normally reached between 20 and 60 seconds. The change in the sensor mass is read as a frequency change (ΔF_1), and is a function of the solvent/solute chemical properties. This will be discussed later when dealing with Linear Solvation Energy Relationships.

(D)   Desorption of Vapour

After the coating has been exposed to the vapour for a set time, the airflow over the sensor is switched to allow ambient air pass over it. The concentration of the vapour in the ambient air is negligible, and so a concentration gradient arises in the opposite direction to that in (C) above. The ambient air will absorb the vapour molecules at or near the surface. This will allow dissolved vapours in the bulk to diffuse towards the surface of the coating, from where it will then be desorbed. This desorption thus regenerates the sensor surface (Figure 2-3). Ideally the sensor frequency will return to F_B, and this is often the case. The process of desorption usually takes longer than the absorption, and is always allowed extra time to avoid any vapour being trapped in the coating, thus minimising memory effects.

33

Uncoated crystal (A)	Coated crystal (B)
Absorption of vapour (C)	**Desorption of vapour (D)**
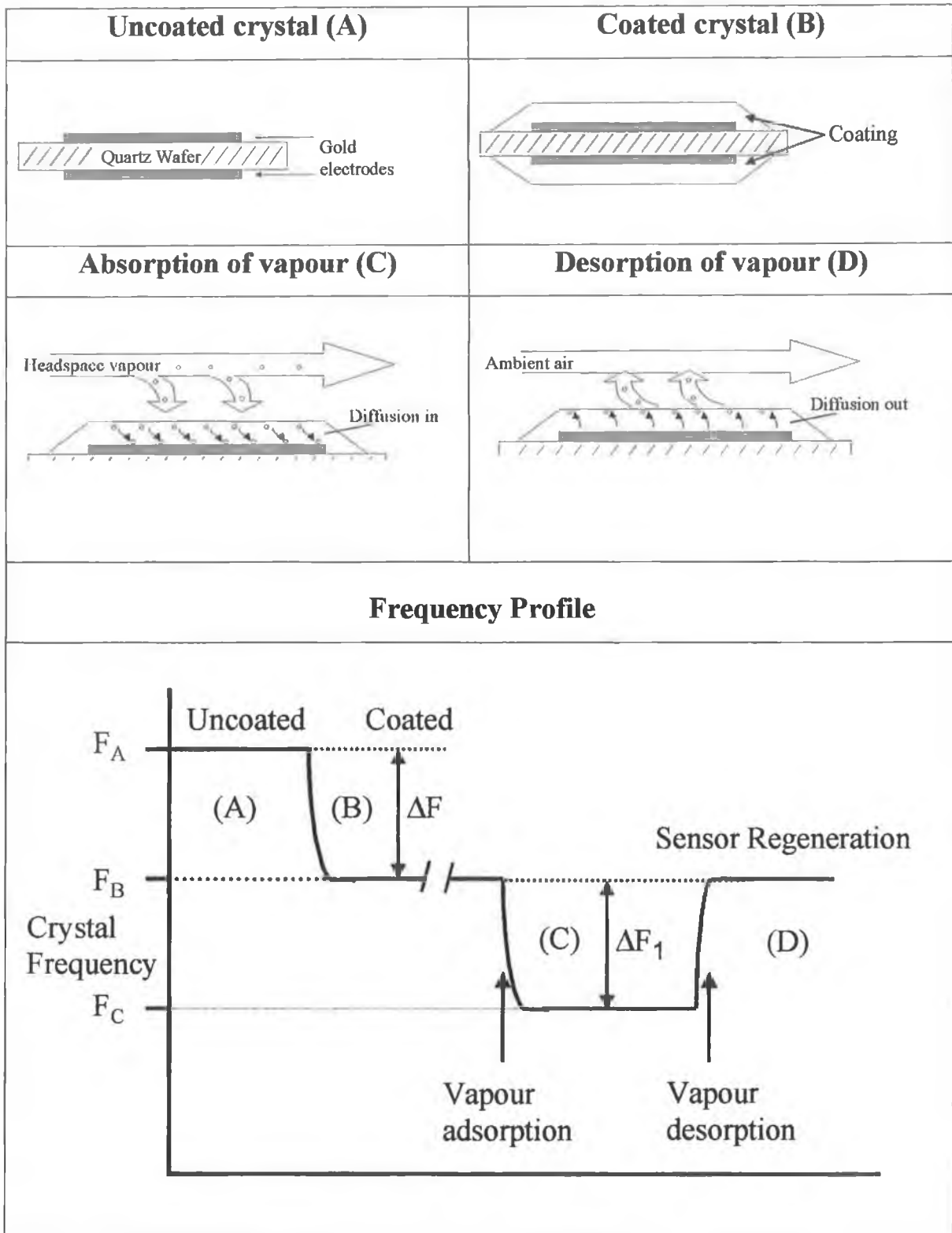
Frequency Profile

Figure 2-3: Frequency profile of quartz crystal from bare uncoated state to regeneration

2.2.1.1   Concentration Profiles

The concentration gradients mentioned in (C) and (D) above, will now be examined. There are four stages of interaction between the headspace and the coating:

(1) $C_G = C_C = 0$

Before any vapour is introduced to the coating, ambient air is passed over the sensors. As the concentration of the vapour in the air and the coating are both negligible, there will be no interactions.
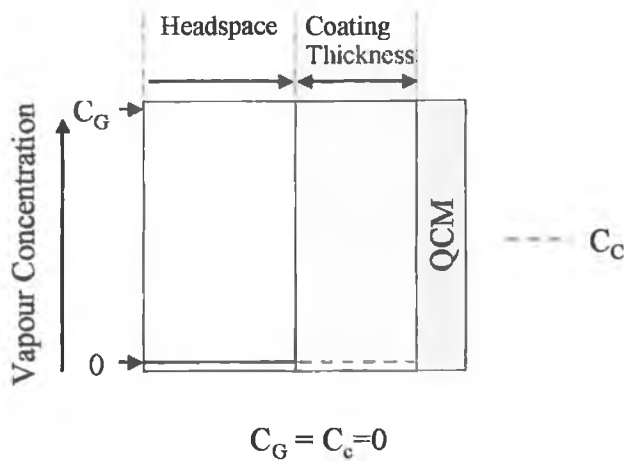
Figure 2-4:   Concentration profile prior to vapour sampling

(2) $Cg > C_G$

When the ambient air passing over the sensors is changed to the analyte vapour there will be an initial adsorption of the vapour onto the surface, as the vapour will find this area of low concentration attractive. The concentration in the bulk of the coating (C_C) at this stage is still zero. Gradually the vapour will diffuse into the coating over time and will approach equilibrium with the headspace.
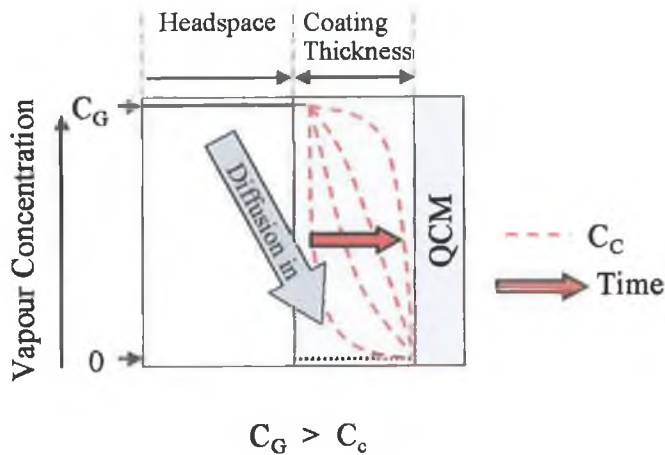
Figure 2-5: Concentration profile during vapour sampling

(3) $Cg = C_G > 0$

At equilibrium, C_G will equal C_C. Ideally this stage should be reached as quickly as possible, as this is the "rate determining step" in the sampling cycle.
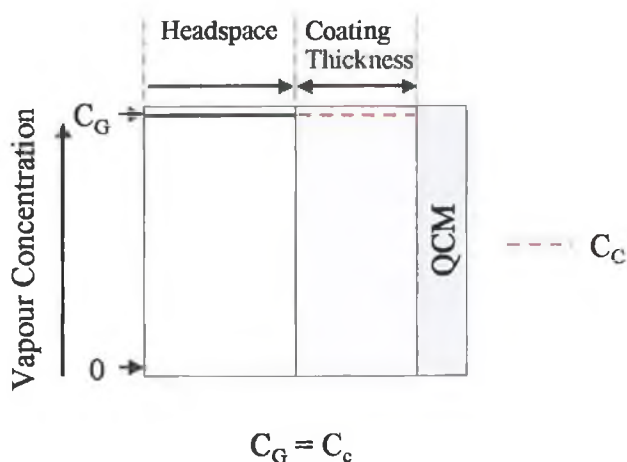
Figure 2-6: Equilibrium concentration profile during vapour sampling

(4) $Cg\ (\approx 0) < C_G$

When switching occurs again, ambient air is passed over the sensor, and C_G returns to zero. Therefore the dissolved vapour will find the ambient air more attractive and diffusion out of the coating begins. When all of the vapour has left the coating, C_C

will reduce to zero and the system returns to **(1)** above, thereby completing the regeneration.
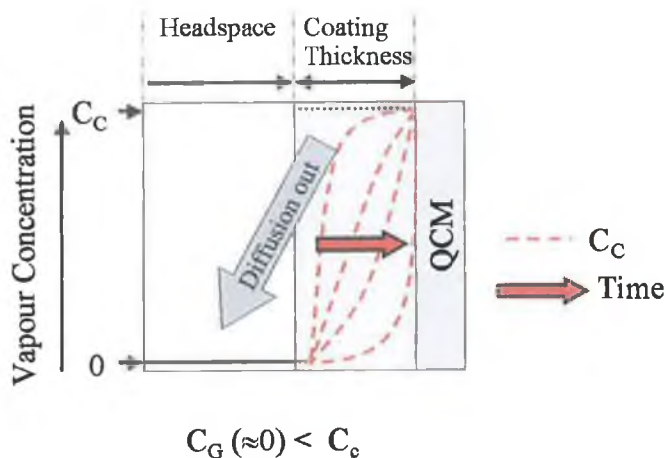
Figure 2-7: Concentration profile during ambient air sampling

2.3 Selectivity

For a BAW sensor to be useful in a continuous flow system it has to make use of weak interactions, in a thin coating. As already pointed out in the previous chapter, strong interactions give rise to poor reversibility. The weak interactions required for these kinds of sensors are hydrogen bonding, dispersion interactions and Van der Waals interactions. The bond strength of these interactions are generally smaller in comparison to ionic and covalent interactions (Table 2-1), and so breaking of these bonds easily occurs at ambient temperatures.

Interaction Type	Energy ($kJmol^{-1}$)
Covalent	200-800
Ionic	80-400
Hydrogen Bond	4 - 40
Dispersion	~6
Induction	0.4 - 4
Dipolarity	0 - 4

Table 2-1: Indication of relevant interaction strengths

The ideal coatings properties have been discussed in the previous chapter (Sec. 1.3.6), but can be briefly summarised as follows:

- The coating should be non-volatile. The coating should be resistive to chemical and physical degradation, and be able to interact with analyte vapours without reacting with them.
- The coating should be soluble in a volatile solvent to allow for easy application.
- The coating should allow rapid facile diffusion of vapours to and from sites of selective interaction. Such reversibility is necessary for complete regeneration of the sensor coating.
- The physical state of the coating should not change with use nor give rise to hysteresis effects.
- Material must be compatible with the gold surface.

These requirements are satisfied by non-volatile liquids and by amorphous oligomers and polymers. Elastomeric polymers, such as poly(ethylene glycol) have better sorption, quicker diffusion and reversibility than more rigid crystalline glassy polymers, such as poly(acrylic acid).

The chemical nature of the coating determines how it will interact with volatile samples, and hence defines the sensor sensitivity and selectivity. Functional groups that will cause increased interaction with the vapour of interest should be present provided that they do not cause significant self-association in the coating. Therefore the selectivity of a coating material will be greatest if we select a particular solubility interaction sympathetic to the target analyte and maximise it while trying to minimise all others. The following forms of interaction cover a wide range of possibilities.

(A) Hydrogen bonding

Hydrogen bonding is an attractive interaction between two closed-shell species that arises from a link of the form A—H···B, where A and B are highly electronegative

elements and B possesses a lone pair of electrons. Hydrogen bonding is conventionally regarded as being limited to N, O and F but if B is an anionic species (such as Cl⁻), then it may also participate in hydrogen bonding. There are then three subsets in this category: Hydrogen bond basicity (with minimal dipolarity), Hydrogen bond basicity and dipolarity, and Hydrogen bond acidity.

Hydrogen-bond basicity (minimise dipolarity)

Hydrogen bond basicity is the interaction between an electropositive hydrogen, of a molecule, with an electron rich functional group, through a lone pair of electrons. Water would possess such electropositive hydrogen's and this explains its high boiling point compared to methanol for example. There are several functional groups that provide basicity but most of them are also dipolar. Strong basicity accompanied with little dipolarity can be obtained from the mildly electronegative nitrogen of amines, which have only one lone pair.

Example: Poly(ethylenimine)
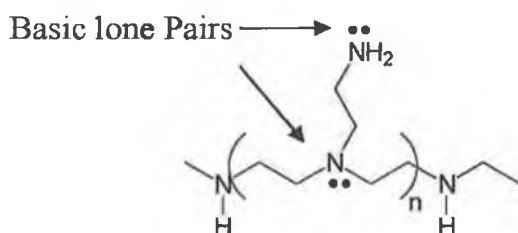
Figure 2-8: Chemical Structure of poly(ethylenimine)

Hydrogen-bond basicity and dipolarity

Typical coatings would contain electronegative groups, which could donate electron density towards a hydrogen bond. For this category there is plenty of choice including amides, sulphoxides, phosphoryl groups being the strongest with esters being weaker but more readily available.

Example: Poly(vinyl propionate)

Strongly polar oxygen with
basic lone Pairs ⟶
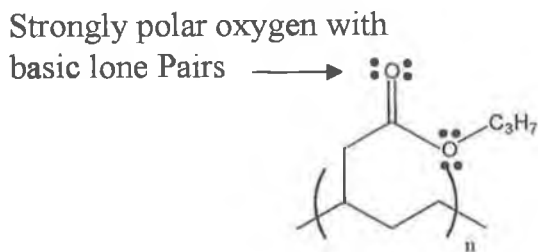
Figure 2-9: Chemical Structure of Poly(vinyl propionate)

Hydrogen-bond acidity

A coating is said to be a hydrogen bond acid when it partially donates a hydrogen to an electronegative molecule. The principal functional group for this class would be OH groups in alcohols and phenols and sometimes non-aliphatic NH groups can be considered. Aliphatic NH groups will have negligible acidity, but not aromatic amines. Carboxylic acids can dimerise and so aren't considered. The acidity in alcohols can be increased using electron withdrawing halogen substituents. These compounds cannot be purchased directly and must be synthesised.

Example: Fluoro Allyl bisphenol
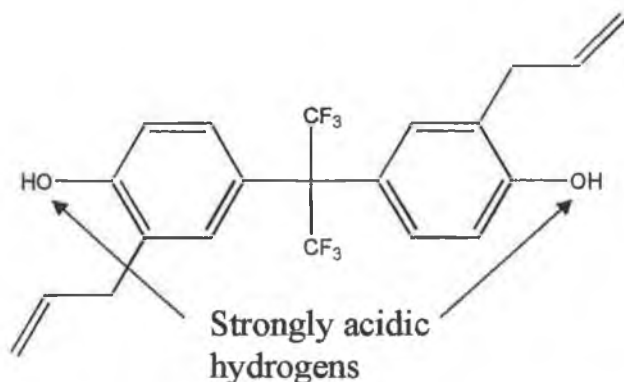
Figure 2-10: Chemical Structure of Fluoro Allyl bisphenol

(B) Dispersion interactions

Dispersion interactions are also known as induced-dipole/induced-dipole interactions or *London* forces, and are seen between aliphatic hydrocarbons in the condensed phase. Although individually weak the summation of all these forces can be quite substantial. An example of a compound, which has a high degree of dispersion

interactions, is Polyisobutylene (PIB). These interactions arise from the electric field produced by the very rapidly varying dipoles between nuclei and electrons in molecules with zero-point motion. Induced dipoles are formed in phase with the instantaneous dipoles producing them. They are present in all solute/solvent systems. They are the only source of interactions between non-polar molecules and the interactions are independent of temperature.

Example: Polyisobutylene
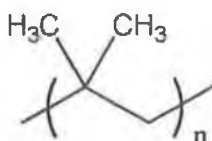
Figure 2-11: Chemical structure of Poly(isobutylene)

(C)   Induction

Induction (or *Debye*) forces arise from the interaction of a permanent dipole with a polarisable molecule. Polarisability refers to the formation of a dipole in a material due to the influence of an external electric field. The presence of aromatic groups or heavy halogen atoms in a compound promotes polarisability. Polarisable materials will have greater interactions with dipolar vapours via dipole/induced-dipole interactions. Should the polarisable coating molecule be also aromatic there may be a possibility of intramolecular π-π interactions, or even π-π stacking with aromatic analytes. It should be remembered that polarisable refers to the ease with which a dipole is induced whereas dipolar refers to a dipole that already exists.

Example: Phenylsilicones such as Poly(phenylmethylsiloxanes) OV17 (50% Phenyl Substitution), OV25 (75% Phenyl Substitution)(*Oxygen's in the chain are very weakly basic*)

41
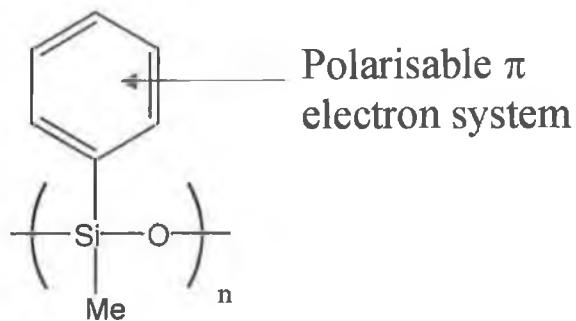
Figure 2-12: Chemical structure of OV17

(D) Dipolarity

Dipolarity involves the incorporation of dipolar groups into a material to increase the sorption of dipolar vapours by orientated dipole/dipole interactions. Sorption of polarisable vapours will also be increased by dipole/induced-dipole interactions. Dipolarity is greatest in heteroatomic functional groups, but these are also basic. Hence we have to consider how to maximise dipolarity and minimise basicity. Widely available cyano groups are popular for this type of interaction.
Example: Silar 10C(*Siloxane with 100% cyanopropyl substitution*),
Tris(cyanoethoxy)propane.
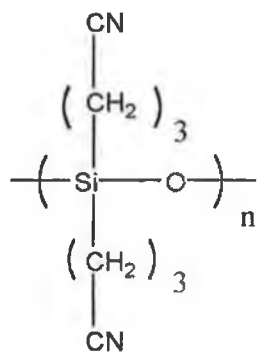
Figure 2-13: Chemical structure of Silar 10C

2.3.1 Estimation of Solute-Solvent Interactions: Linear Solvation Energy Relationships (LSER)

In the analysis of any system it is necessary to estimate the total absorption of any solute (vapour) by a solvent (sensor coating), using a partition coefficient, K, as previously introduced in this chapter:

$$K = \frac{Conc_{Solvent}}{Conc_{Solute}}$$

Equation 2-1

This partition coefficient can be related to the standard Gibbs's free energy of solution of a gaseous solute, ΔG_s^o by

$$\Delta G_s^o = -RTLnK$$

Equation 2-3

where the standard states are unit concentration in the gas phase. The partition coefficient is very useful as it can be directly related to the frequency shifts of BAW's on vapour sorption. It can be noted that the most strongly sorbed vapours are those with hydrogen-bonding capabilities. Lesser-sorbed vapours are dominated by dispersion interactions.

Considerable attention has been paid to the parameters that regulate the solubility properties of solvents. Such parameters were initially collected from UV spectra of various indicator dyes dissolved in solvents and are often referred to as solvatochromic parameters [1]. However these were bulk properties and so revised parameters had to be devised that would characterise monomeric solutes, and are known as solvation parameters. These parameters, obtained experimentally, can be used to compare vapours (solutes) with one another. For clarity, solvents will be denoted using the subscript 1, while solutes will be denoted using the subscript 2.

Solvation Parameter	Symbol	Explanation
H-Bond Acidity	α^H_2	Measure of the H-bond acid strength, derived from equilibrium constants for acid-base reactions using reference bases such as pyridine. eg. EtOH = 0.33, Phenol = 0.6, Trifouroacetic acid = 0.96
H-Bond Basicity	β^H_2	Measure of the H-bond base strength, derived from equilibrium constants for acid-base reactions using reference acids such as 4-fluorophenol. e.g. Alkanes = 0, Acetone = 0.5, long chained amines=0.7
Dispersion	L^{16}	Related to the Gibbs free energy, it's a combination of exothermic dispersion interactions, coupled with endothermic cavity terms. For Alkanes Log L^{16} is related to Boiling Point
Polarisability	R_2	Ability of a solute to interact with a solvent through $\pi + n$ e⁻ pairs 1(aromatic) ⇔ 0.5(Halogenated HC) ⇔ 0(others)
Polarity	π^*_2	Ability of compound to stabilise a neighbouring charge or dipole. Cyclohexane = 0 (By definition),EtOH = 0.4, Nitrobenzene =1.0

Table 2-2: Table of solvation parameters

The following table quantifies these parameters for some solutes [2].

Solute	Solute Factor				
	Polarisability R_2	Dipolarity π_2^*	H-Bond Acidity α_2^H	H-Bond Basicity β_2^H	Dispersion log L^{16}
Hexane	0.0	0.0	0.0	0.0	2.688
Toluene	0.601	0.55	0.0	0.14	3.34
Chloroform	0.425	0.58	0.2	0.02	2.48
Methanol	0.278	0.40	0.37	0.41	0.922
Propan-2-ol	0.212	0.40	0.32	0.47	1.821
Ethylacetate	0.106	0.55	0.0	0.45	2.376

Table 2-3: Solvation parameters for solutes

When a solute interacts with a solvent there will be a variety of interactions depending upon their intrinsic chemistries. To consider all these interactions a method has to be devised. Such a method must be applicable to materials used as coatings, including non-volatile liquids, liquid polymers and solid elastomeric polymers. One such method is to use Linear Solvation Energy Relationships (LSER's).

The general form of a LSER is as follows:

$$LogK = c + rR_2 + s\pi_2^* + a\alpha_2^H + b\beta_2^H + lLogL^{16}$$ **Equation 2-4**

Where the symbols are explained in Table 2-2 and Table 2-4

It should be noted that GLC literature quoting LSER values are based on high temperatures whereas piezoelectric work is based at room temperature. For our purposes the LSER parameters can only be used as an indicator of solute-solvent interaction strengths. Therefore it will act as a guideline for choosing polymers and volatile organic solvents for this study.

Coefficient	Complementary to:	Explanation:
K	-	Partition coefficient
c	-	c arises from the derivation using regression techniques
r	R	Measure of the ability of a phase to interact with n and π electrons (usually +ve but –ve if Fluorine's are present)
s	π_2^*	Measure of the liquid phase dipolarity.
a	α_2^H	Measure of the liquid phase H-bond basicity
b	β_2^H	Measure of the liquid phase H-bond acidity
l	L^{16}	Combined measure of (a) Dispersion Interactions and (b) Cavity Effects.

Table 2-4: Table of LSER Solvent coefficients

2.4 Response Time

For a continuous flow system to be able to compete with established techniques such as GC, it must use sensors that have a quick sample throughput. Therefore the sensors that it uses must be fast (~30 seconds per sample), and reversible.

Most BAW sensors are fast, with equilibrium response times sometimes between 10 and 15 seconds. However some sensors are not as quick and this is due to their absorption properties.

When a sample interacts with a BAW sensor it first binds to the sensor surface and then is absorbed into the bulk of the coating. The rate at which this happens depends upon its functionality and affinity for the coating (solvent). Therefore the response time of the sensor is dependant on two factors, the chemical nature of the sample, and its subsequent rate of diffusion. The functionalities that govern chemical interactions have been covered in the previous section and now we will look at the adsorption and diffusion processes. A useful explanation of these processes given by Janata [3] is presented in *Appendix 1*.

When a chemical species (X) interacts with a sensor (S), an equilibrium is reached:

$$X + S \underset{k_r}{\overset{k_f}{\Longleftrightarrow}} XS \qquad \text{Equation 2-5}$$

The overall rates of the forward (k_f) and reverse (k_r) reactions together with the mass-transport parameters of the species involved in the transduction mechanism, such as size and concentration, determine the response time of the sensor.

By a simple manipulation it can be shown that if there is a change in sample activity then the sample will interact with the sensor, once the variation in the standard free energy is negative ($\partial G^o < 0$). However if ∂G^o is large, it will give rise to a high

46

binding constant. For sensor applications a high binding constant implies that equilibrium will be reached very quickly, but may cause problems with reversibility and this would be undesirable for a BAW sensor. Therefore there is a need to look at a more passive situation where equilibria are reached over relatively longer periods of time.

By just considering the rates of reaction, the interactions between the sample and the sensor can be expressed in terms of activities of the sample and sensor coating. With some manipulation it can be shown that the output of a BAW is logarithmic. This is the case when we are only dealing with an equilibrium situation.

However there is also a contribution to the response due to mass transport, for which concentration can be shown to be the determining variable.

As BAW sensors involve mass-transport to a point where equilibrium is reached, then they can be said to be dependant on both concentration and activities. For an ideal dilute solutions these can be considered equivalent. The concentration determines the amount of signal produced while the activities determine the type of signal produced. Taking these conditions into consideration, the overall reaction must be within a range where there is no risk of hysteresis, thereby giving a sensor with satisfactory reversibility.

2.5 Reliability

The reliability of a sensor is critical to its success, and BAW sensors being used for repeated exposures in a continuous flow system have to be reliably consistent under a variety of conditions; temperature, pressure *etc*.

The reliability of a sensor is dependant upon the coating, which should be stable between the upper and lower operating temperature ranges. For BAW's that range is usually 20 to 60°C, depending upon the polymer. As the temperature increases the crystalinity within the polymer will start to decrease and the polymer may undergo

creep, seen as a negative drift in the sensors signal over time, thereby shortening the lifetime of the sensor.

The sensor will be exposed to various samples, some of which may find the polymer coating very attractive. An example of this would be poly(ethylene glycol) being exposed to a solvent such as chloroform. If the levels of chloroform are high enough, it might overload the sensor, and hence interfere with the binding between the polymer and the gold, as the polymer could swell. This could result in the coating becoming viscoelastic, thereby causing unharmonic oscillations. Over time this drift will have an effect on the reproducibility of the sensors results.

Humidity is a constant problem for environmental samples, but can be considered to be just another component of a sample headspace. Under saturated conditions water will form a monolayer on the surface of a bare crystal, which represents a frequency change of about 10Hz for a 10 MHz crystal. This can then be compensated into the responses of other sensors, should it become a problem. An alternative method is to use a dryer, which is essentially a Nafion® coated tube encased within a box of molecular sieves. While the dryer removes most of the water it can also interfere with similar size analytes such as ammonia *etc*.

Most operational work is carried out at room temperature under normal pressures, and so variations in pressure are minimal. If there were a variation in pressure it would change the gas phase concentrations of the analytes, thus nullifying any work done. Consequently variable pressure must be avoided.

2.6 Repeatability

For BAW sensors in a continuous flow system, the analyte will remain within the coating matrix until it's concentration in the headspace drops below that in the coating. This only happens when the sampling has been switched off and the cleaning process has begun. However if the sample does not come out of the coating as quickly as it went in there may be significant problems. Such a problem would be hysteresis, where the rate of diffusion in does not equal that out. Therefore if the

cleaning time is not sufficient some of the analyte will remain in the coating. This will then be seen as an increase in the baseline signal. Over the period of a sampling run this additive accumulation of analyte will cause the absorption capability of the coating to decrease. This drift then is represented as a tailing off or saturation at higher concentrations. The solution to this is to use longer cleaning times, with higher flow rates. An alternative would be to introduce an additional step such as running something like methanol or every second run or so. This introduction of a solvent might dissolve the analyte into the methanol vapour, thus cleaning the sensor.

All BAW sensors are exposed to various organic solvents after coating, to gain an initial understanding of their sorption properties. This allows one to determine the length of cleaning time required to fully desorb any absorbed analyte. Thankfully most samples desorb quickly, and so a cleaning time of double the sampling time is usually sufficient.

2.7 Reproducibility

Comparison of sensor-to-sensor work using BAW's is possible once the results being used are presented as the normalised responses. This is due to the fact that as the thickness of coating upon a sensor increases so does its response to analytes. However there sometimes arises the situation where sensors made at the same time using the same amount of polymer, and coated in the same manner may give different responses. This is a problem but does not occur very often. The failure could have something to do with the crystal itself, rather than the coating material being the source of trouble. Sometimes the crystal being supplied can have faulty connections, or insufficient levels of glue holding the crystal within the mounting. Such faulty transducers must be identified and screened out of arrays, as the data collected could be completely spurious.

2.8 Reference methods

2.8.1 Characterisation of Coatings by Surface Analytical Techniques

When dealing with coatings on surfaces there is a need for adequate characterisation, to answer the following questions [4]:

- ➢ Is the coating adhering to the substrate?
- ➢ Is its composition and structure as expected?
- ➢ Are there any visible surface defects, or ruptures?
- ➢ Is there corrosion beneath or within the coating?

To this end there are various techniques that can be used:

2.8.1.1   *Optical Microscopy*

Optical Microscopy uses diffuse reflected light, and has a maximum spatial resolution of 250nm with low image distortion. Use of high sensitivity analog and digital imaging systems can view poorly reflecting areas and shadowy areas with little difficulty. This technique is used consistently in the analysis of paints on metal surfaces in the automobile industry on a daily basis.

2.8.1.2   *Scanning Electron microscopy / Energy Dispersive X-ray Analysis (SEM/EDX)*

SEM/EDX has become very popular in the last 15 years. SEM uses a beam of focused electrons rather than light to form images. The use of electrons gives higher resolution (<5nm) and allows for greater depth of field. As a result of the increased improvements in SEM sources problems that would have required Transmission Electron Microscopy (TEM), can now be easily tackled. Example of this would be the deposition of Ruthenium complexes on silicon wafer by chemical vapour deposition. The dispersive X-ray analysis gives elemental information on the near-surface region of the coating.

The model of SEM used for this study was a Hitachi S3000N, which is capable of operating under variable pressure (chamber pressure = 1-270 Pa). Such variable pressures allow for gas molecules, present in the chamber, to strip surface of potential accumulating charges. Also it avoids dehydration of soft coatings unlike high vacuum SEM systems.

Previous models were dependant on the surface of interest being coated, with gold for example, in order to accurately generate an image. Unfortunately this method made the sample unusable for future applications. However this has now been avoided and SEM has become a standard tool for non-destructive surface analysis.

2.8.1.3   Infra Red Spectroscopy

Reflectance Infrared Spectroscopy can be used to verify the presence of a chemical coating on the surface of a piezoelectric crystal. The crystal is mounted in a horizontal attenuated total reflection accessory (HATR), which allows for a blank crystal to be inserted as a reference and then compared after being coated.

2.8.2   Gas Chromatography

Traditional headspace analysis has been carried out using gas chromatography. This offers a quantitative and qualitative analysis of the headspace components. Coupled with Mass Spectroscopy, a library of analytes can be built up and used as a reference point. Such libraries can hold huge numbers of reference chemical profiles, thereby automatically identifying unknowns.

2.9   Molecular Recognition

For a sensor to be able to discriminate between analytes, its properties have to be examined on a molecular level. At this level there are two factors that govern molecular interactions.

The first factor is charge distribution, and is controlled by the functionality of the sensing layer and that of the analyte of interest. In the liquid phase ions are strongly

bound to a sensing layer due to their high charge density. However in the gas phase weaker interactions are more dominant, and so forces such as hydrogen bonding, or dipolar interactions dominate. Therefore using complexes that have electron rich and deficient centres can take advantage of such functionalities, such as metal centred pthalocyanines [5].

The second factor that determines the behaviour of analyte-sensor interactions is morphology. In this case an ensemble of weak interactions yields the efficient binding of properly aligned weak interactions centres of analyte molecules. This allows molecules to be classified according to their size, molecular shape, and subunit arrangement.

2.9.1 Molecularly Imprinted Polymers

One area of coatings that is attracting attention is that of molecularly imprinted polymers (MIP's). Such polymers are used to create sensors with predetermined selectivity towards particular molecules in the gas phase. The sensor coatings are highly cross-linked macroreticular polymers possessing microcavities complementary in size, shape and functionality to that of the original template molecule [6]. Such polymers however tend to have problems releasing the template molecule, which often cannot be fully washed out. The most popular of such polymers tend to be styrene based, but are proving difficult to perfect.

2.10 References

1 J.W. Grate, M. Abraham, Solubility interactions and the design of chemically selective sorbent coatings for chemical sensors and arrays, *Sensors and Actuators B*, **3** (1991) 85-111
2 M.H. Abraham, J. Andonian-Haftvan, C.M. Du, V. Diart, G.S. Whiting, J.W. Grate, and R.A. McGill, *J. Chem. Soc. Perkin Trans.*, **2** (1995) 369
3 J. Janata, *Principles of Chemical Sensors*, Plenum, NY, 1989
4 N.S. McIntyre, R.D. Davidson, S. Ramamurthy, M.J. Walzak, & M.C. Biesinger, *Characterisation of Coatings by Surface Analytical Techniques*, Metal Finishing, (October 1997)
5 F.L. Dickert, A. Haunschild, Sensor materials for solvent vapour detection: donor-acceptor and host-guest interactions, *Advanced Materials*, **5(12)** (1993) 887-895
6 H-S. Ji, S. McNiven, K. Ikebukuro, I. Karube, Selective piezoelectric odour sensors using molecularly imprinted polymers, *Anal. Chim. Acta*, **390** (1999) 93-100

Chapter 3

3 Experimental

3.1 Introduction

This chapter will deal with the experimental approach taken with the supplied gas sensing system, its modifications, and subsequent applications. The topics covered will include the supplied system, instrumentation, sampling methods, data acquisition and subsequent interpretation (Figure 3-1).

Supplied System

Instrumentation
- Pumps, valves, & Tubing
- Circuitry → Swithable Reference
- Sensors → Evaluation of Coating Methods
- Sensor Housing → New Chamber Design
- Sampling Vessels

Sampling Method
- Sampling
- Switching
- Cleaning
- Sampling Time

Data Aquisition → Export Data as CSV

Data Interpretation
- Data Evaluation → Kinetic Modelling
- Molecular Modelling → Chem 3D, Spartan
- Classification → PCA, CA, DFA

Figure 3-1: Overview of Experimental Topics

3.2 Supplied System

A gas sensing system was purchased from Quartztec Ltd. (Quartz Technology Limited, Hemel Hampstead, Herefordshire, UK)(Figure 3-2). The system (Figure 3-3) consisted of a pump, switching valves (SV), tubing, and circuit board with integrated sensor housing, sampling interface, and sampling vessels and data acquisition software.

Figure 3-2: Gas sensing system and Laptop Computer
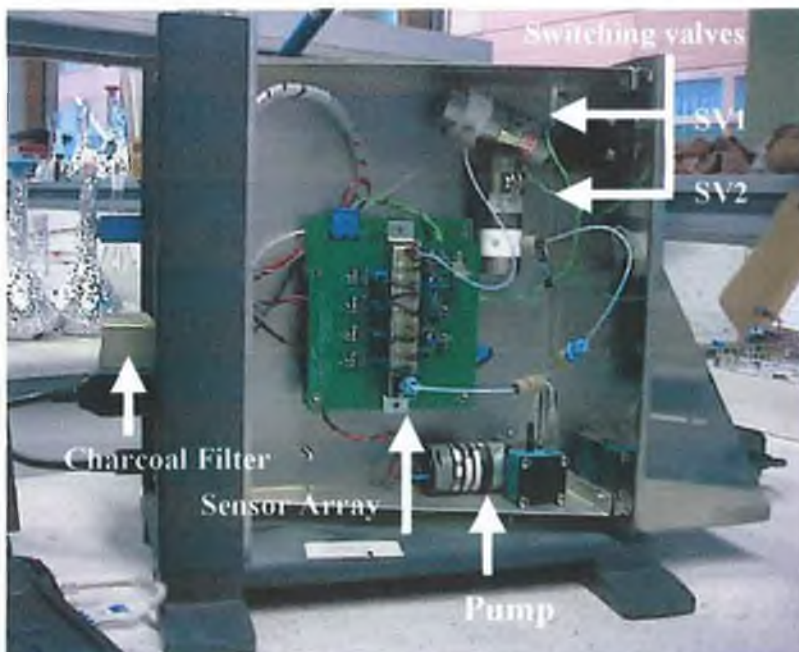
Figure 3-3: Gas sensing system with some components labelled

3.3 Instrumentation

3.3.1 Pumps, Valves and Tubing

(A) Pump

The pump supplied with the system is a Teflon® diaphragm pump. It draws the sample from the headspace above the liquid/solid. The DC power supplied to it from the circuitry is 5V, and at this voltage has a flow rate of 160 ml/min. Incorporating a potential divider between the pump and the circuitry allows for control over the DC voltage. By adjusting the voltage to the pump, the flow rates can be adjusted down to a lower limit of 100 ml/min.

(B) Valves

The Teflon® 3-way switching valves SV_1 and SV_2 (Figure 3-3) operate on a 5V supply from the circuitry. Switching these valves allows the pathways of the airflow through the instrument to be changed. In sampling mode (Sec. 3.4) only the sample headspace passes over the sensors, while in cleaning mode ambient air is drawn over the sensors. An electronic analogy would be that the sample headspace acts as a (open circuit) shunt.

(C) Tubing

The Teflon ® tubes supplied ($\varnothing$ = 1.53mm o.d.) were fitted with airtight connections which matched those of the switching valves and the end blocks of the sensor array. The tubing was made as short as possible to minimise the dead volume within the sampling loop.

3.3.2 Circuitry

The circuitry is required to run the various pumps and valves, but primarily exists to provide electrical conditions that will encourage the quartz crystals to oscillate at their maximum efficiency. The circuitry contains various amplifiers and filters, but essentially, incorporates the quartz crystals as tuning elements in a NAND gate

configuration. This configuration is considered to be a compromise between the gain needed to generate a signal and detrimental aging effects in the crystal. The current passing through the crystal is then compared to a hermetically sealed reference crystal on the circuit board. As different crystals were used during this body of work it was necessary to modify the connections of this reference crystal to the board. To facilitate easy and rapid change between reference crystals a male HE14 socket (Radionics (Irl) Ltd) was interposed between the crystal and the board. The currents are read by the PC via a RS232 9 pin D-type cable, as frequency differences using the QuartzTec software.

3.3.3 Sensors

The system was supplied with eight sealed quartz sensors. No information was provided on the structure of their respective coatings, however a brief explanation of their respective chemistries was given. For this reason it was decided to coat our own crystals where the specific chemistries would be known. Therefore various different coating methods had to be evaluated, and the one that gave the best uniformity with greatest ease of application and control would be chosen. An ideal coating method would be one where sensors could be coated uniformly to a specific frequency reproducibly. The uniformity would be determined using scanning electron microscopy (see Chapter 2).

3.3.3.1   Coating method and application details

(1)   Airbrush

The airbrush technique involves spraying a polymer solution (in a recycle loop possibly), using high pressure N_2 or air, and passing the crystal through the resulting mist. Once the pressure is high enough the mist will be adequately fine to ensure a relatively even finish. However if the mist is too coarse, then there may be problems with the solvent creeping and dripping from the crystal. With a more volatile solvent, *e.g.* hexane, there are no such problems with dripping, as the solvent will

evaporate from the surface quite rapidly. Using this technique the level of coating can be adjusted by simply changing the spraying time, until the desired level is reached. From the SEM image (Figure 3-4 B) a satisfactory coating can be observed for PIB. The coating at low magnification appears patchy, but is very even at higher magnification.

Advantages: Efficient, fast, uniformity, repeatable

Disadvantages: Large polymer volumes required
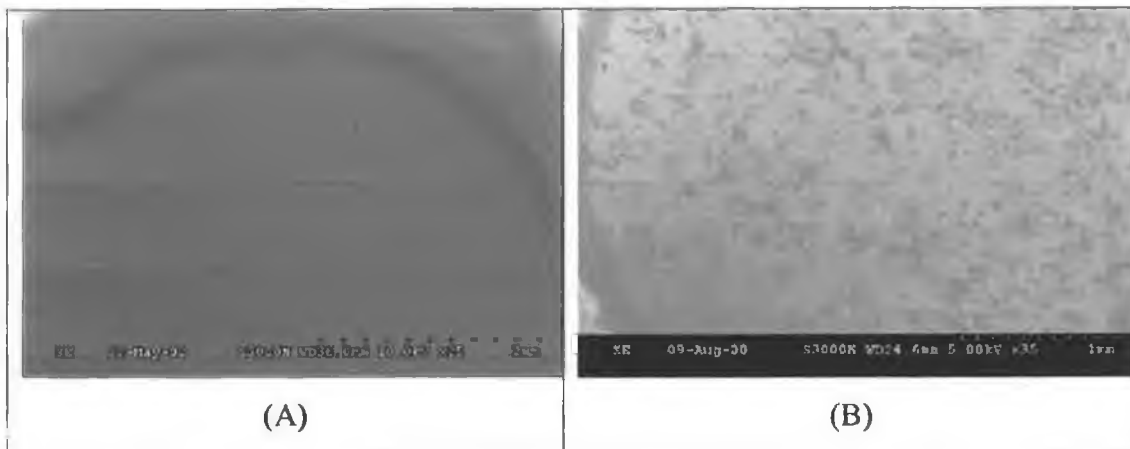
Figure 3-4: SEM image of (A) an uncoated QCM and (B) a PIB Spray-coated QCM (x40)

(2)   Drop Coating:

Drop coating involves applying drops of a set amount of a polymer solution to the centre of a crystal and allowing the solvent to evaporate leaving a polymer layer on the crystal. This has to be done to both sides of the QCM in separate steps. The crystal has to be left in a horizontal position between steps so that the drop remains centred, and avoids trailing. The SEM image (Figure 3-5a) displays a phase separation while (Figure 3-5b) shows a light coating on the gold surface with congealed polymer on top of this again. The problem with this technique is that the amounts of polymer being dropped are of the order of μL, and so reproducibility and control are difficult to maintain. Also with large solvent amounts, there is a chance that the coatings may coagulate, as seen in Figure 3-5(a).

Advantages: Simple, Fast,

Disadvantages: limited reproducibility

(a)   (b)
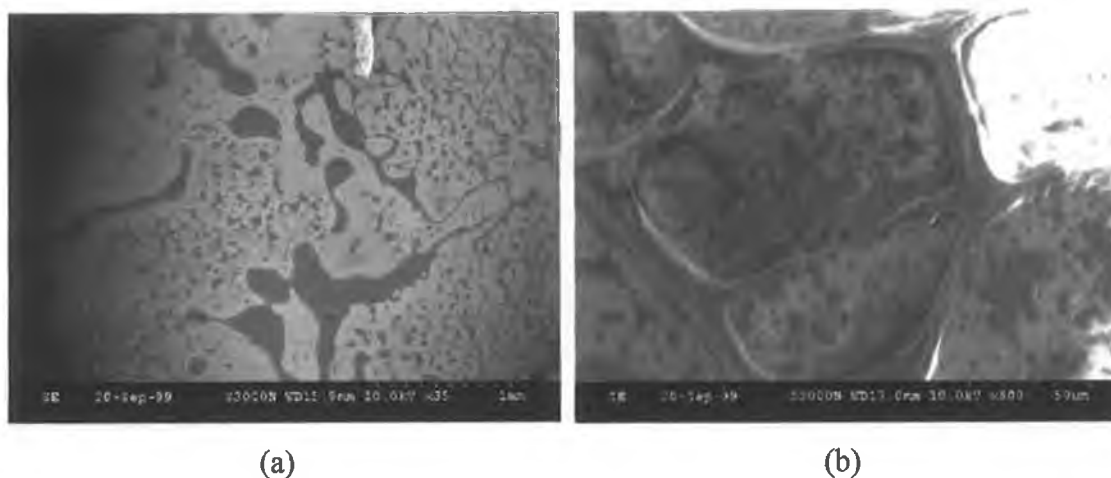
Figure 3-5: SEM image of PVC Drop-coated QCM (a) (x35) & (b) (x800)

(3)   Dip Coating:

This technique involves lowering the crystal into a polymer solution and then raising
it with a coating attached. The technique is very simple and inexpensive, but
unfortunately is not very reproducible (unless thiolated monolayers are being
attached). The problem of trailing can arise if the coating is thick enough. This
means that the coating at the bottom will be thicker than that at the top. The SEM
image (Figure 3-6) is for an area just below the centre, over the bare quartz wafer.
The coating is quite thick here, but the charging of the quartz brightens the picture.
The coating is very light higher up the crystal face and very patchy, probably due to
trailing.

Dipping Advantages: Simple, fast
Dipping Disadvantages: Poor reproducibility
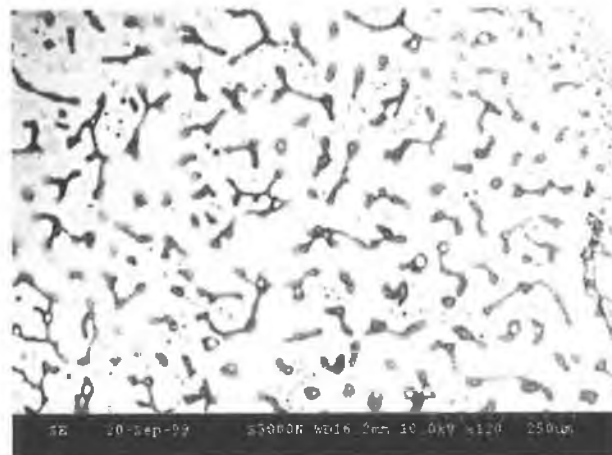
Figure 3-6: SEM image of PVC dip-coated QCM (a) (x120)

(4) Spin Coating:

Spin coating involves dropping a solution onto a surface, which rotates at high speeds (*ca.* 2000 rpm) ensuring that the polymer is spread out over the surface due to the centripetal forces. This coating method normally ensures that a uniform thin film thickness is obtained. This method was not used due to the physical form of the crystal, such as the electrode connections and the time required to disassemble and reassemble the crystal within the arms.

Advantages: Reproducible, uniformity, fast application times.

Disadvantages: Awkward (depending on crystal size), slow preparation
times.

(5) Smearing:

Smearing involves brushing the surface of the crystal with a solution of the polymer. The technique suffers from poor reproducibility, where dried out polymer from previous brush strokes may be re-dissolved in later applications giving varying results and possible contamination. The SEM images shown (Figure 3-7 a & b) are for a small area, which gives similar results to (3), but is not representative of the coating on a macroscale, where brush strokes will be uneven.

Advantages: Simple, Fast,

Disadvantages: Poor reproducibility, very uneven with poor coverage

59
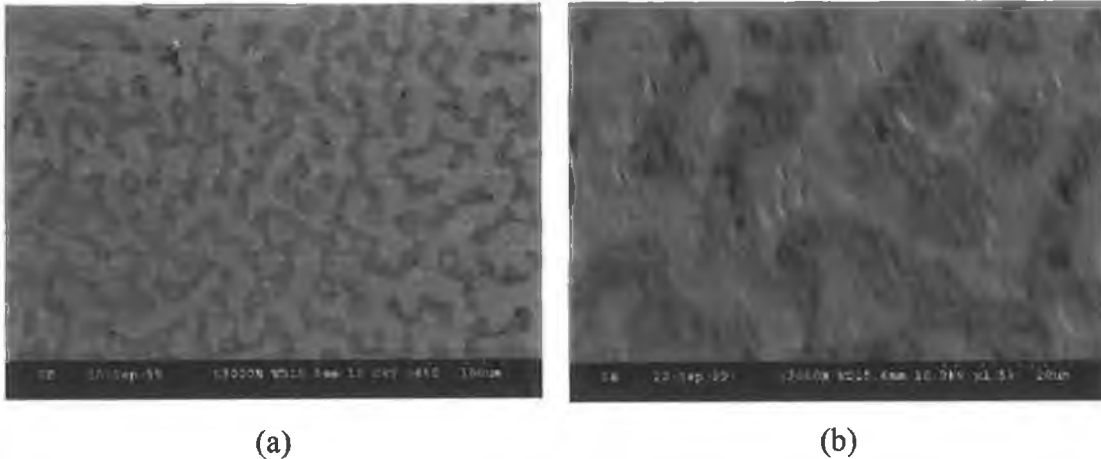
Figure 3-7: SEM image of PVC Smeared QCM (a) (x430) and (b) (x1,500)

(6)   Physical Adhesion:

If a polymer is cured in the form of a thin layer it might be possible to physically attach it to the surface of a crystal. This process may require the use of high pressures and temperatures. The use of tackifiers (glue-like chemicals) and plasticisers may reduce the amount of work necessary to get good adhesion.

Advantages: Reproducible

Disadvantages: Slow, tedious, and unsuitable for microscale work

(7)   Application Details:

For our purposes the technique chosen was spraying due to the ease of application, good reproducibility and control over the coating level (Figure 3-8). The system was covered and placed in a fume hood. It was then attached to a portable personal computer (Laptop), which facilitated real-time monitoring of the mass being absorbed onto the crystals surface (see Figure 3-9). An air-operated spray gun (Radionics Irl. Ltd.) was used to coat the crystals, generally at a distance of 30 to 50 cm from the crystal (see Figure 3-10). At this distance using a suitable pressurised carrier gas (N_2 at 60psi) the polymer solution will be adequately fine enough to obtain a light even coating. The coating process takes as little as 30 seconds per QCM side using a suitably volatile solvent such as hexane. Less volatile solvents

such as ethanol take longer (~2 minutes per side). The coatings were allowed to dry standing with their original protective covers, left loosely on, to avoid particulate contamination. After being allowed to dry for up to 2 days the crystals were then tested to monitor the change in frequency. Some times the frequency change would be significant in the case of solvent systems of low enough volatility. This would happen for some coatings like PEG, if it had been coated using ethanol as solvent. The ethanol would take up to a day to fully evaporate from the crystal surface. Therefore more volatile polar solvents were used, such as chloroform. Polymer coatings using highly volatile solvents such as hexane (*e.g.* PIB) would reach a stable frequency in well under an hour.
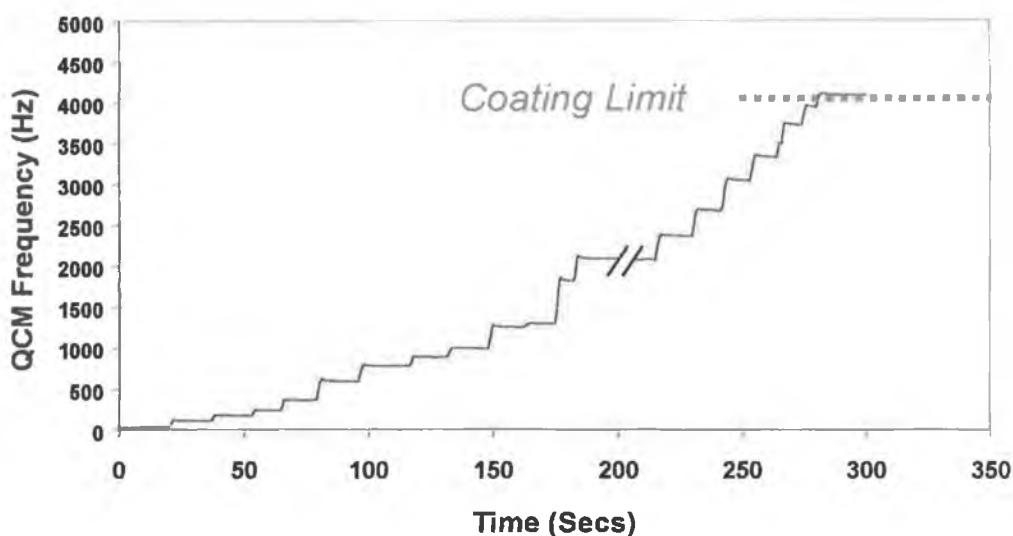
Figure 3-8: Real-time frequency profile of a crystal being coated

(8)   Overloading

The Sauerbrey equation (Chapter 1) relates the oscillating frequency of a quartz disk to its mass. One of the assumptions made in the derivation of this equation requires that the additional mass be negligible in comparison to that of the quartz disk. Therefore there is a mass or "loading limit" that a QCM can sustain before the energy losses cause the harmonic oscillations to cease. When an absorbent coating is attached to the surface its mass may not reach this limit, but on interaction with a suitable vapour, the combined masses will exceed it. When this additional mass loading exceeds the limit, then the crystal is said to be "overloaded". When this

61

happens the apparent sensor signal can couple with other sensor signals and becomes no more than electrical noise. This can occur with volatile vapours such as chloroform or hexane partitioning into particularly favourable coatings such as PEG or PIB for example. Therefore, when coating a crystal, there is a "coating limit" which cannot be exceeded (Figure 3-8) and from experience it is usually taken as being about half of the loading limit, typically 8,000 Hz, depending on the quality of the crystal.
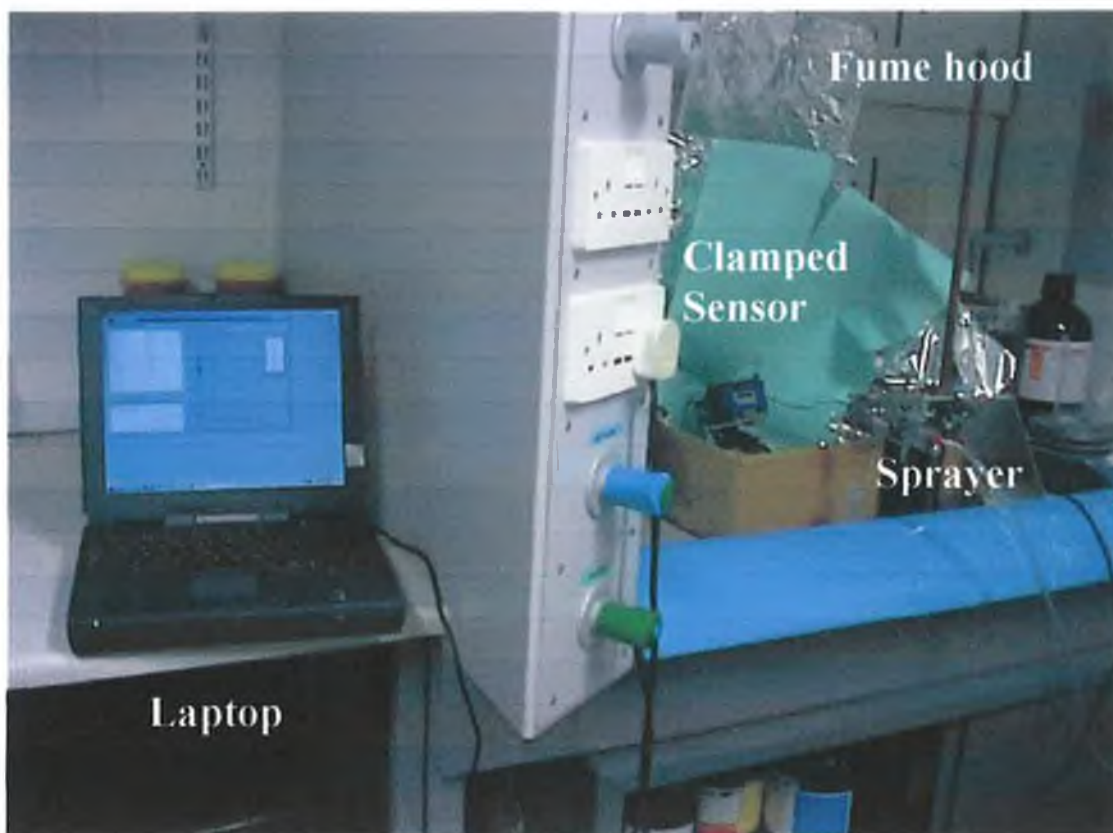
Figure 3-9: Photo of Array in Fume hood
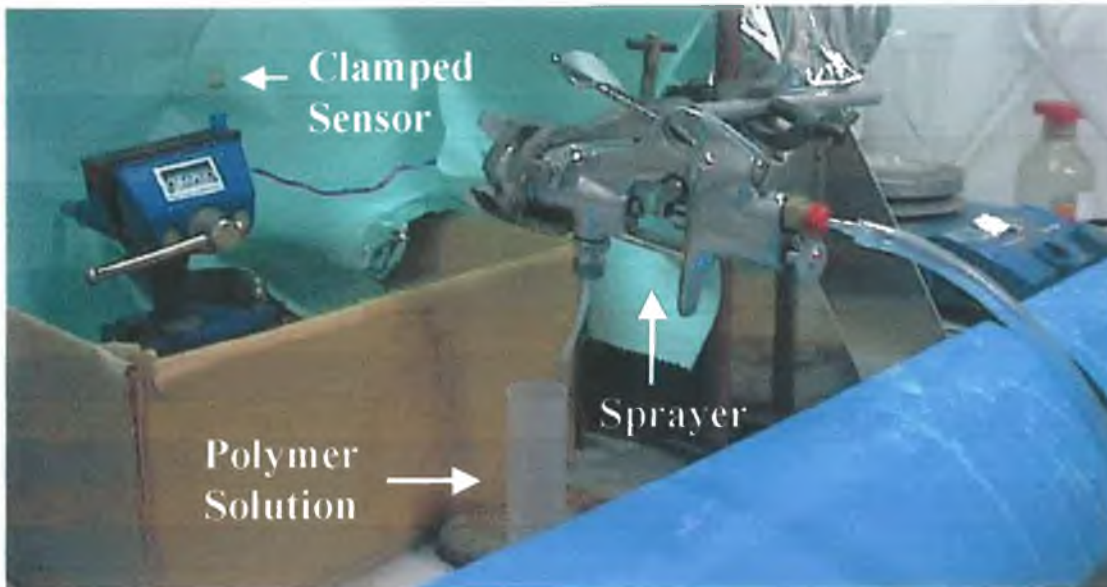
Figure 3-10: Photo of Sprayer and Clamped Sensor

3.3.4 Sensor Housing

The original sensors were supplied individually encapsulated using an epoxy resin in a Delrin® holder, which was then fitted with the corresponding electrical connections for attachment to the circuitry (Figure 3-11). The design of these holders means that the QCM's themselves act as the baffles, thereby aiding interaction with the analyte (Figure 3-12(b)). The dimensions of the holder are 18mm(H) x 13mm(W) x 8mm(D).
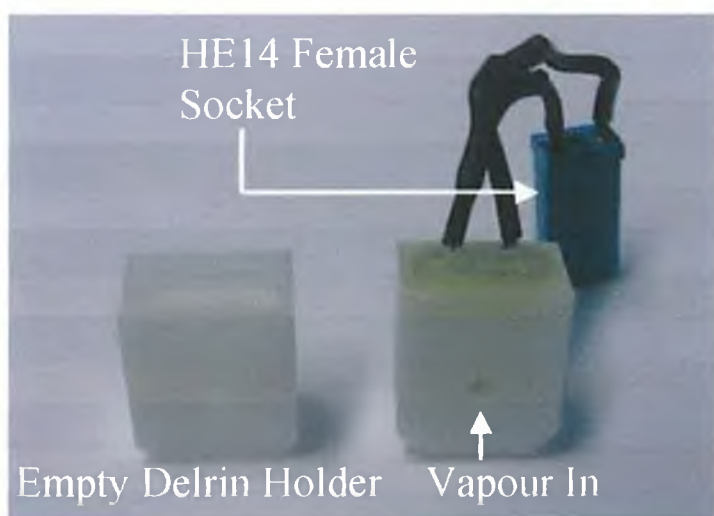
Figure 3-11: Photo of Delrin® Holder with and without sensor

Original Crystal Chamber Setup

Epoxy Resin

QCM

Delrin Holder

End View **Front Elevation**

Vapour in → ⋯⋯⋯ → Vapour out

(a)   (b)
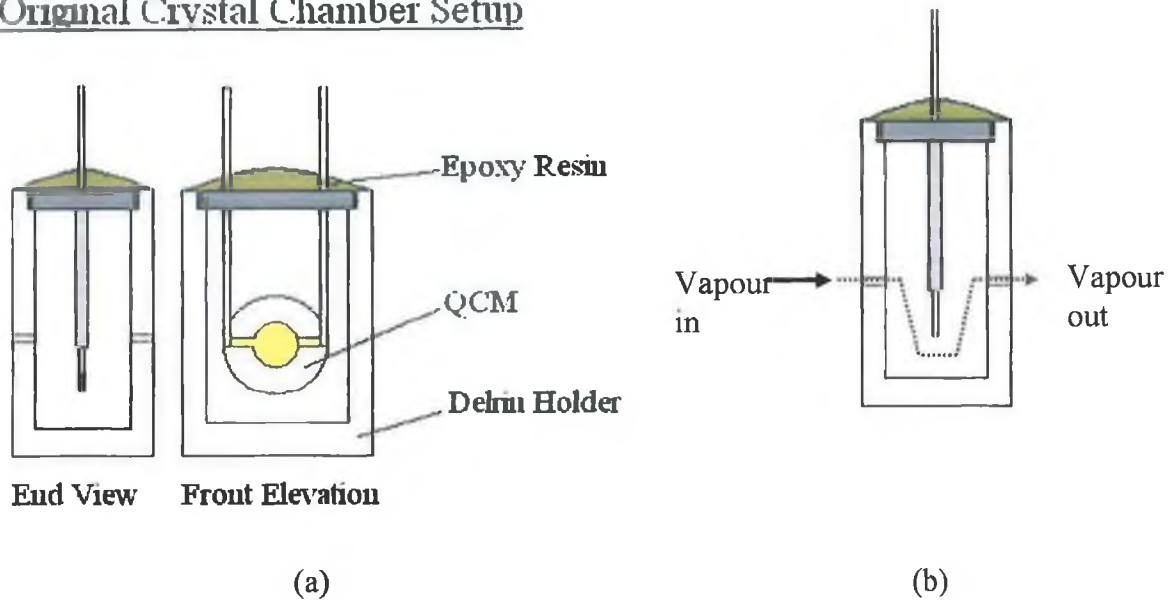
Figure 3-12: (a) Original Crystal Chamber Setup, End View and Front Elevation and (b) Vapour movement schematic.

While this approach is efficient in terms of sampling, it was found to be inflexible when devices had to be replaced. When a new coating had to be tested it had to be placed in an empty chamber and glued using an epoxy resin. The replacement time was determined by the time for the resin to dry (typically in the order of 2-4 hours). Therefore an integrated array block was designed and fabricated based on the original holder design (Dimensions: 64 mm(W) x 25 mm (H) x 18 mm (D)) using Perspex® (Figure 3-13). The new design allowed for rapid sensor changes (eight sensors being replaced in less than 5 minutes!). The sensors are placed in the chamber resting on the o-ring (See Figure 3-14), and then the lid is placed over them pressing them tight thereby achieving an airtight seal (the lid being screwed into the array housing). Again the sensors act as baffles disturbing the airflow over the sensors (Figure 3-15).
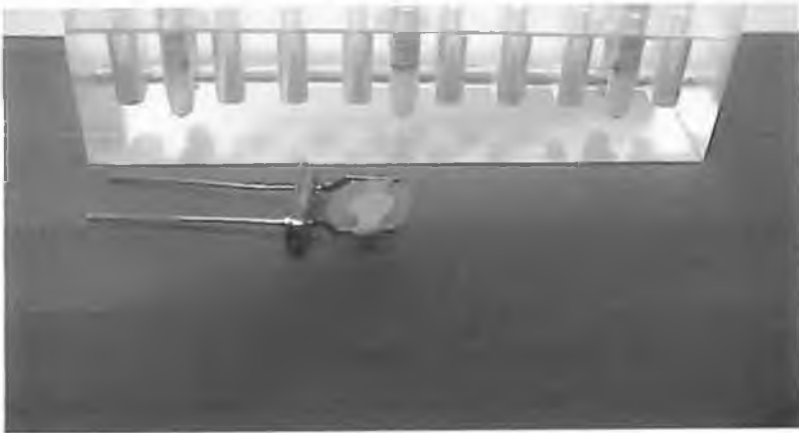
Figure 3-13: Photo of In-House Designed and Fabricated Array Chamber

Perspex Array Lid

O-Ring

QCM (BAW)

Perspex Array Chamber
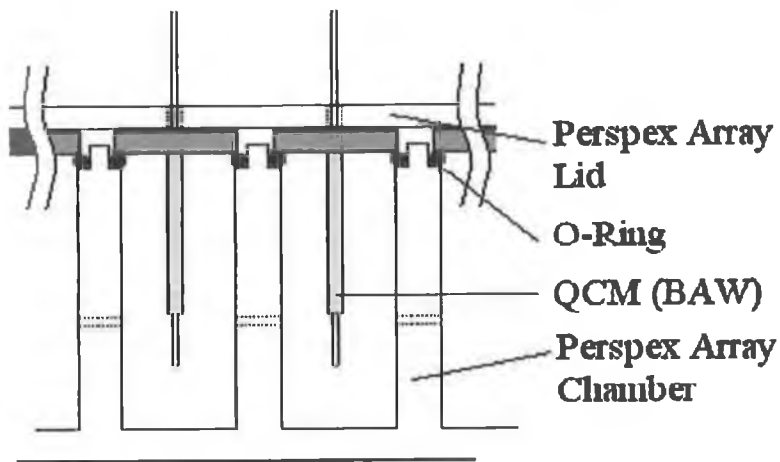
Figure 3-14: Schematic of fabricated array chamber

Vapour in

Vapour out
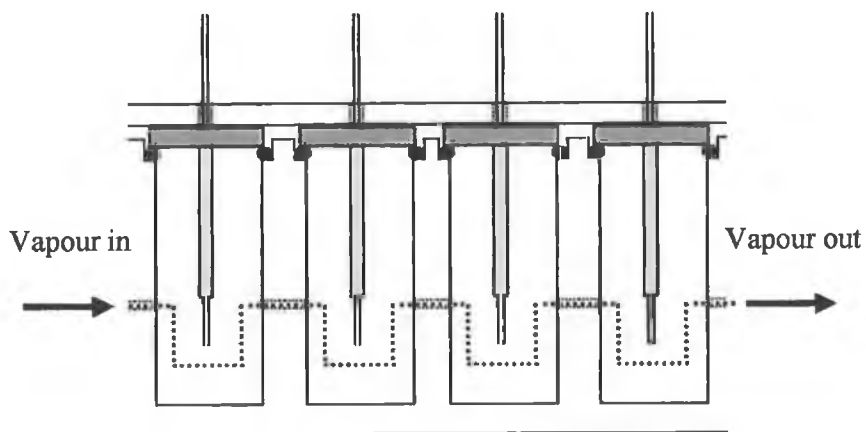
Figure 3-15: Schematic of sample vapour movement through array chamber

3.3.5 Sampling Vessels

The system was supplied with two attachments for sampling.

The first attachment allowed for the sampling of small sample volumes using 2ml polypropylene vials (Whatman Int. Ltd., UK). Up to 1ml of a sample is placed in the vial, which is then just simply screwed into the housing attachment (Figure 3-16).

The second attachment can be connected to a 200-500ml Duran® glass bottle for sampling the headspace over from larger liquid samples. This setup facilitates the bubbling of the headspace gas within the bottle through the sample liquid itself thereby saturating it. Should the influence of humidity be required to be removed then it can be passed through a "dryer" which is a Nafion® tube encapsulated in a gas tight box filled with molecular sieves of a desired size (4Å). However, the dryer constitutes a large dead volume in the system and lengthens sampling times, and its use must be carefully considered.

Figure 3-16: Photo of the Vial Headspace Sampling Attachment

3.3.6 Software

The software supplied controls all system operations such as pump on/off, switching valves, sensor monitoring, data acquisition, processing and presentation.

3.4 Sampling Method

There are two different types of sampling that can be carried out;

(i)   Batch Sampling (for determining sensor sensitivities)

(ii)   Dynamic Sampling (for comparing vapour headspaces)

3.4.1 Batch Sampling

The QTS instrument was modified to facilitate calibration for up to 4 sensors, in an airtight sampling chamber of fixed volume (Figure 3-17). The sampling chamber was a 3-necked round bottom flask, with the coated QCM sensors sealed within one of the necks, a septum for injection of analyte in the second, while the third neck was fitted with two 3-way valves to control the purging with nitrogen. Aliquots of volatile analytes, calculated to give various concentrations when vapourised within the flask upon magnetic stirring, were injected through the septum into the sampling chamber. The stabilised response of each sensor to each injection, considered to be $\pm 1Hz$ over 30s, was recorded (Figure 3-18). The system was then purged with N_2 for 2 min or until the sensor response returned to baseline before subsequent injections. All measurements were made in triplicate, for exposure to each vapour and recorded using a personal computer. The data was then exported to MS Excel where means and relative standard deviations were generated. This procedure allowed sensor calibrations and comparisons to be carried out.
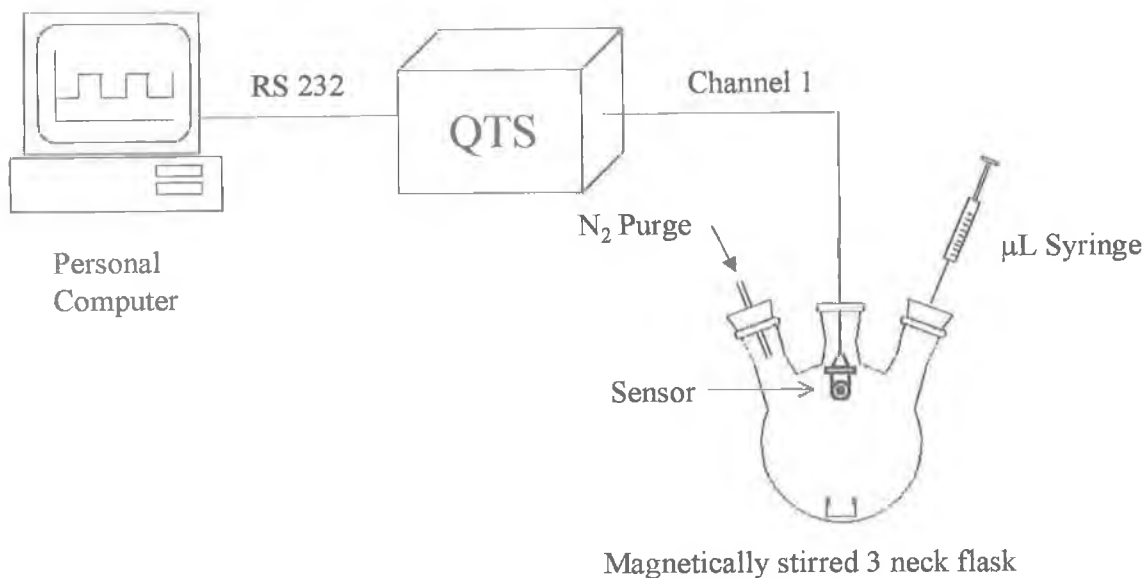
Figure 3-17: Schematic of Static Sensor Calibration
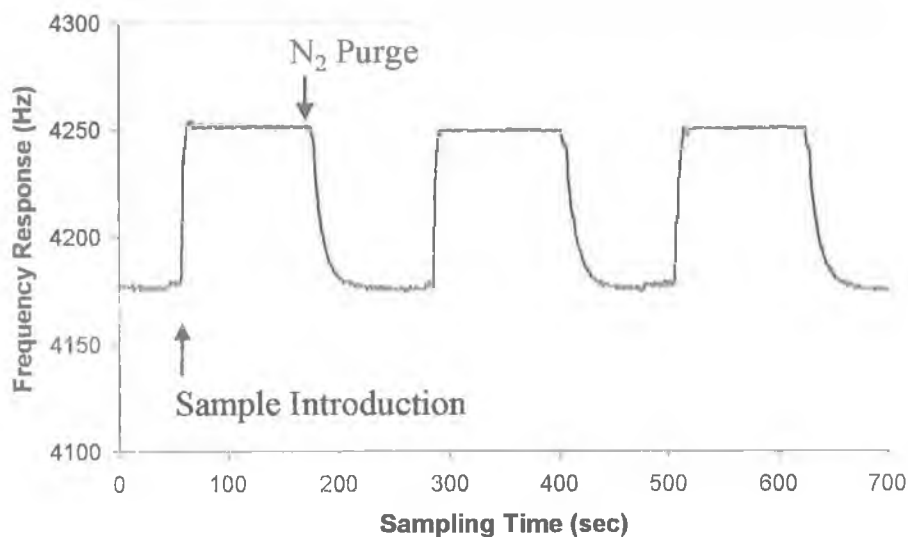
Figure 3-18: Frequency profile of OV17 on exposure to ethyl acetate (x3)

3.4.2 Dynamic Sampling

Dynamic sampling involves sampling vapour headspaces above liquid, or solid samples. The concentration of the sample in the headspace will be dependant on the volatility of the sample, or in the case or organic solvents, on their vapour pressures. There are three possible arrangements:

1. Ambient air is drawn through a charcoal filter over the sensor array (**Route A**).

2. The sample headspace is drawn over the sensors in a recycling loop (**Route B**).

3. Ambient air is drawn through the recycling loop with <u>no sample</u> attached
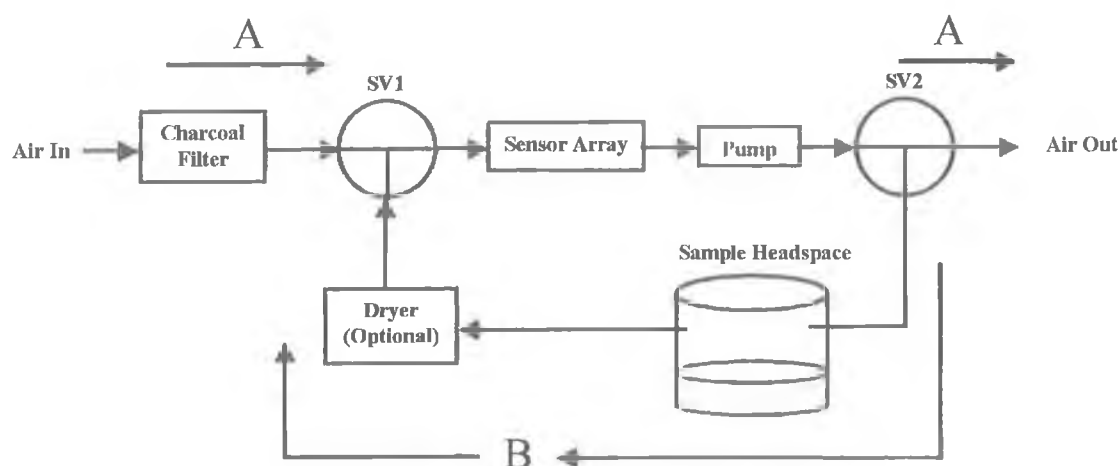
Figure 3-19: Schematic of experimental setup

A typical sampling process involves 5 steps, which are designed to ensure maximum reproducibility of the polymer coating-vapour interaction for each run. These 5 steps are (a) Pre-Condition, (b) Pre-Clean, (c) Sampling, (d) Clean-Sensors, and (e) Clean-Piping. A schematic of each is presented in Table 3-1. (a) and (b) are optional, but are found to improve response patterns. The position of the switching valves (Figure 3-19) is given in the square brackets ([ ]).

(a) Pre-Condition:

Pre-conditioning is where the crystals are exposed to the sample for a short period of time to allow the polymer to equilibrate. The precondition flushes the sample headspace thereby ensuring that there is a constant equilibration time for the sample headspace to settle every time. Without this there can be no kinetic comparisons of the data. The duration of the pre-condition is defaulted to half that of the sampling time. **[SV1, SV2 = (B)]**

(b) Pre-Clean:

Pre-cleaning is where the headspace over the crystals is flushed through with air drawn through an activated charcoal filter on line, on switching of SV1 & SV2 (Figure 3-19). This step is to remove any sample that has been absorbed by the sensors. The duration of the pre-clean is defaulted to half that of the Sampling time. **[SV1, SV2 = (A)]**

(c) Sampling:

Sampling then takes place when the SV1 & SV2 (Figure 3-19) have returned to their original position. **[SV1, SV2 = (B)]**

If the diffusion coefficient for the analyte within the polymer coating is high it is easier to get the sample in and also easy to get it out of the coating . Consequently if the coefficient is low it will be harder to get the sample to diffuse in and out. From a kinetic viewpoint the saturation time will also depend on the mass of the coating. An increase in crystal frequency on exposure can result from the polymer coating becoming less viscous, therefore becoming more rigid and therefore reducing the damping capability. The sampling time should be long enough to achieve equilibrium.

(d) Clean-Sensors:

This step is identical to the Pre-Clean cycle, except the time specified is independent of the sampling time, and should be long enough to allow for efficient regeneration of the sensors. **[SV1, SV2 = (A)]**

(e) Clean-Piping:

This step is identical to the sampling cycle with the exception that no sample vial is inserted into the housing, thereby allowing the system to flush air through the sampling loop. **[SV1, SV2 = (B)]**
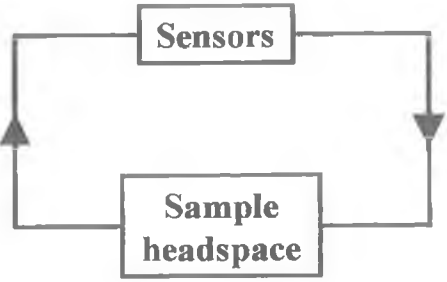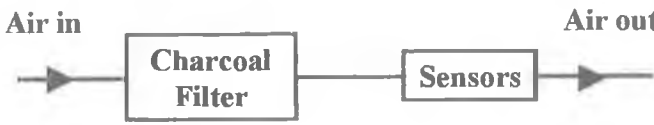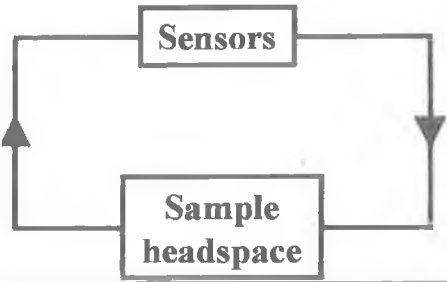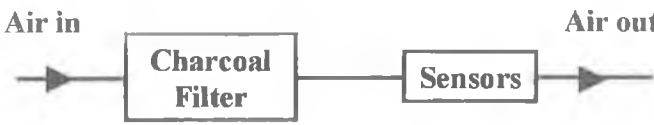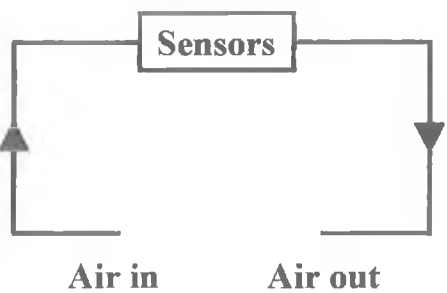
Schematic	Description
Sensors → **Sample headspace** (circulating loop)	**(A) Pre-Condition:** Sample headspace is circulating over the sensors to condition the sensors. **Typical Time Period:** 30 seconds
Air in → **Charcoal Filter** → **Sensors** → Air out	**(B) Pre-Clean:** Air is drawn through the filter over the sensors regenerating them. **Typical Time Period:** 30 seconds
Sensors → **Sample headspace** (circulating loop)	**(C) Sampling:** Sample headspace is circulating over the sensors. **Typical Time Period:** 60 seconds
Air in → **Charcoal Filter** → **Sensors** → Air out	**(D) Clean-Sensors:** Air is drawn through the filter over the sensors regenerating them. **Typical Time Period:** 50 seconds
Sensors (loop) Air in Air out	**(E) Clean-Piping:** Ambient air is drawn over the sensors, thereby cleaning the piping. **Typical Time Period:** 10 seconds

Table 3-1: Sampling schematic, description and respective time period.

3.4.3 Sampling Time

The sampling time is usually taken as the time taken for the sensors to reach
equilibrium with the sample vapours. For some samples this can be quite short (~15-
20 sec) while it can be much longer for others (~1-2 mins).
For this reason a nominal time of 45 or 60 seconds is sometimes taken, as a
compromise between these extremes. If a sample set includes 10 samples being
sampled 5 times for 60 seconds, and cleaning for 60 seconds, then the overall run
time will be 2 ½ hours [(30s + 30s + 60s + 60s) x 10 x 5]. Clearly this would be
doubled if a sampling time of two minutes was chosen, and could be unfeasible.

3.4.4 Typical Response Profile

A typical frequency profile is seen in Figure 3-20. This response represents the
difference between the coated QCM and the uncoated reference QCM. The
responses of each sensor to each solvent were then averaged and relative standard
deviations (%RSD's) generated. A selectivity factor, K, is then determined for each
solvent and represents the molar ratio of the response of each analyte relative to that
of the lowest response. This K then represents the relative interaction of different
samples to each sensor coating. The average responses are then plotted in the form
of frequency profiles, with RSD's as error bars, upon data export (Sec. 3.5.2).

72
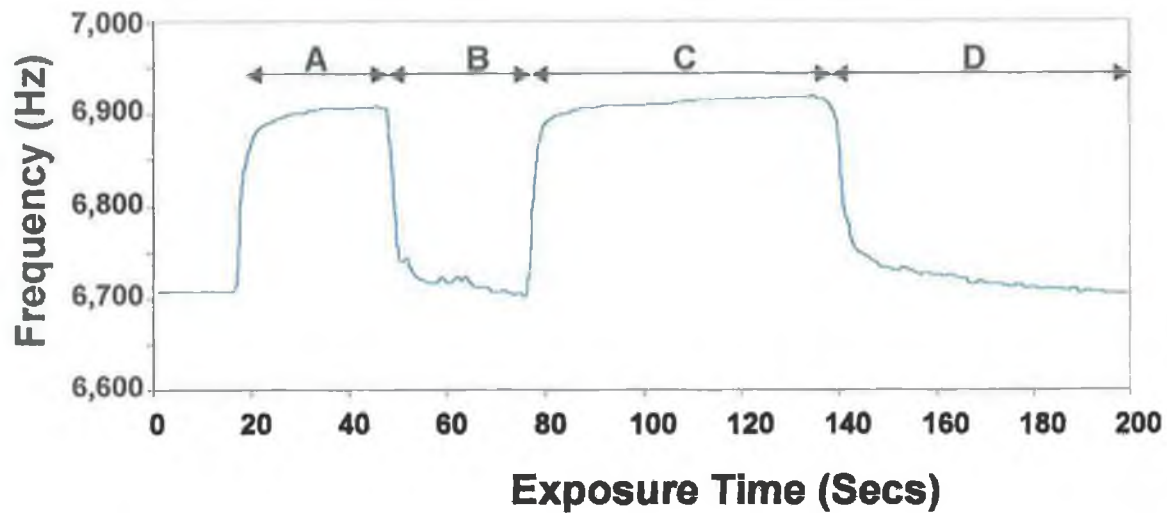
Figure 3-20: Typical frequency profile of a PEG coated sensor on exposure to Toluene, during sampling procedure (For an explanation of A-D see Table 3-1)

3.5 Data Acquisition

Through the QuartzTec software the sampling parameters are entered for the sampling process, such as sample names, number of sample, number of repeats, sampling time, cleaning time, whether or not to include the pre-sampling/pre-cleaning.

The sensors are then exposed to a range of sample vapours when prompted by the software. The software records the sampling frequency every second, and all data is stored in the form of a project file (*.prj). This file can then be opened using another supplied program, Filer.exe, and various options are then presented.

3.5.1 Analysis using Built-in Software

The filer.exe program on activation prompts the user for a project file to open. When chosen, the options for the project file are presented in Figure 3-21.

> ➢ View the raw data under **Measurements**
> ➢ View the sample names and markers under **Groups**
> ➢ View *saved* multivariate **Models**
> ➢ Generate **Reports**
> ➢ Insert **Comments**
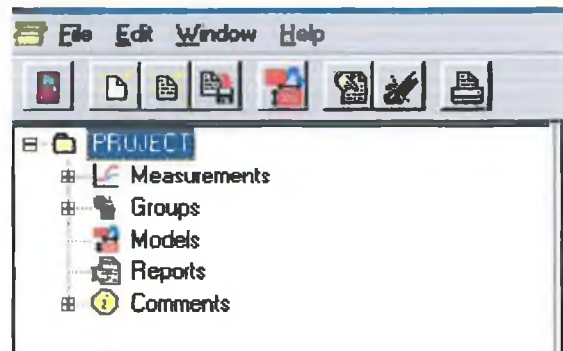
Figure 3-21: Filer Options for Project Files

To create a model, the model icon, , is selected and the Create/Edit Model window appears (Figure 3-22), and various options are presented in Table 2. When the relative steps have been followed, the end result is a 2-D plot (Figure 3-23), which graphically displays the classification result.

74
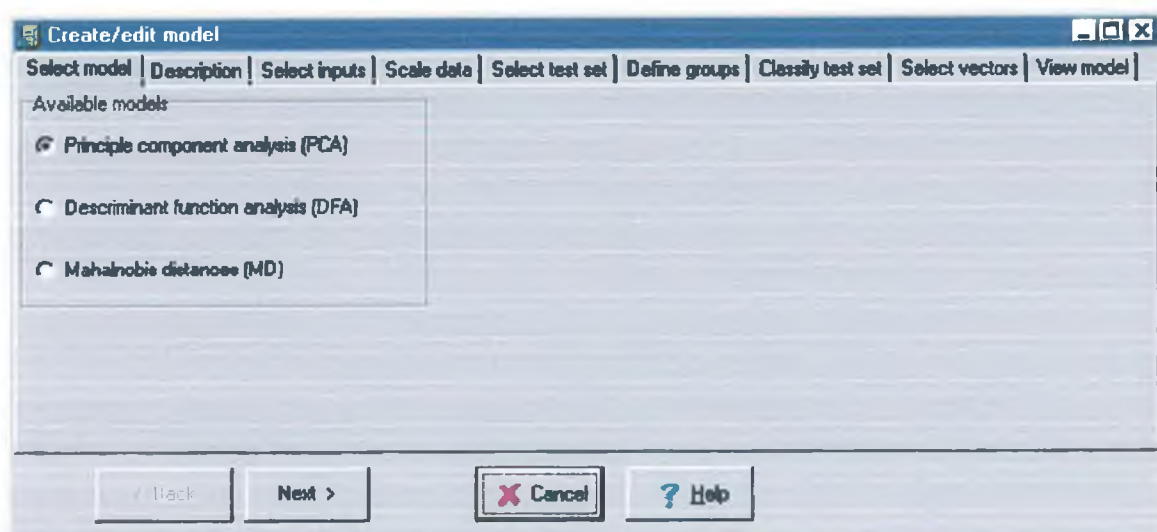
Figure 3-22: Create/Edit Model Window

Option	Explanation
Select model	Choose between PCA, DFA or MD (see Sec.3.6.3 for details)
Description	Choose a name to give to the model
Select Inputs	Select the time slice(s) to be used
Scale Data	Select a data scaling method for the frequencies, *e.g.* F, Δf *etc*.
Select Test Set	Select sample runs to be analysed
Define Groups	Confirm group names and markers
Classify Test Set	Confirm samples to be modelled
Select Vectors	View and choose the vectors generated using the model
View Model	View a 2-D plot of the chosen vectors (Figure 3-23)

Table 2: Create/Edit Model options with explanations
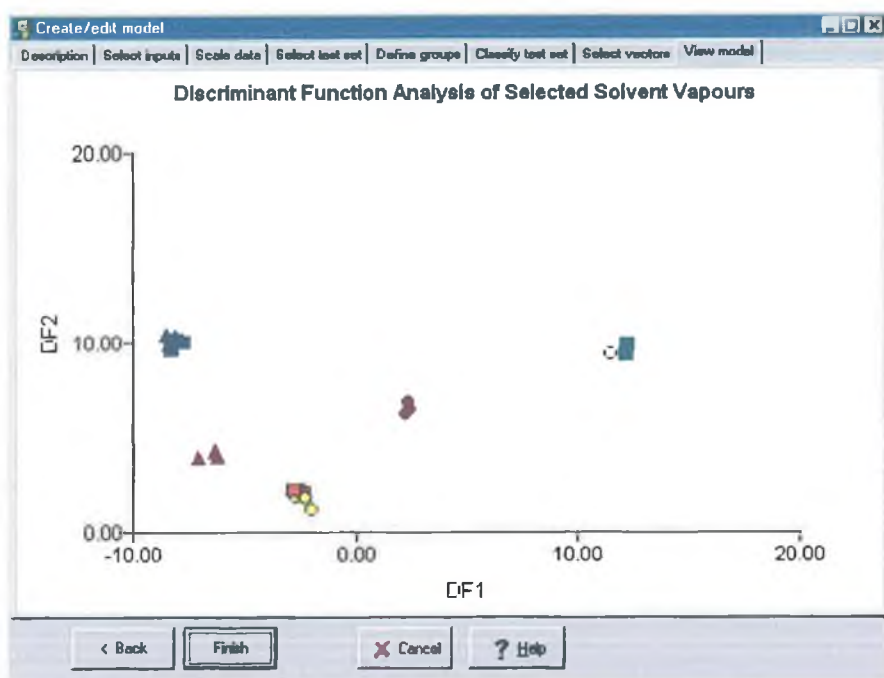
Figure 3-23: Graphical output of a DFA model with an unknown displayed as (O)

3.5.2 Data Export

The filer.exe program will process the data and present the data in the form of a 2-D plot, but it is rather limited in display options and raw data viewing. Therefore for a complete analysis of the results it is necessary to export the raw data to a spreadsheet package such as MS Excel®. To do this, the results are exporting in comma separated variable (*.csv) format. Data can be exported in its entirety for each sample or as a specific time slice for all samples. With some rearrangement and processing the mean and standard deviation for each sensor can be determined and easily presented in the form of a histogram or x-y scatter. Time slices are imported and saved in MS Excel, before they are exported to Minitab® where multivariate analysis can be carried out.

3.6 Data Interpretation

When data is obtained from the sensors and exported to MS Excel® it can be quickly evaluated by simply plotting frequency profiles, standard deviations, and histograms. Interpretation of this data is very important when considering the merits of each

sensor. A sensor that provides a high response is desirable, but the variability of the response must be small to be of any use. In other words sensors with small relative standard deviations (%RSD) are desirable. The response must also be sufficiently different from sample to sample, as blanket responses are of no use.

3.6.1 Evaluation

(A) Sampling Profiles and Histograms

Frequency profiles of sensor responses are the simplest and quickest way of presenting a complete picture of the properties of a sensor. Adding error bars to the profile then gives an indication of the repeatability of the measurement (Figure 3-24).
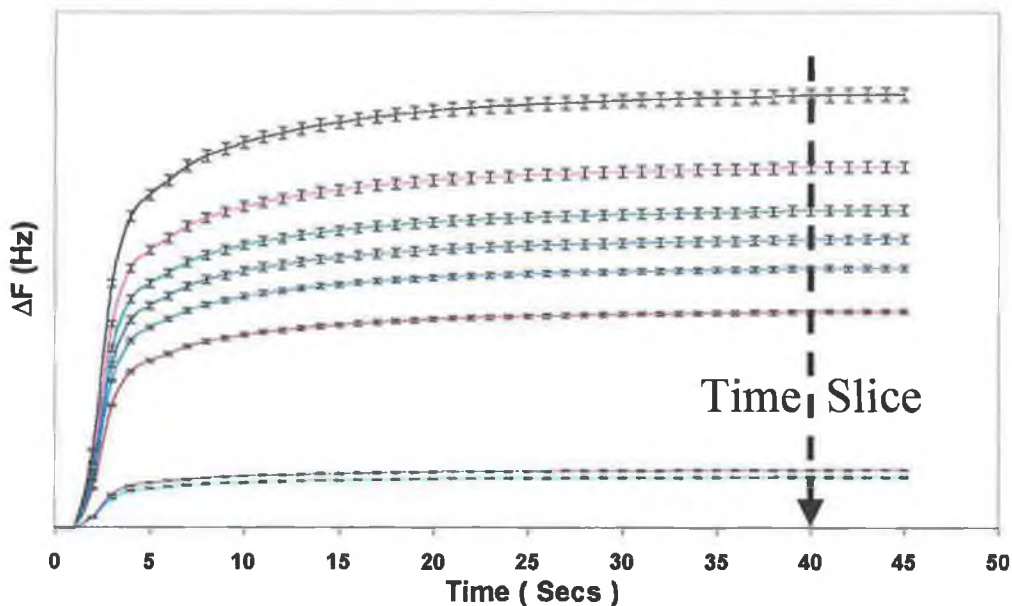
Figure 3-24: An idealised frequency response of eight sensors to an analyte with standard deviations as error bars (n = at least 3), with a "Time Slice" indicated

Taking a "Time Slice" of this profile somewhere in the equilibrium region, at a particular time, and presenting it as a histogram gives us an indication of the relative responses of each sensor (Figure 3-25).
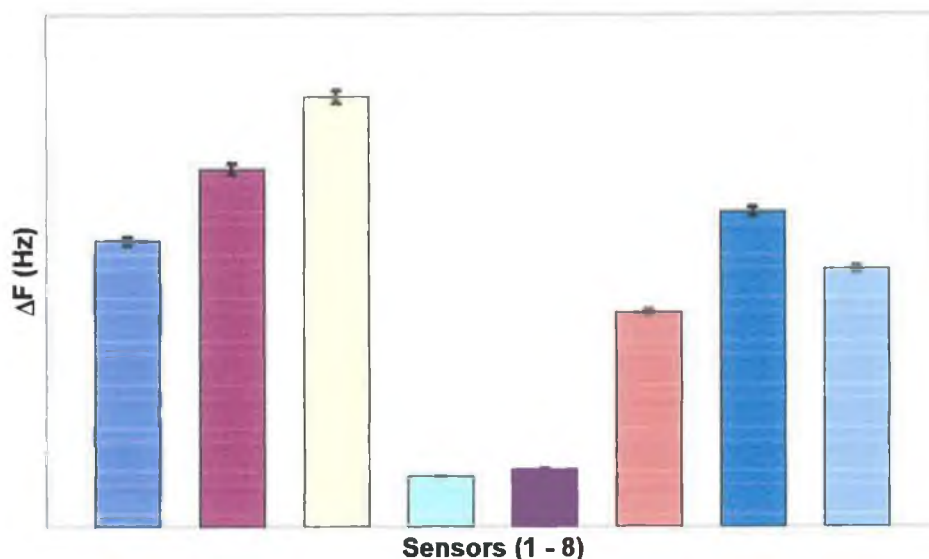
Figure 3-25: Ideal time slice histogram of eight sensors with standard deviations as error bars

This histogram can now be considered to be a fingerprint of the analyte to the particular array of sensors. Using such fingerprints classification techniques could identify this analyte from a compiled library.

(B)   Kinetic Modelling

The sorption of vapour molecules into the QCM coating has been described as a bulk interaction and sometimes QCM's are called bulk acoustic wave devices in recognition of this phenomenon. Bulk interactions are 2-stage; the species is firstly absorbed onto the surface before it then partitions between the vapour phase and the sensor. To determine the rates of the sorption stages, the response of a sensor can be modelled using some rather simplistic assumptions. Those being that the interactions are first order or pseudo first order. This means that the response can be assumed to be the sum of two exponential interactions;

$$\text{Response} = A_0 - A_1(-e^{-K_1 t}) - A_2(-e^{-K_2 t}) \qquad \textbf{Equation 3-1}$$

where K_1 is the rate constant for the absorption of the analyte, and K_2 is the rate of diffusion of the analyte into the coating, A_0 is the initial frequency of the QCM sensor. Such a model has been successfully employed previously [1], where it was

78

found that changes in the coating mass would increase the magnitude of the response but not its kinetic characteristics. The coatings concerned were GC stationary phases, which upon exposure to various vapours, were modelled with RSD's of less than 5%. For the system concerned in this thesis a dead time component has to be incorporated into the model and this usually takes the form of A_0 up until 3 seconds, whereupon the double exponential model (Equation 3-1) starts.

The modelling can be carried out in MS Excel® using Solver, a programme that uses iterative search algorithms, in order to minimise the total residual, or error, between the model and the real data. By creating a 2-series plot of the model and the data, a graphical indication displays the "goodness of fit" achieved (Figure 3-26).
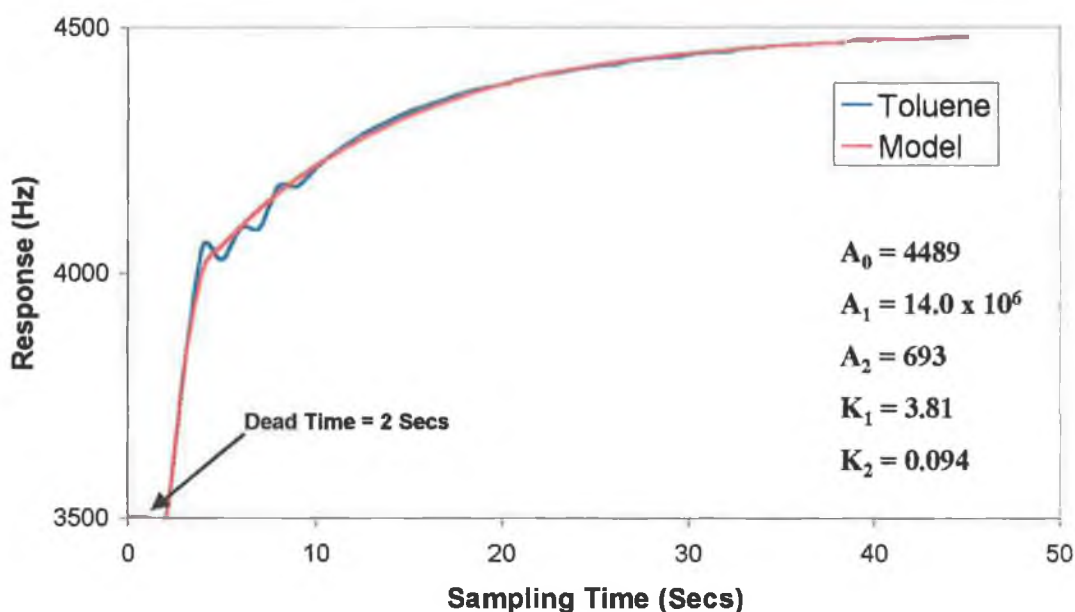
Figure 3-26: 2-Series plot of PIB coated sensor on exposure to Toluene (Blue) and subsequent model (Red)

If desired, residual plots can be generated, and r^2 values reported along with the sum of squared residuals to facilitate inter-comparison of "goodness of fit".

3.6.2 Molecular Modelling

To gain an insight into the interaction of molecules it is useful to create simulations using suitable modelling packages. The package used in this case was Chem 3D.

Supplied by as a component of ChemOffice, Chem 3D is a modelling package that uses MM2, MOPAC and Gaussian energy minimisation techniques to arrange molecules in their lowest estimated energy state. Using certain methods, such as the Austin Model 1 (AM1), this package can give an insight into the relevant distances and energies associated with various compounds. There are limitations with this package with respect to model size, parameter availability and computer resources so it can't be used on all compounds. For that reason when polymers are being modelled with vapours only a small component of the chain can be used. Obviously the interaction strengths will vary from real data, but the approximation is usually satisfactory for illustrative purposes.

The most common requirements of any method are: Single point energy calculations, geometry optimisations, and property calculations. Chem3D can calculate these efficiently. There are more specialised functions, such as conformational searches and molecular dynamics simulations, but these are beyond the scope of the work covered here.

3.6.3 Multivariate Analysis

Chemometrics has been agreed as being "how to get chemically relevant information out of measured chemical data, how to represent and display this information, and how to get such information into data" [2]. It has found great success in applications where pattern recognition, classification and discriminant analysis are required. When faced by large sets of data, multivariate techniques can quickly reduce and simplify the problem. However there is cause for prudence in applying such techniques, as bad data cannot be changed into good data. In other words if the sensors aren't working well, no amount of statistical analysis will change that.

There are two different situations that can arise, with samples in this work.

1. There is no information about the data obtained from the array. This means there is no '*a priori*' information for multivariate techniques to use. Therefore the techniques used will try to group the *present* objects based upon their intrinsic properties.

2. There is information about the data, obtained from the array. Using this information it can be possible to create rules that will allow for classification of *future* objects.

Taking this into consideration, Principal Components Analysis, Cluster Analysis, and Discriminant Function Analysis will now be discussed and their applications explained.

(A) Principal Components Analysis

Principal Components Analysis (PCA) is a method that is mainly used for data reduction as it can maintain the total variance within the data set while reducing the number of variables used. PCA is an unsupervised method that changes the original data set into a relatively smaller and simpler one that can still adequately give the same amount of information, by removing redundant variables. Of course some information is lost but the improvement in ease of use of the information compensates for this.

Suppose we have a spread of points in a two dimensional plane with the axes X and Y. Assuming that the origin for these axes is where the mean centre would be, it can be seen that the axes cover all the points. However using a different set of axes X' and Y' could reduce the density of the points per axis unit. These axes would still be orthogonal and would use the same origin (see Figure 3-27). Therefore the "spread" or variance of points would be increased.
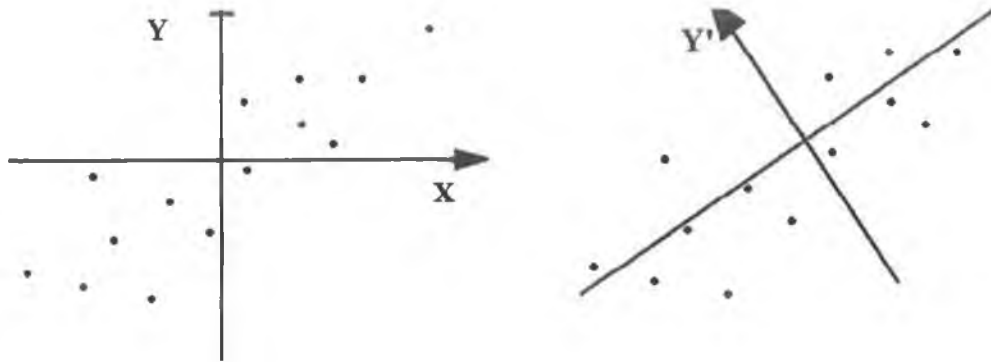
Figure 3-27: Rotation of orthogonal axes to align with greatest variance in data points

To reduce the number of descriptors or variables, data points must be transformed onto a new axis. To do this they are projected onto a new axis, whose orientation maximises the variance of the data. Figure 3-28 illustrates how a 2-D system can be reduced to a 1-D system by orthogonal projection of all data points onto the new axis, X'.
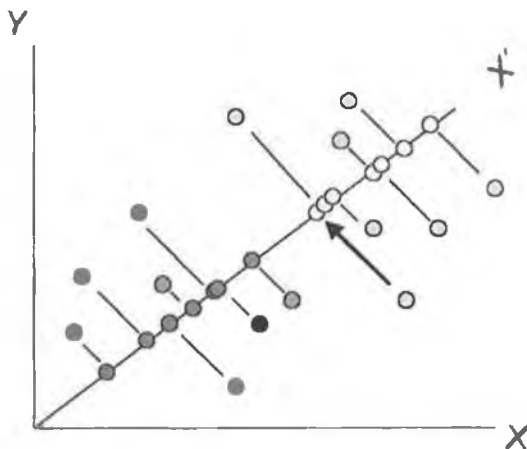
Figure 3-28: Data reduction from a 2-D system to a 1-D system

From the original data set the first principal component is calculated and this contains most of the information about the variance of the data set. The second principal component, being orthogonal to the first, then contains information on the remaining variances and so on for subsequent principal components. The original data matrix is product of a scores matrix and transpose of the corresponding loading matrix (Figure 3-29).

82

The general equation is

$$X = TL^T \qquad \text{Equation 3-2}$$

where X is the original data matrix with *n* rows (objects) and *p* columns (features), T is the scores matrix with *n* rows and *d* columns (Principal components) and L^T is the transpose of the loading matrix with *p* rows and *d* columns. By simply multiplying both sides by the *L* we get T on its own where the first set of principal components make up the first column and the second set of components make up the second column and so on. These components are graphically represented as PC1, PC2 *etc*.
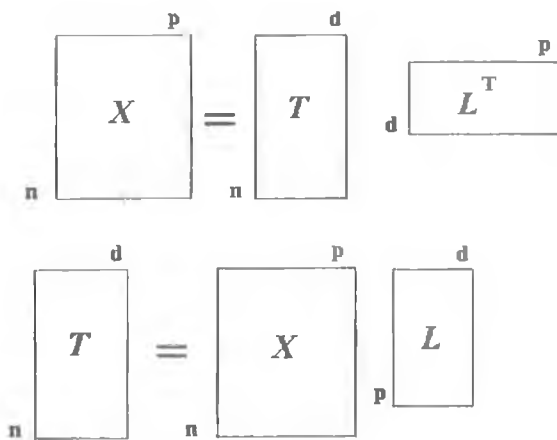
Figure 3-29: PCA explained though matrices

Essentially this method generates eigenvectors for our defined eigenvalues (sensors in this case). These eigenvectors then relate the amount of information that the eigenvalue contributes to the overall variance. Those with the greatest eigenvectors are therefore the most important.

(B)   Cluster Analysis

Cluster analysis is an "unsupervised" method, which groups objects together on the basis of the similarity of their common features. The method is unsupervised in that the experimenter may know how many groups there are but nothing else. The term cluster describes a group of objects that are more similar to each other than to objects outside the group [3]. There are two methods in which objects are clustered together, hierarchical and non-hierarchical. Hierarchical cluster analysis combines

objects according to their similarities, and there are two different techniques for this method, divisive and agglomerative. Divisive techniques split a whole set of objects into clusters, whereas agglomerative techniques start with one object and merges them into larger object groups. Non-hierarchical cluster analysis involves partitioning objects into different groups and their membership to that group is then tested. Their membership is then either confirmed or not, whereupon the object would then be repartitioned. The clustering process can be described diagrammatically in tree form, *i.e.* a *Dendrogram*. A dendrogram shows the points that are closest to each other, which is quoted by their percentage similarity or distance apart.

Figure 3-30 show how an initial four points (A, B, C, & D) are grouped together. Firstly the closest two points (A &B) are joined and they form a new point AB[*]. Then the closest pair of AB[*], C, & D are paired. In this case it would be C and D. These two points are joined and form a new point CD[*]. As AB[*] and CD[*] are the only points left they are joined. These successive joining operations or fusions are represented in the dendrogram, where the vertical component of the plot is the distance between the points joined.

There are various different dendrograms that can be generated from one set of data, and they are dependant on the method of determining distances (Distance Method) and the method of joining points (Linkage Method). An example of a distance method would be Euclidean, which is essentially the Theorem of Pythagoras in a 2-D problem. An example of a linkage method would be Average linking, where the result is the average of linking all points of one cluster to those of another.
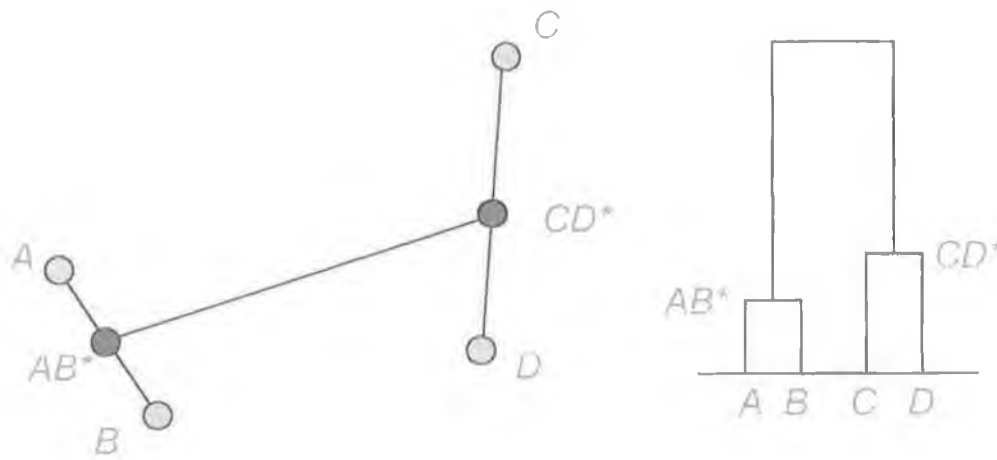
Figure 3-30: An example of agglomerative hierarchical cluster analysis and the resulting dendrogram

(C)   Discriminant Function Analysis (DFA)

For some types of analysis it might be necessary to distinguish between two different <u>known</u> populations. To this end it might be necessary to devise a rule or function that would allocate an object to a specific group. Such a function is known as a *Discriminant Function* and the type of analysis is known as *Discriminant Function Analysis (DFA)*. Therefore it is necessary to construct a *Classification Rule* which will allocate individuals to pre-assigned groups with the lowest error rate. Discriminant functions aim to maximise separation between groups of (<u>available</u>) individuals, while classification rules aim to minimise the misclassification rate over all possible (<u>future</u>) allocations. Probabilistic classification rules are based on the premise that a large number of individuals will in the future need to be classified, and hence the classification rule should be chosen in such a way to minimise the expected consequences of mistakes made in this series of allocations [4].

A brief simplified mathematical explanation s now given:

In Discriminant Function Analysis the *Standard Distance* gives a dimensionless measure of the separation between two groups (similar to *t*-statistic)

$$D = \frac{\left| \overline{X_1} - \overline{X_2} \right|}{s}$$

where $\overline{X}$ is the mean of groups 1 and 2, and s is the standard deviation

Any member of a group can be described using the following expression:

$$Y_i = \beta_0 + \beta_1 X_1 + \beta_2 X_1 .. + \beta_p X_p$$

And will have its own coefficients $\beta_0, \beta_1, \beta_2, \beta_3 .. \beta_p$.
Therefore each group will have a mean and standard deviation, implying that the standard distance will be dependant on the values of the coefficients $\beta_0, \beta_1, \beta_2, \beta_3 .. \beta_p$., *i.e.*

$$D(Z) = D(\beta_0, \beta_1, \beta_2, \beta_3 .. \beta_p)$$

And therefore the Multivariate Standard Distance, D_p, will be the greatest distance attainable between the two groups.

$$D_p = \max D(\beta_0, \beta_1, \beta_2, \beta_3 .. \beta_p)$$

The linear combination of coefficients for which the maximum D(Z) is achieved is called the Discriminant Function. Using this function it will be possible to create a classification rule that would assign unknowns to pre-determined groups.

In a visual sense this means that if one looks at the two groups of data in Figure 3-31 from the traditional orthogonal X view (green arrow), there is a region of overlap where group membership would be shared. The same would be true for the corresponding Y view. However if a view from an alternative angle is taken, X', then a clear separation is obtained. So essentially DFA aims to find the best angle to look at data so as to maximise the space between known groups.
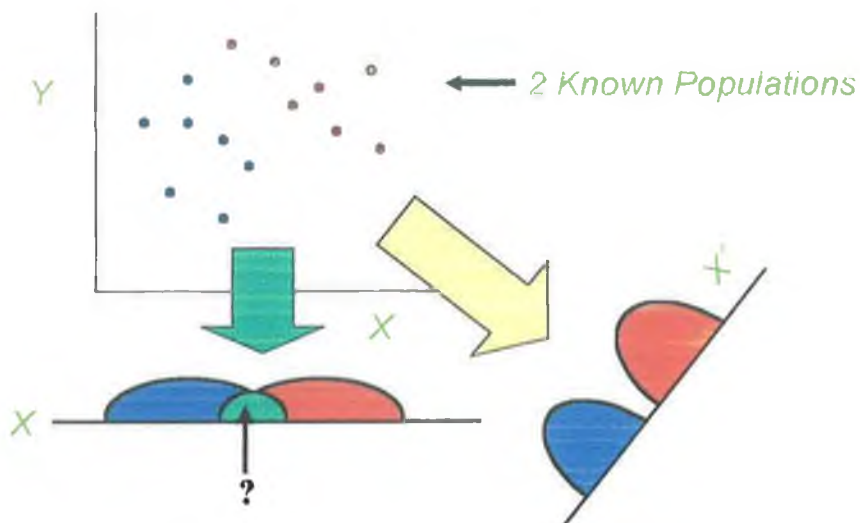
Figure 3-31: Visual interpretation of DFA

3.7 References

[1]   N.J. Freeman, I.P. May, D.J. Weir, Response kinetics of polymer-coated bulk acoustic wave devices on exposure to gases and vapours, J. Chem. Soc. Faraday Trans., **90(5)**, 1994, 751-754

2   S. Wold, M. Sjöström, Chemometrics, present and future success, *Chemometrics and Intelligent Laboratory Systems,* **44**, 1998, 3-14

3   Otto, M., Chemometrics: Statistical and Computer Application in Analytical Chemistry, *Wiley-VCH,* 1999

4   M.J. Krzanowski, Principles of Multivariate Analysis, *Oxford Statistical Science series, Clarendon Press, New York,* 1988

Chapter 4

4 Gas Chromatography Phases as BAW Coatings

4.1 Introduction

Gas Chromatography has been one of the most significantly developed tools in analytical chemistry in the latter half of the twentieth century. It represented a gigantic leap forward in the studies of complex mixtures of organic compounds and inorganic gases. Its most popular characteristics were quickly identified as being sensitivity, selectivity, accuracy, reliability and relative speed. The success of the technique is based on the wide range of stationary phases available, which can be tailored for specific needs and budgets. However the cost initial cost of purchasing a GC system can be expensive, often running into several thousands of euro. Bearing this in mind, techniques that make use of the range of GC coatings with lower operating costs are desirable.

BAW's coated with GC coatings have been investigated since 1964 [1] when King investigated their applications as GC detectors. By coating the crystals with a similar coating to that of the column, eluents could be detected by changes in the resonance frequency of the crystal. The initial choice of detector coatings was popular materials such as squalene, polyethylene glycol, silica gel and metal complexes such as lead acetate. Favourable results in comparison to thermal conductivity detectors, in terms of signal generated and consequently sensitivity were observed.

Since then several papers and comprehensive reviews were published [2,3,4] dealing with the use of stationary phases.

In this body of work the GC polymers studied were poly(isobutylene), poly(ethylene glycol), OV17, OV225, poly(epichlorohydrin), poly(vinylpropionate), tri-dodecyl amine (Not real GC).

4.2 Chemicals

The polymers to be used as coatings (PIB, PEG, OV17, OV225, PECH, PVP and TDDA) were all purchased from Sigma Aldrich and were used as received. Volatile

organic solvents (methanol, ethanol, isopropanol, ethyl acetate, toluene, hexane, cyclohexane, chloroform, dichloromethane) were all supplied by Labscan Ltd. (Dublin)

4.2.1   Choice of Volatile Organic Solvents

The solvents used for sensor evaluation (Table 4-1) were chosen due to their varying respective properties such as hydrophobicity, acidity, aromaticity *etc.* To quantify these properties, LSER data is presented in Table 4-2, along with respective vapour pressures, and consequent ambient gas phase concentrations.

Name	Description	(Non-)Specific	Classification
Cyclohexane	Hydrophobic	Non-specific	Alkane
Chloroform	Hydrophobic	Specific	Acid
Toluene	Hydrophobic	Specific	Aromatic
Ethyl acetate	Hydrophilic	Specific	Base
Propan-2-ol	Hydrophilic	Specific	Acid/Base
Ethanol	Hydrophilic	Specific	Acid/Base
Methanol	Hydrophilic	Specific	Acid/Base

Table 4-1: Description of VOC's used for sensor evaluation [5]

Solute	R	π^*	$\Sigma\alpha$	$\Sigma\beta$	$Log(L^{16})$	V.P. (KPa)	C_g (ppm)
Cyclohexane	0.305	0	0	0	2.964	13.0	441.6
Chloroform	0.425	0.49	0.15	0.02	2.48	26.2	1262.4
Toluene	0.601	0.52	0	0.14	3.325	3.79	140.9
Ethyl acetate	0.106	0.62	0	0.45	2.314	12.6	448.0
Propan-2-ol	0.212	0.36	0.33	0.56	1.764	6.02	146.0
Ethanol	0.246	0.42	0.37	0.48	1.485	7.87	127.3
Methanol	0.278	0.44	0.43	0.47	0.97	16.9	218.6

Table 4-2: Summary of solute parameters [6,7]

From the C_g data it is clear that chloroform has the highest gas phase concentration, and coupled with its range of LSER parameters would be expected to interact with most coatings.

Ethyl acetate can easily interact with most coatings, but is limited in its ability to donate hydrogen towards H-bonding ($\Sigma\alpha = 0$). A C_g value of over 400ppm indicates that ethyl acetate will strongly concentrated in the gas phase.

Cyclohexane would be expected to interact strongly with coatings through dispersion interactions, and weakly through polarisable forces. However it will be not able to interact in any H-bonding, and with a high C_g value it's interactions should be similar to that of ethyl acetate.

Toluene has similar properties to that of ethyl acetate, with the exception of higher polarisability. This is due to the aromatic nature of toluene, with its electron rich ring. However a low vapour pressure means that the concentration of toluene will be lower in the gas phase than ethyl acetate.

The alcohols are included to show the effects of increasing the size of the alkyl component of a homologous series. They can act as acids or bases, as recognised by their $\Sigma\alpha$ and $\Sigma\beta$ parameters.

4.3 PIB

Polyisobutylene (PIB) is an elastomeric amorphous polymer, and its chemical structure is given in Figure 4-1. Its structure is very similar to that of squalane (Figure 4-2), one of the first coating materials suggested by King [1] in 1964. As the repeating unit of PIB is completely made up of alkyl groups, it means that transient hydrophobic dispersion interactions are promoted. Although the relative strength of these interactions is small (<4 KJmol^{-1}) the summation of the forces over the entire polymer is quite large (Figure 4-3). Its interactions will be greatest with aliphatic compounds. LSER data provided in Table 4-3 indicate that PIB has some polarisability and hydrogen donating capabilities, but when these are compared to the relative strength of the dispersion coefficient, l, they represent only a fraction of the overall Log K value. As with all aliphatic hydrocarbon stationary phases, dispersion interactions have been found to increase directly in proportion to the molecular weight of solutes [8]. Owing to their inertness, such stationary phases have been very popular for studying all types of organic and inorganic compounds [8].
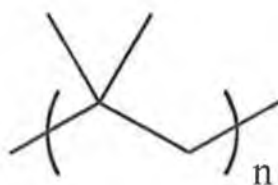
Figure 4-1: Chemical Structure of PIB

Figure 4-2: Chemical Structure of Squalane

Transient Dispersion Interactions
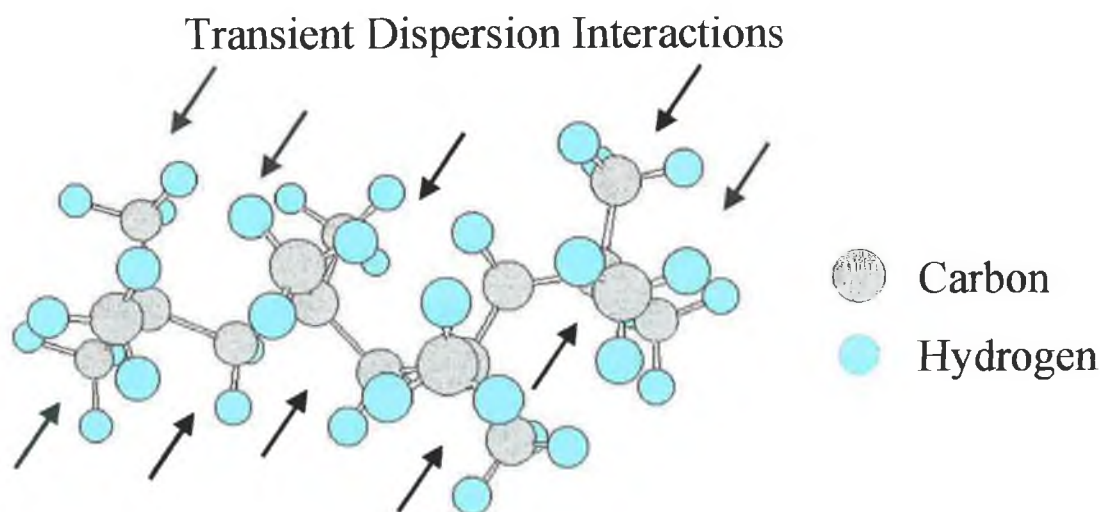
Figure 4-3: Indication of transient dispersion interactions throughout the PIB backbone

PIB	c	r	s	a	b	l
	-0.766	-0.077	0.366	0.180	0.000	1.016

Table 4-3: Table of Solute Coefficients for PIB [9]

4.3.1 Application Details

BAW's were spray coated with a PIB solution (0.1% W/V in hexane). The average coating was ~ 4,500Hz, varying from 3,500 to 6,500Hz. This frequency range corresponded to a mass change of $17 - 27\mu g$. The particular sensor used for solvent evaluation had a coating equivalent to a frequency change of 6,510Hz

4.3.2 SEM Analysis:

The sensor was monitored using SEM, as detailed in Chapter 3. The SEM image of the gold electrode of the PIB sensor (Figure 4-4) initially appears to be "patchy" over the surface. However it is consistent over the entire surface and merely represents where the initial droplet met the gold surface. To minimise the size of these patches a finer spray would be necessary, but this coating still gives a satisfactory response.

Figure 4-4: SEM of PIB-coated BAW (x35)

4.3.3 Solvent Evaluation:

The solvents were sampled as detailed in the previous chapter (Sec.3.4), for 45 seconds. The values are presented in Table 4-4 and Figure 4-5.

Solvents	Response (Hz) @45s	Selectivity Factor, K*	RSD
Cyclohexane (**C.Hex**)	3280	31.22	5.3%
Chloroform (**CHCl$_3$**)	2180	7.26	8.2%
Toluene (**Tol**)	1516	45.23	6.2%
Ethyl Acetate (**EtOAc**)	651	6.11	5.6%
Isopropyl Alcohol (**IPA**)	98	2.82	10.4%
Ethanol (**EtOH**)	74	2.44	6.8%
Methanol (**MeOH**)	52	1.00	9.7%

Table 4-4: Table of frequency responses, selectivity factors and RSD values for PIB-coated BAW.

(* - given as $K = \dfrac{S_i}{S_{min}}$, where S_i is the sensor sensitivity (Hz/ppm) to any vapour i, after 45s, and S_{min} is the lowest S_i attained by any vapour)
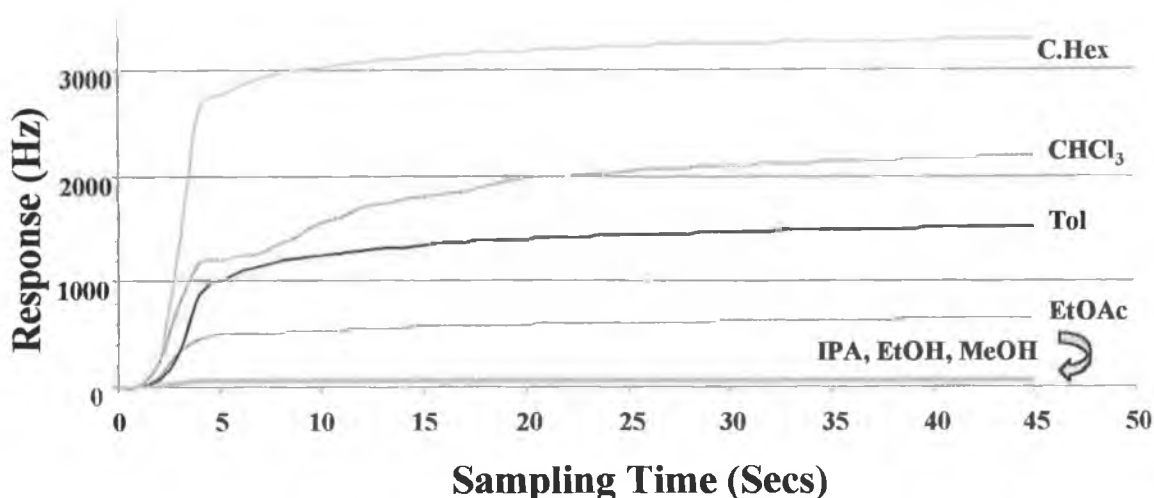
Figure 4-5: Frequency response of PIB-coated BAW to solvents

The response of PIB was greatest for the cyclohexane due to the fact that dispersion interactions are responsible for most of its total interactions. The solute coefficients are shown in Table 4-3 for PIB. Unfortunately there is no complete set of corresponding data for the other polymer coatings at hand.

As can be seen from Table 4-3 the response of solutes to PIB will be dominated by dispersion interactions. The sensor responds well to chloroform with its high L_{16} and π_2^* values, which contribute the greatest towards its Log K parameter. Toluene has also similar properties except that its vapour pressure is only 14% as high as chloroform (see Table 4-2). Ethyl acetate has the next greatest response, which has similar properties to that of chloroform but again has a lower vapour pressure. The alcohols then have the lowest responses as expected. Although propan-2-ol has the lowest vapour pressure it has the highest response due to its alkyl component, through which it interacts with PIB.

From a sensitivity point of view the values for K, in Table 4-4, indicate the order of sensitivity is **toluene > cyclohexane > chloroform > ethyl acetate > IPA > ethanol > methanol**. This implies that even though toluene is present in lower concentrations than most of the other vapours, it interacts very strongly with the coating.

4.4 PEG

Polyethylene glycol (PEG) is a very popular stationary phase and is supplied under the trade name Carbowax. This polymer has been used to detect alcohols, which can be both acidic and basic, through hydrogen-bond acidity via the OH group and hydrogen-bond basicity via the polymer backbone (Figure 4-6). The possible binding sites for these acidic and basic hydrogen bonds are indicated in Figure 4-7. The polymer is supplied in various molecular weights, such as 400, 1560, and 20K. PEG has been applied to the separation of 1°, 2°, and 3° amines, the separation of alcohols, ketones and aldehydes from hydrocarbons [8]. Essentially this stationary phase is used to investigate all compounds that can form hydrogen bonds.
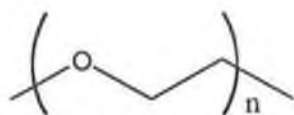
Figure 4-6: Chemical Structure of PEG
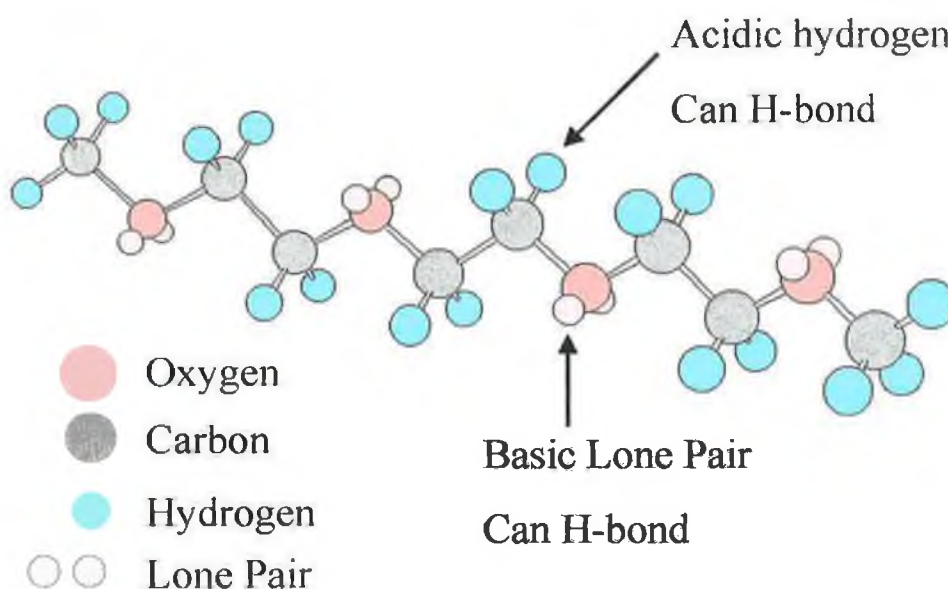
Figure 4-7: Possible H-bonding sites on PEG

4.4.1   Application Details

BAW's were spray coated with a 1540 PEG solution (0.1% W/V in Chloroform).
The average coating was ~ 6,000Hz, varying from 5,500 to 7,500Hz. This frequency
range corresponded to a mass change of $25 - 30\mu g$. The particular sensor used for
solvent evaluation had a coating equivalent to a frequency change of 7,500Hz

4.4.2   SEM Analysis

The sensor was monitored using SEM, as detailed in Chapter 3. At low
magnification (x35) it was difficult to see any coating material, and so a higher
magnification (x1,000) was used. At this new magnification the polymer could be
seen on the surface as black area (Figure 4-8), which indicated that the coating was
probably more uniformly distributed over the surface than PIB. Such coatings if
perfectly uniform over the entire surface would be 60 nm in thickness
approximately.
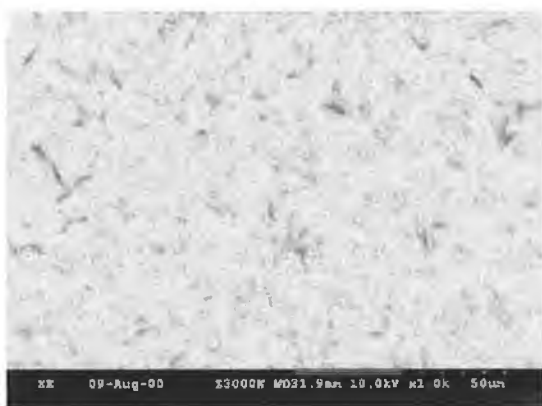
Figure 4-8: SEM of PEG-coated BAW (x1,000)

4.4.3   Sensor Evaluation

The solvents were sampled as detailed in the previous chapter (Sec.3.4), for 45
seconds. The values are presented in Table 4-5 and Figure 4-9. The frequency of
this sensor is close to the loading limit and ceased oscillating harmonically, on

exposure to the highly polar chloroform. This will be avoided in future by using lower coating levels.

Solvents	Response (Hz) @45s	Selectivity Factor, K	RSD
Ethanol **(EtOH)**	725	21.13	21%
Methanol **(MeOH)**	606	10.29	43%
Ethyl Acetate **(EtOAc)**	600	4.97	40%
Isopropyl Alcohol **(IPA)**	293	7.45	24%
Toluene **(Tol)**	230	6.06	28%
Cyclohexane **(C.Hex)**	119	1.00	25%

Table 4-5: Table of frequency response of PEG-coated BAW to solvents
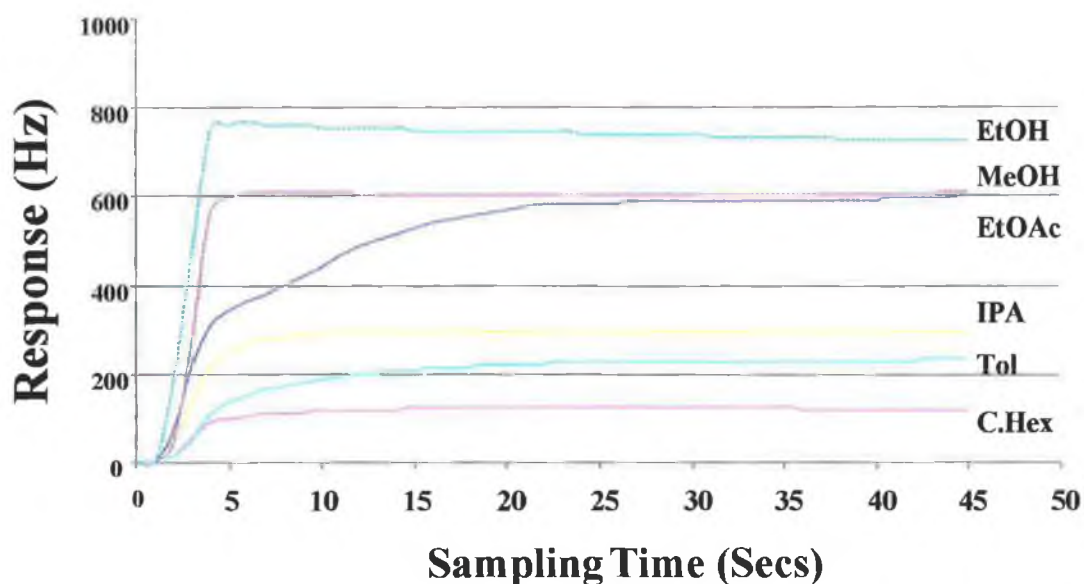
Figure 4-9: Frequency response of PEG-coated BAW to solvents (Overloading was seen on exposure to Chloroform).

The response of chloroform was seen to be the greatest and it overloaded the sensor. Chloroform being polar has a proton capable of strong hydrogen bonding, and has a α_2^H value of 0.2 that although lower than that of the alcohols, however it is very likely that the overloading was simply due to its high ambient concentration. Ethanol was seen to have the greatest response of the alcohols that can be attributed to its balance of hydrogen bond acidity and basicity. The response of ethyl acetate was lower than expected but a large RSD value (42.7%) indicates that the response is

97

quite variable. As expected cyclohexane and toluene have the lowest responses due to their α_2^H coefficients being equal to zero.

The sensor was observed as being most sensitive to ethanol (K = 21.1), followed by methanol (K = 10.3) and least sensitive to cyclohexane indicating the hydrophilic nature of the coating. The large RSD values are possibly due to memory effects as when the coating was subsequently exposed to ethanol ten times in succession, the RSD value dropped to less than 10%.

4.5   OV17

Poly(organosiloxanes) are the most popular and most used stationary phases in GC
[8]. They exhibit chemical inertness, good thermal behaviour, wide selectivities and
have the possibility of introducing substituents, of varying polarities, into the
polymer backbone. After poly(dimethylsiloxanes), phenyl containing polysiloxanes
are the most popular liquid stationary phases and enjoy high selectivity, due to
strong dispersion interactions and high polarisability capabilities of the phenyl
groups. The phenyl component of polysiloxanes increases the rigidity of the
polymer, and hence their thermal stability. The poly(phenylsiolxane) used in this
study is OV17 (Figure 4-10) and is made up of 50% phenyl substitution and 50%
methyl substitution. With these components OV17 maximises dipolar interactions
and enhances dipole/dipole and dipole/induced-dipole interactions through the
existence of a permanent dipole in the structure. The possible binding sites are
indicated in Figure 4-11. The presence of the phenyl group enhances the
polarisability of the polymer, and while the oxygen's will confer some basicity ($\Sigma\beta =$
0.16 [10]), it is small and comparable to benzene ($\Sigma\beta = 0.14$ [10]).

**Figure 4-10: Chemical structure of OV17**

Figure 4-11: Available binding sites of OV17

4.5.1 Application Details

BAW's were spray coated with an OV17 solution (0.1% W/V in Chloroform). The average coating was ~ 4,500Hz, which corresponded to a mass change of 22µg. The particular sensor used for solvent evaluation had a coating equivalent to a frequency change of 3,900Hz

4.5.2 SEM Analysis

The sensor was monitored using SEM, as detailed in Chapter 3. Similarly to PEG, the polymer coating was undetectable at magnification of x35(Figure 4-12(a)), and so a magnification of x500 was used to see the coating (Figure 4-12(b)). The coating can be seen as a series of spots on the surface (typically 1-10µm in size). As the surface is uneven below micrometre level, the coating solution settles into crevices on the surface.

(a)   (b)

Figure 4-12: SEM of OV17 coated BAW (a) x40 (b) x500

4.5.3   Sensor Evaluation

The solvents were sampled as detailed in the previous chapter (Sec.3.4), for 45 seconds. The values are presented in Table 4-6 and Figure 4-13.

Solvents	Response (Hz) @45s	Selectivity Factor, K	RSD
Chloroform $(CHCl_3)$	1419	2.56	2.0%
Cyclohexane **(C.Hex)**	588	3.03	2.1%
Toluene **(Tol)**	588	9.50	1.2%
Ethyl Acetate **(EtOAc)**	438	2.23	2.4%
Ethanol **(EtOH)**	105	1.88	2.4%
Isopropyl Alcohol **(IPA)**	99	1.54	5.0%
Methanol **(MeOH)**	96	1.00	6.8%

Table 4-6: Frequency response of OV17-coated BAW to solvents

101
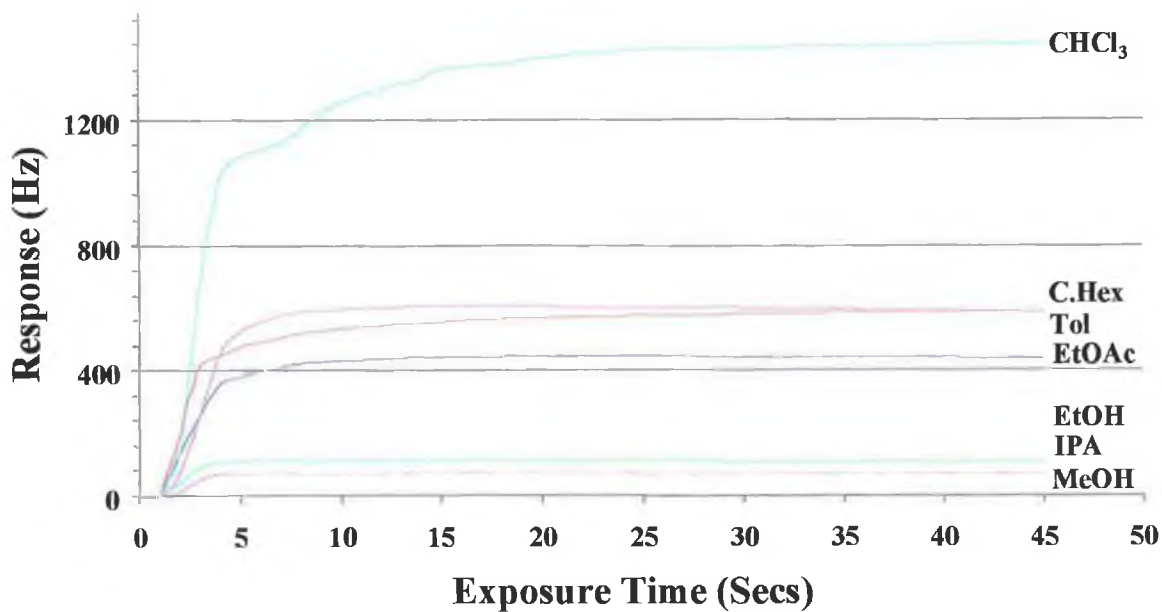
Figure 4-13: Frequency response of OV17-coated BAW to solvents

The highest response seen was for chloroform due to its polarity, π_2^*, value (0.58), and polarisability coefficient (0.425) and high vapour pressure. Cyclohexane also interacts strongly due to OV17 being 50% methyl substituted. Toluene interacts with the phenyl group of OV17 through π-π interactions and, as it has a high dispersion coefficient, will interact with the methyl substituents as well. However its low vapour pressure will mean its response will be lower than that of the more volatile cyclohexane. However from a sensitivity point of view the coating finds toluene more than 3 times more attractive than chloroform or cyclohexane.

4.6   OV225

OV225 (Figure 4-14) is an example of a cyanoalkylsilicone, one of the most important families of stationary phases, that combines high polarity and selectivity with reasonable thermal stability [8]. The cyano group attached to the siloxane backbone via two or three methylene groups is dipolar and strongly electron attracting, hence displaying dipole-dipole, dipole-induced dipole, and charge transfer interactions. Also the unshared electron pair may form intermolecular hydrogen bonds with suitable hydrogen donors, *e.g.* phenols, however this is weak due to the stability of a charged nitrile (*i.e.*, ⎯C≡N⎯).
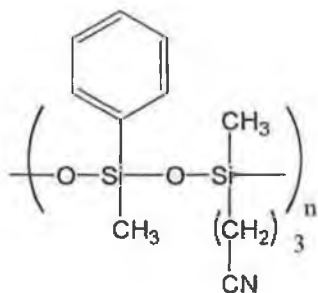
Figure 4-14:   Chemical structure of OV225
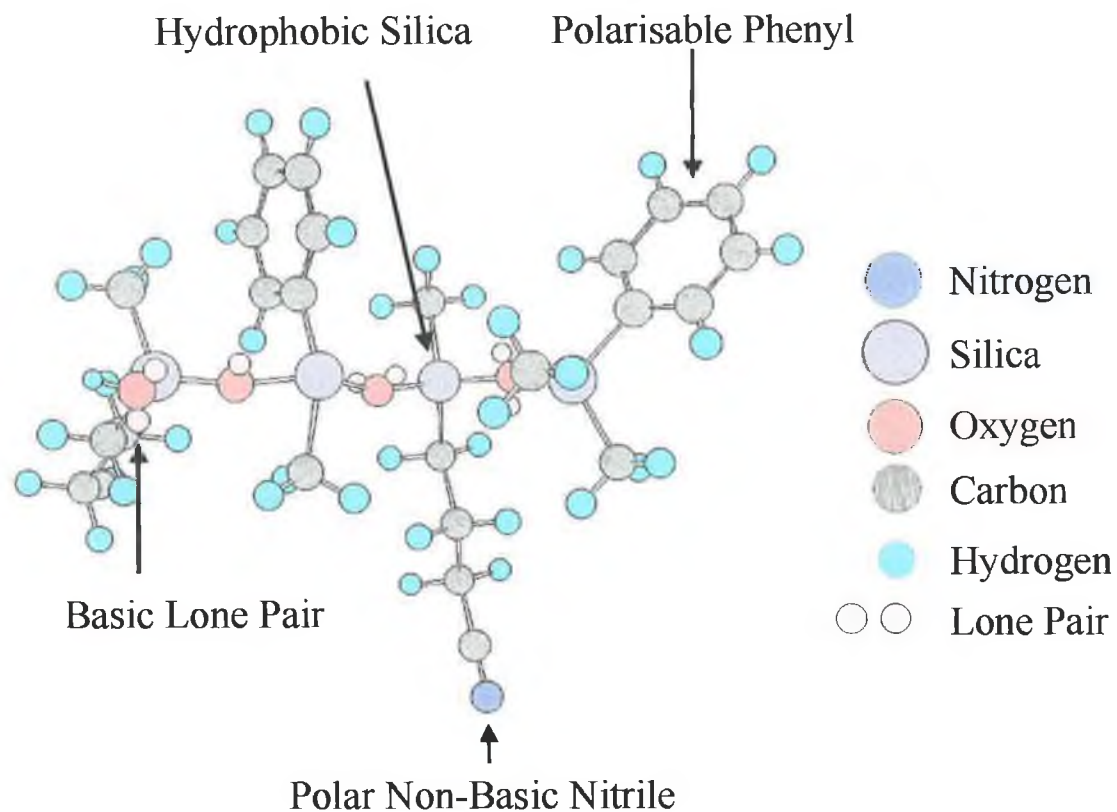
Figure 4-15: Possible binding sites on OV225

Patte et al [11] developed a hybrid LSER for OV17, OV225 and some other polymers. Although this LSER varies from that in that in Chapter 2, the coefficients are still a comparable reflection of the coatings chemical properties. Using this hybrid LSER all interactions are quoted relative to the individual coatings dispersion capabilities, as seen in Table 4-7.

	Dispersion	Dipolarity	Polarisability	H-Bond Acidity	H-Bond Basicity
OV17	211	230	267	135	160
OV225	211	333	316	230	285

Table 4-7: Solute factors for OV17 and OV225 (Taken from Patte et al [11])

Clearly the diffusion parameters of OV225 are more dependant on polar, polarisable, and hydrogen bonding than OV17. This implies that the dispersion component of OV225 will be lower than that of OV17, if the other forces are equivalent.

104

4.6.1 Application Details:

BAW's were spray coated with an OV225 solution (0.1% W/V in Chloroform). The average coating was ~ 4,000Hz, which corresponded to a mass change of 20μg. The particular sensor used for solvent evaluation had a coating equivalent to a frequency change of 3,900Hz

4.6.2 SEM Analysis

The nature of the OV225 coating is very similar to OV17, as would be expected due to their similar chemistries.

Figure 4-16: OV225 coated BAW (x400)

4.6.3 Sensor Evaluation

The solvents were sampled as detailed in the previous chapter (Sec.3.4), for 45 seconds. The values are presented in Figure 4-17 and Table 4-8. Clearly the response of OV225 and OV17 are very similar, considering almost identical loading masses, but OV225 interacts better with the polar solvents. This is displayed in Figure 4-18. As expected from the hybrid LSER data, the relative response of OV225 to cyclohexane purely based upon its dispersion interactions is less than

105

OV17. The properties of OV17 and OV225 are very similar, despite the fact that the solute factors for OV225 are higher (Table 4-7) due to the presence of the cyano group. A simple plot of the responses of the organic solvents against each other represents this similarity (Figure 4-18). The presence of the polar cyanopropyl group in OV225 reduces the interaction of cyclohexane considerably compared to OV17. Should only the polar solvents be considered the correlation coefficient between the two phases reaches 0.995. As seen with OV17 this polysiloxane sensor is most sensitive to toluene, being three times more sensitive than the closest, chloroform.
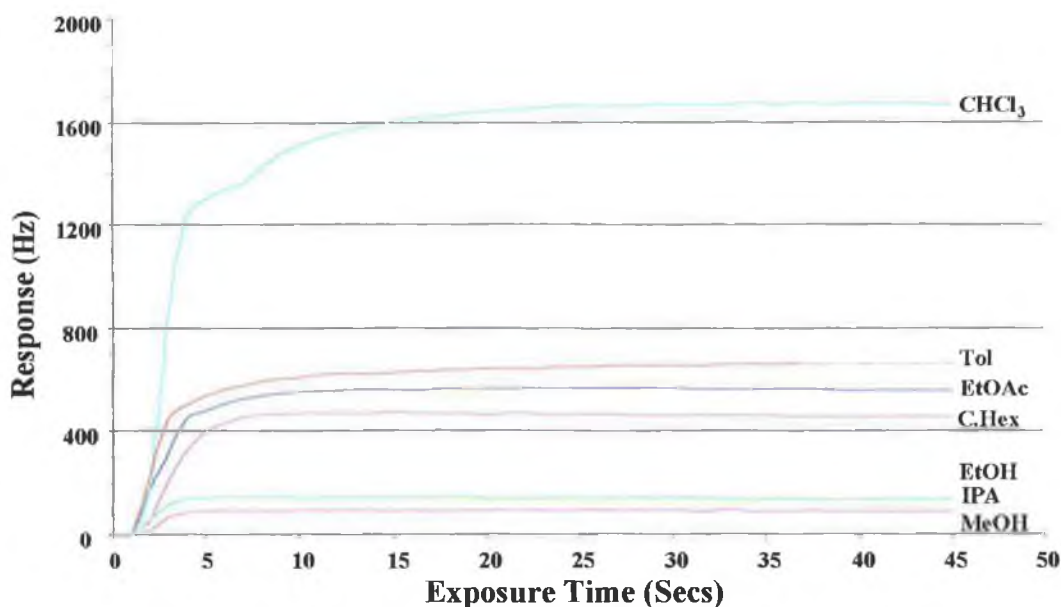
Figure 4-17: Response of OV225-coated BAW to solvents

Solvents	Response (Hz) @45s	Selectivity Factor, K	RSD
Chloroform (**CHCl₃**)	1646	3.28	2.5%
Toluene (**Tol**)	657	11.72	2.0%
Ethyl Acetate (**EtOAc**)	556	3.12	2.7%
Cyclohexane (**C.Hex**)	447	2.54	6.7%
Ethanol (**EtOH**)	129	2.55	4.6%
Isopropyl Alcohol (**IPA**)	123	2.12	11.0%
Methanol (**MeOH**)	87	1.00	5.0%

Table 4-8: Table of frequency response of OV225-coated BAW to solvents
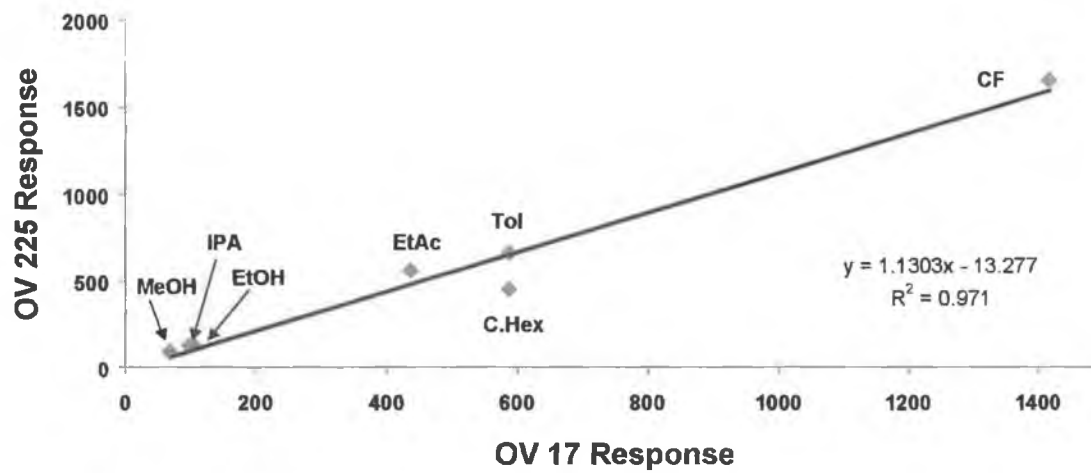
Figure 4-18: Comparison of responses of OV17 and OV225

The chart shows data points labelled MeOH, IPA, EtOH, EtAc, Tol, C.Hex, and CF, with axes "OV 225 Response" (vertical) and "OV 17 Response" (horizontal). The trendline equation is:

$$y = 1.1303x - 13.277$$
$$R^2 = 0.971$$

4.7 PECH

Polyepichlorohydrin (PECH) (Figure 4-19) is an amorphous polymer that promotes dispersion interactions through the methylene groups, as well as dipolar interactions through the chlorine atoms (Figure 4-20). The strength of this dipolarity is seen in Table 4-9, along with its ability to donate electron density to form hydrogen bonds. This polymer has been used for the detection of aromatic vapours and chlorinated hydrocarbons [12].
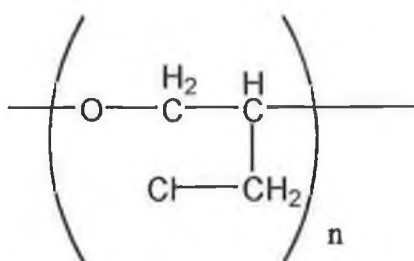
Figure 4-19: Chemical structure of PECH
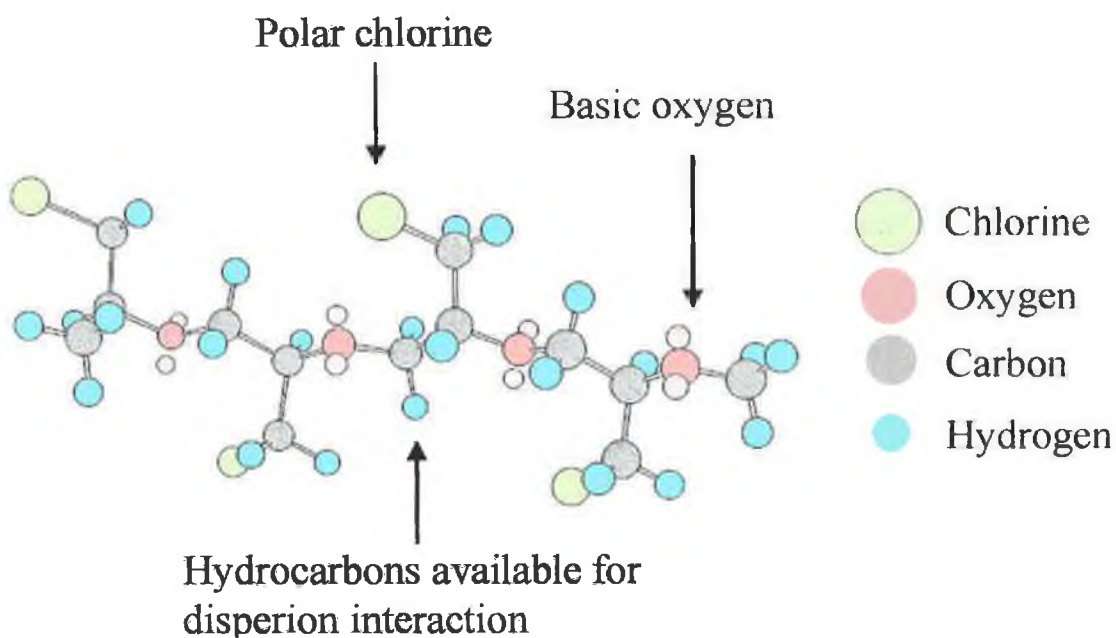
Figure 4-20: Possible binding sites on PECH

PECH	c	r	s	a	b	l
	-0.749	0.096	1.628	1.450	0.707	0.831

Table 4-9: Table of Solute Coefficients for PECH [9]

4.7.1 Application Details:

BAW's were spray coated with a PECH solution as detailed in Chapter 2. The average coating was ~ 4,500Hz, corresponding to a mass change of 20µg. The response displayed in Figure 4-21 is for a coating of 2,650Hz.

4.7.2 Sensor Evaluation

The solvents were sampled as detailed in the previous chapter (Sec.3.4), for 45 seconds.
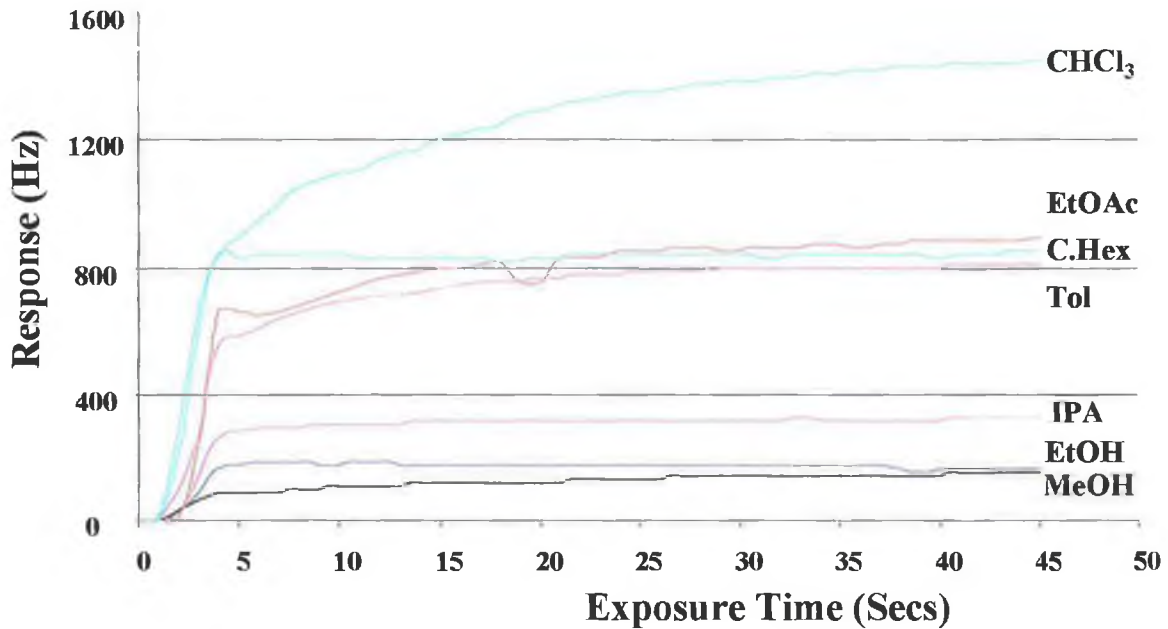
Figure 4-21: Response of PECH-coated BAW to solvents

Solvents	Response (Hz) @45s	Selectivity Factor, K	RSD
Chloroform (CHCl$_3$)	1447	1.68	4.7%
Ethyl Acetate (EtOAc)	890	2.91	8.7%
Cyclohexane (C.Hex)	844	2.80	3.7%
Toluene (Tol)	804	8.37	3.6%
Isopropyl Alcohol (IPA)	320	3.22	1.5%
Ethanol (EtOH)	159	1.83	9.4%
Methanol (MeOH)	149	1.00	13.5%

Table 4-10: Table of frequency response of PECH-coated BAW to solvents

From Table 4-9, it is seen that PECH will absorb polar compounds that can hydrogen-bond (both basic and acidic). It is therefore no surprise that the highest response seen was for chloroform due to its polarity and volatility. Ethyl acetate being a hydrophobic polar solvent, capable of basic hydrogen bonding, finds PECH a very attractive medium. Cyclohexane also interacts strongly due to PECH having an alkyl component within the repeating unit. Toluene is also strongly attracted to the polymer due to polarisability factors. However its low vapour pressure (3.79 KPa) will mean its response will be lower than that of the more volatile cyclohexane (13 KPa). Although the alcohols have the lowest responses, PECH is more sensitive to IPA than any other vapour, with the exception of toluene, due to its polarity and hydrogen bonding ability.

The %RSD values obtained indicate this polymer would be a good coating material for a sensor within an array.

4.8 PVP

Poly(vinyl propionate) (PVP) is a polarisable polymer that promotes hydrogen-bond basicity via the oxygen's in the ester groups along its hydrophobic backbone.

Figure 4-22: Chemical structure of PVP

Figure 4-23: Possible binding sites for PVP

4.8.1 Application Details

BAW's were spray coated with a PVP solution as detailed in Chapter 2. The average coating was ~ 4,400Hz, corresponding to a mass change of 19μg. The response displayed in Figure 4-24 and Table 4-11 is for a coating of 3,300Hz.

4.8.2 Sensor Evaluation

The solvents were sampled as detailed in the previous chapter (Sec.3.4), for 45 seconds.
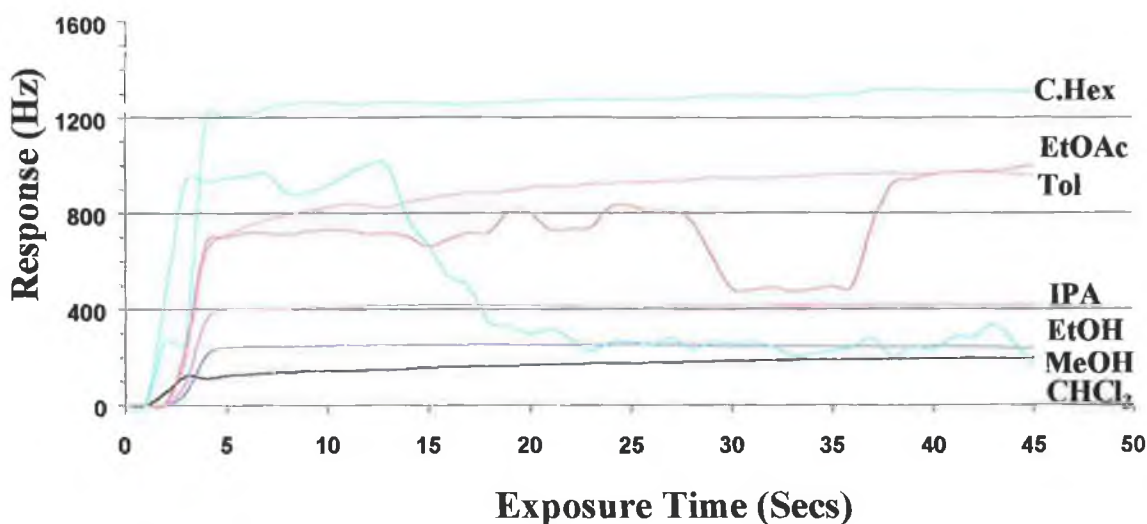
Figure 4-24: Single response of PVP-coated BAW to solvents

Solvents	Response (Hz) @45s	Selectivity Factor, K	RSD
Cyclohexane (**C.Hex**)	1032	2.50	24.9%
Ethyl Acetate (**EtOAc**)	522	1.25	78.9%
Toluene (**Tol**)	461	3.51	92.8%
Isopropyl Alcohol (**IPA**)	345	2.53	32.3%
Methanol (**MeOH**)	204	1.00	4.9%
Ethanol (**EtOH**)	194	1.63	36.6%
Chloroform (**CHCl₃**)	240$^{\#}$		50.6%

$^{\#}$ = response became noisy after 8 seconds

Table 4-11: Table of frequency response of PVP-coated BAW to solvents

112

PVP is a hydrophobic polymer that has an ester group within the repeating unit and is therefore polarisable and incapable of acidic hydrogen bonding. The highly volatile chloroform found the polarisable nature of PVP very attractive and possibly overloaded the sensor. Cyclohexane being totally hydrophobic found this sensor very attractive, as did the polarisable base, ethyl acetate. However the coating was more selective towards the polarisable toluene. Although the hydrophilic alcohols had the lowest response, PVP was more selective to IPA than cyclohexane, indicating its high hydrogen bonding capabilities. The sensor was seen to have large %RSD values, which may suggest that the polymer may have a limited lifetime. The sensor suffered some stability problems with the polarisable ester ethyl acetate. The stability problem could be due to the strength of the interactions between these highly compatible compounds.

4.9 TDDA

Tris(dodecyl amine) (TDDA) is a hydrophobic hydrocarbon (Figure 4-25). At its centre is the basic nitrogen, but is closed surrounded by 3 long alkyl chains.

$$\left(\!\!\begin{array}{c} CH_3 \\ | \\ CH_2 \end{array}\!\!\right)_{11}$$

$$N-\left(\!\!\begin{array}{c} H_2 \\ | \\ C \end{array}\!\!\right)_{11}-CH_3$$

$$\left(\!\!\begin{array}{c} CH_2 \\ | \\ CH_3 \end{array}\!\!\right)_{11}$$
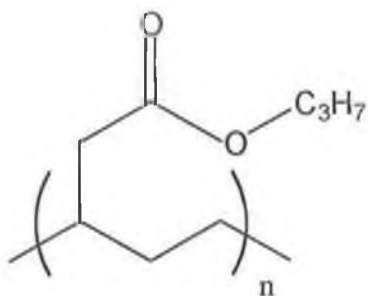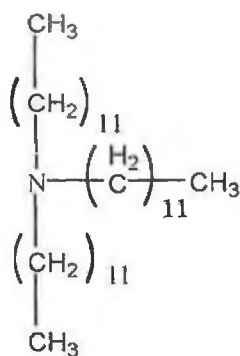
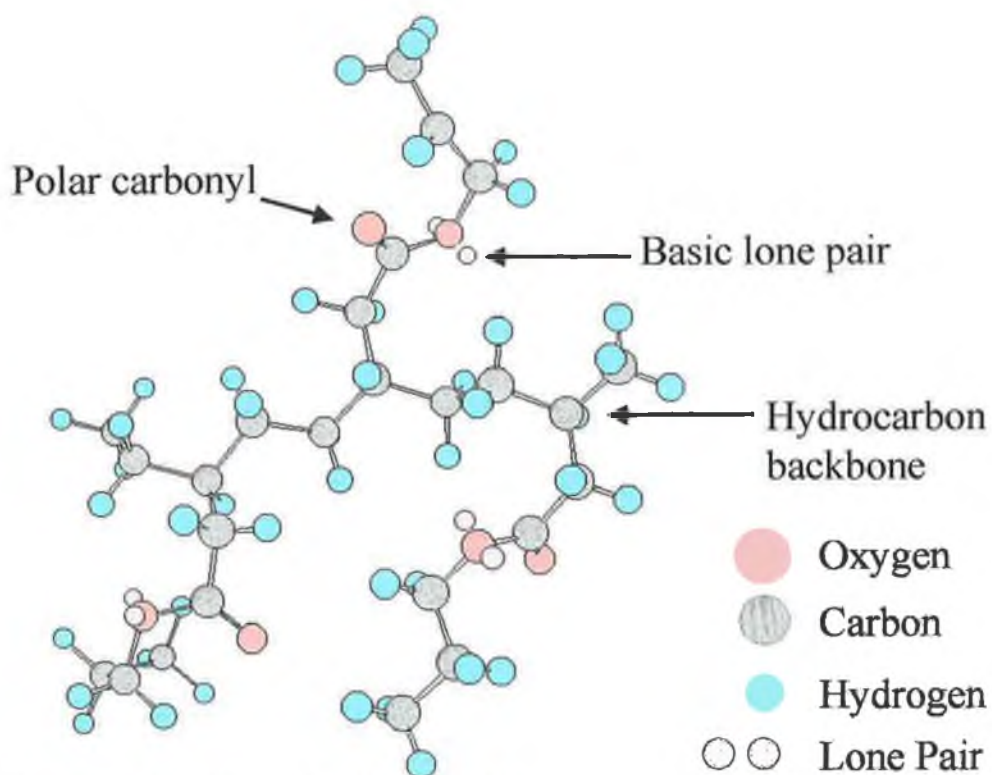**Figure 4-25: Chemical structure of TDDA**
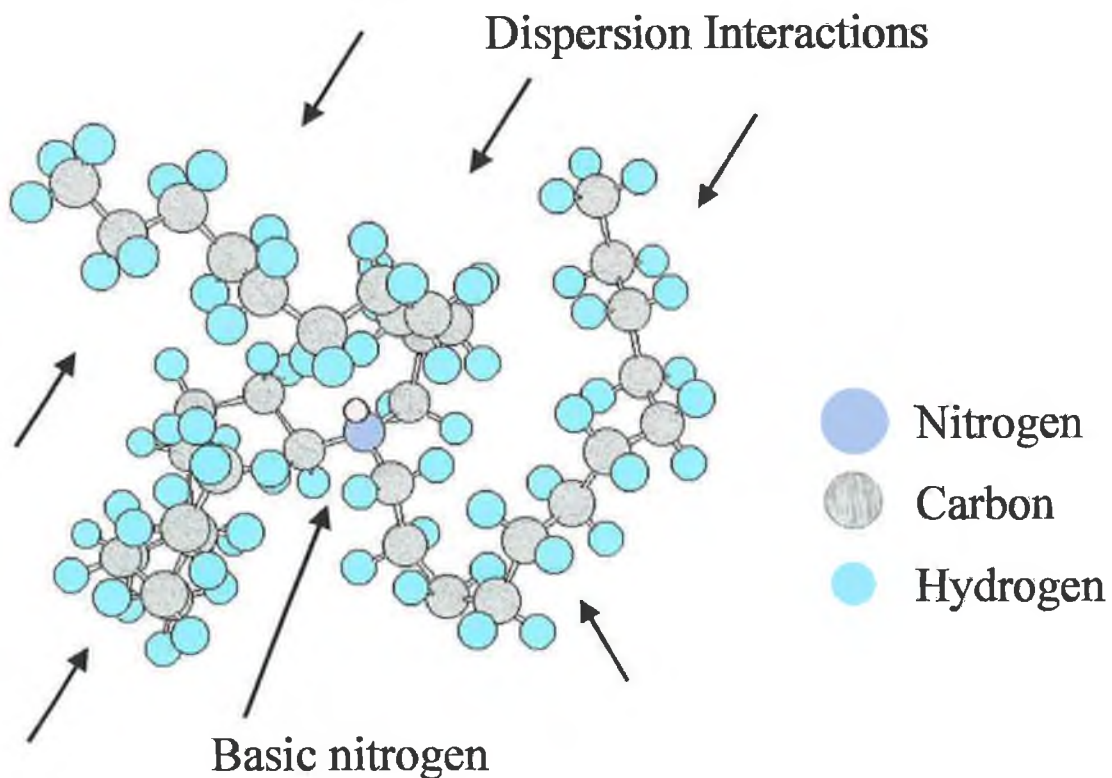
Figure 4-26: Possible binding sites for TDDA

4.9.1 Application details

BAW's were spray coated with a TDDA solution as detailed in Chapter 2. The average coating was ~ 3,700Hz, corresponding to a mass change of 19µg. The response displayed in Figure 4-24 and Table 4-11 is for a coating of 3,250Hz

4.9.2 Sensor Evaluation

The solvents were sampled as detailed in the previous chapter (Sec.3.4), for 45 seconds
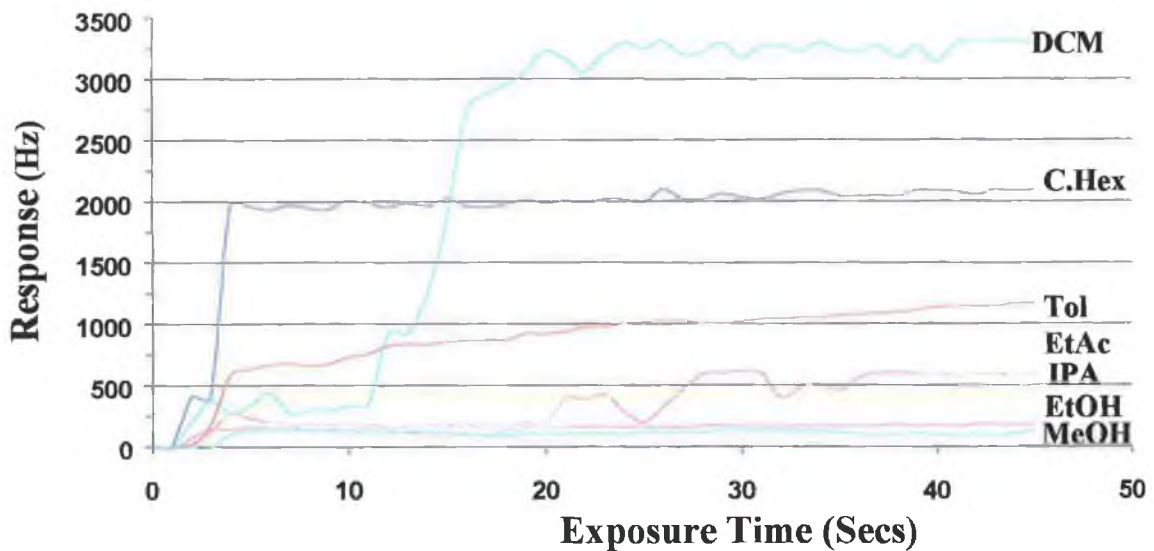
Figure 4-27: Response of TDDA-coated BAW to solvents

Solvents	Response (Hz) @45s	Selectivity Factor, K	RSD
Chloroform (CHCl₃)	2906	3.00	11.4%
Cyclohexane (C.Hex)	2167	6.39	3.6%
Toluene (Tol)	1760	16.25	29.8%
Ethyl Acetate (EtOAc)	994	2.89	77.6%
Isopropyl Alcohol (IPA)	283	2.52	65.8%
Methanol (MeOH)	168	1.00	29.2%
Ethanol (EtOH)	140	1.43	62.0%

Table 4-12: Table of frequency response of TDDA-coated BAW to solvents

115

TDDA has a polar amine centre surrounded by 3 long hydrophobic alkyl chains. It is a new coating to be employed as a BAW sensor coating. The long alkyl chains will be attractive to hydrophobic compounds while the amine centre is capable of basic hydrogen bonding. The response of chloroform is two step, with step one involving the initial surface adsorption while step two involves the diffusion process occurring after about ten seconds. This response is almost equivalent to a 90% increase in mass loading. Surprisingly the %RSD for this solvent is only 11%. Cyclohexane found the alkyl chain of TDDA very attractive and a response of 66% to that of the sensor loading resulted. A 3.6% RSD value was very encouraging. The hydrophobic toluene and ethyl acetate showed the next greatest responses but had high respective %RSD values (29.8% and 77.6%). The alcohols again found such a primarily hydrophobic polymer unattractive.

4.10 Sensitivity

The sensitivity of the sensors was found to be quite good, and a calibration plot is presented in Figure 4-28 for a PIB sensor responding to cyclohexane, in a fixed volume at 22°C, as described in Chapter 3. An R^2 value of 0.9987 indicates good linearity over this range, and is found to be quite reproducible (standard deviations are shown as error bars but may be too small to be seen). The lowest unit that can be read is 1Hz, and S/N ratio of 3:1 means that the lowest concentration that can be read could be 1ppb approx. (4Hz). Similar linear plots were observed with most sensor coatings.

PIB Calibration Plot

$y = 4.1669x - 1.817$
$R^2 = 0.9987$

Cyclohexane Concentration
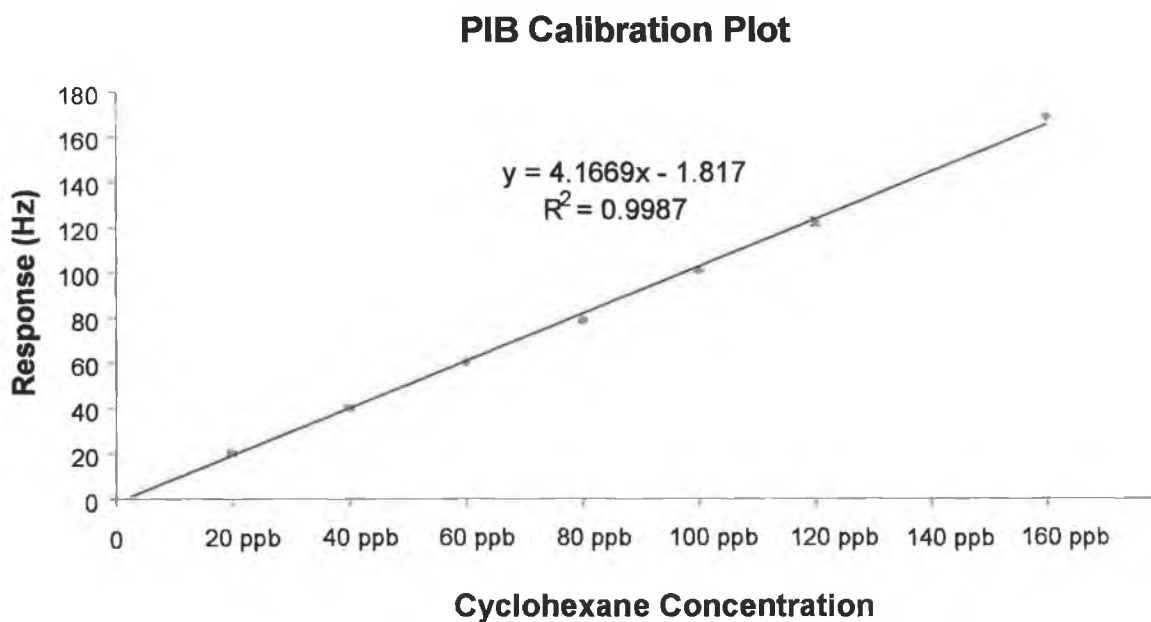
Figure 4-28: Calibration plot for the response of PIB sensor to cyclohexane, in a fixed volume of 320ml at ambient temperature, 22°C.

4.11 Solvent Classification

As discussed in Chapter 3, if the responses of a range of different sensors upon exposure to various solvents are displayed as histograms, it might be possible to distinguish between their generated characteristic patterns. Figure 4-29 shows a simple response histogram for just 3 sensors to a range of solvents, arranged with hydrophobic non-polar hexane on the left, hydrophobic polar solvents next, with the hydrophilic alcohols on the right. PIB is responsive to the hydrophobic solvents, (but not to the hydrophilic alcohols), PEG is responsive to alcohols and polarisable solvents, while OV17 is responsive to the hydrophilic solvents, especially the polarisable ones. The response of PEG to chloroform is significant and overloads the sensor due to the high concentration of chloroform in the headspace (37.1g/L) compared to that of toluene (1.40 g/L) [13]. Using a different sensor with a coating level of 3,500Hz (15.4 μg) gave a response to chloroform that was 10 times greater than that of ethanol!

Therefore using an array of sensors with different chemical properties, will allow specific "fingerprint" responses for each solvent to be generated. Therefore a library can be set-up, which will contain the characteristic responses of the various sensors to different solvents. Using these fingerprints, it will be possible to discriminate between these solvents.
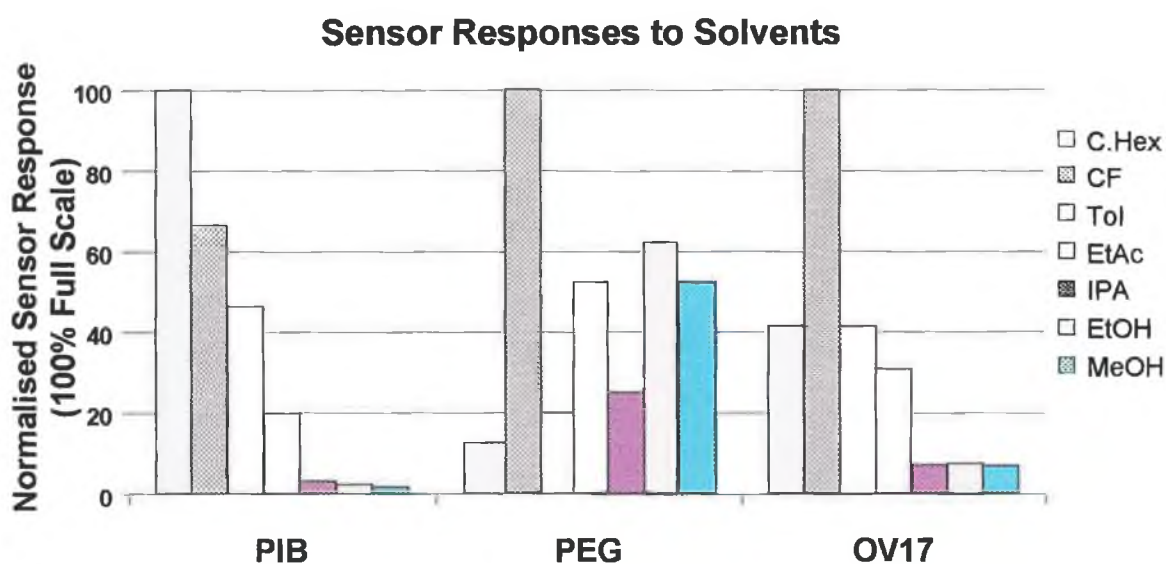
Figure 4-29: Histogram of PIB, PEG, and OV17 responses to solvents

Therefore seven sensors coated with PIB, PEG, OV17, OV225, PECH, PVP, and TDDA along with a blank reference were placed within the in house designed sampling chamber (see Chapter 3). These sensors were then exposed to 7 different vapours, randomly in triplicate within a recycling loop, for 45 seconds. The response of each sensor was then obtained by comparing it to the blank reference BAW. The responses of the 7 sensors to the 21 exposures was then analysed using PCA, CA and DFA.

4.11.1 Principal Component Analysis (PCA) of Solvents:

The frequency responses for each sensor after 45 seconds exposure to each solvent were exported via Excel into Minitab as a 21x7 data matrix and analysed using PCA. From this 21x7 matrix PCA generates 6 eigenvectors (EV1-EV6), which are listed in order of decreasing information content. EV1 contains 49.9% of the information, EV2 contains 23.0%, EV3 contains 16.1% with EV4-6 sharing the remaining 11%. These eigenvectors together form a loading matrix, as explained previously. A transpose of this matrix is given in Table 4-13. Multiplication of the data matrix by the loading matrix generates a scores matrix, which contains the principal component scores, PC1 - PC6. PC1 and PC2, the first two principal component scores, contain the majority of the information (73.2%), and these were plotted against each other to generate a 2-D output plot, Figure 4-30, which represents the output for the classification of various solvents, chosen for their range of chemical properties. If required, a 3-D plot, with PC3 as the additional axes, can be used to gain more insight into the spatial separation between respective sample groups. In general the performance of the array was very successful for classifying the different classes of solvents.

The eigenvectors EV1-6, for PC1-6, are given in Table 4-13.

	PIB	PEG	OV17	OV225	PECH	PVP	TDDA
EV1	-0.422	0.186	-0.396	-0.169	-0.464	-0.484	-0.39
EV2	-0.046	0.486	0.147	-0.6	-0.309	0.222	0.485
EV3	0.03	-0.635	-0.518	-0.512	0.121	0.037	0.223
EV4	-0.888	-0.104	0.187	-0.006	0.308	0.263	0.033
EV5	0.027	-0.439	0.719	-0.328	-0.211	-0.332	-0.163
EV6	0.069	-0.144	-0.02	-0.065	-0.408	0.731	-0.518

Table 4-13: PCA eigenvectors in tabulated form

From examination of the eigenvectors EV1-3, it can be determined that dispersion interactions dominate PC1 (EV1 < -0.4 for PIB, PECH, PVP, and TDDA), dipolar interactions (including hydrogen bonding) dominate PC2 (EV2 > 0.4 for PEG and TDDA while < -0.3 for OV225 and PECH), while polarisable interactions dominate PC3 (EV3 < -0.5 for PEG, OV17 and OV225). It can be seen from EV1 that PIB, OV17, and PECH have eigenvectors of at least –0.4, which suggests that dispersion interactions are dominating the responses. The high magnitude of the TDDA eigenvector is due to a combination of dispersion interaction of the three alkyl chains and hydrogen bonding abilities of the amine centre. This hypothesis is then supported by the high magnitude of the EV2 eigenvector for PEG, OV225, PVP and TDDA (all polar polymers). The eigenvector components of PC3 are represented typically by OV17 whose phenyl component is highly polarisable.

Figure 4-30 shows that the alcohols clustered together, and had the highest PC1 scores. Cyclohexane being totally hydrophobic had the lowest PC1 score while the highly polar $CHCl_3$ was totally discriminated by having the lowest PC2 score. The $CHCl_3$ samples were seen to have the lowest PC2 score. Ethyl acetate and toluene were then seen to fall somewhere between $CHCl_3$ and cyclohexane.
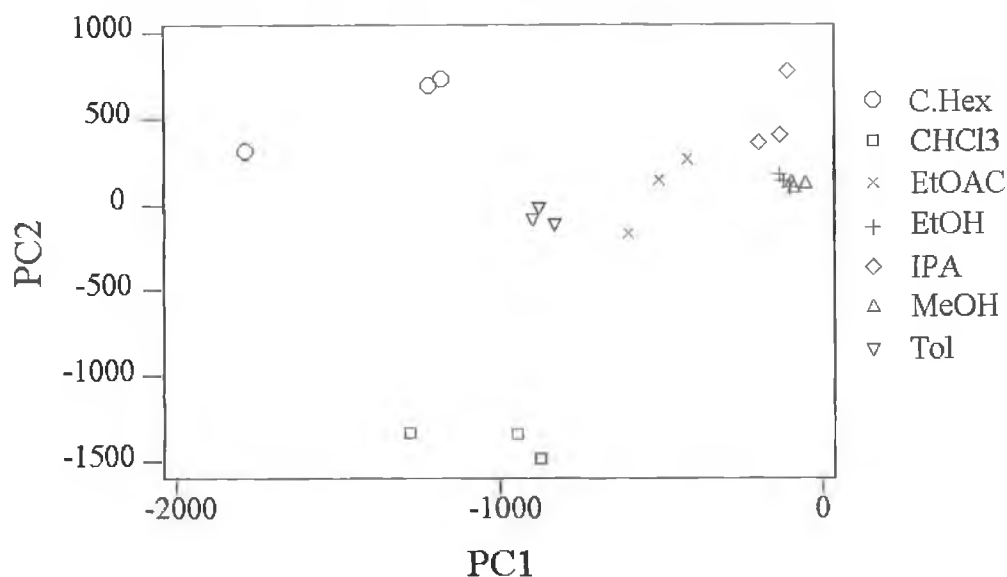
Figure 4-30: PCA plot of solvents

4.11.2 Cluster Analysis (CA) of Solvents:

Using the same data as before, in the PCA, cluster analysis was carried out. Using a complete linkage method and Euclidean distances, a dendrogram was obtained (Figure 4-31). Similar results to those seen in PCA were obtained. Three main clusters were identified in the dendrogram enjoying satisfactory separation according to their chemical properties. These three groups being the hydrophilic alcohols (methanol, ethanol and isopropanol), polarisable hydrophobic solvents (toluene, chloroform and ethyl acetate), and non-polar hydrophobic cyclohexane. Clearly the polarisable hydrophobic solvents toluene, chloroform and ethyl acetate clustered together although not as tightly as the alcohols. Cyclohexane was seen to be totally distinct from the other solvents indicating it's totally hydrophobic and non-polarisable nature.

Similarity

Complete Linkage with Euclidean Distances
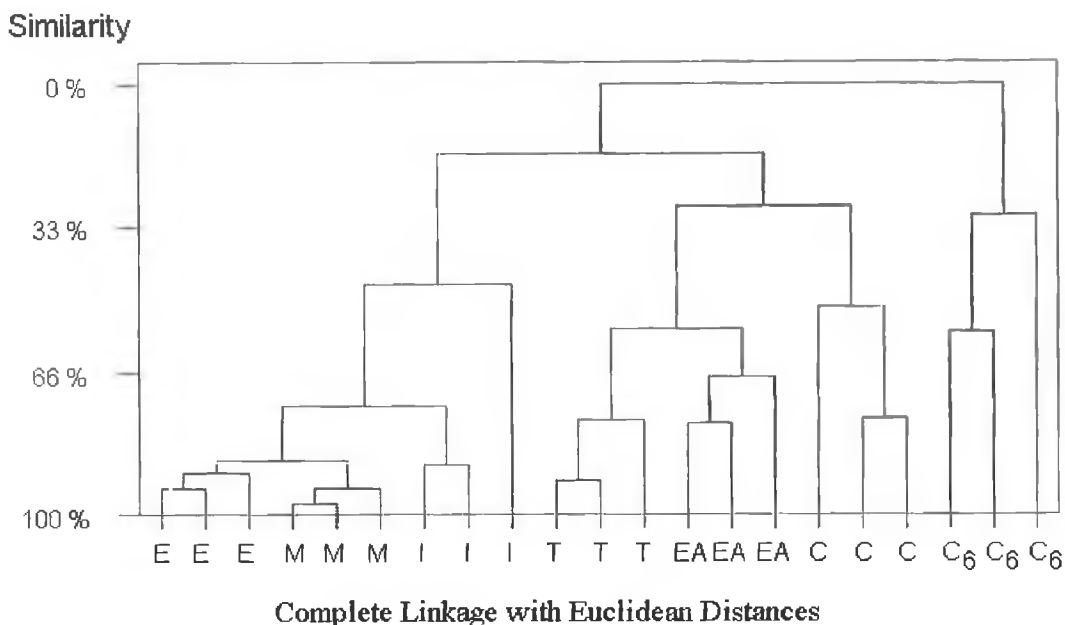
Figure 4-31: Dendrogram obtained by CA on solvent responses (E = Ethanol, M = Methanol, I = Isopropanol, T= Toluene, EA = Ethyl Acetate, C= Chloroform, C_6 = Cyclohexane)

4.11.3 Discriminant Function Analysis (DFA) of Solvents:

Using the same data as before, in the PCA and CA, DFA was carried out. Being a supervised method DFA is expected to give better discrimination and this is displayed in the resultant 2-D plot, Figure 4-32, using the first two discriminant factors, DF1 and DF2. Further spatial separation between the groups was achieved by introducing a third axis, namely the third discriminant factor, DF3 (Figure 4-33). When this data is presented in table form, Table 4-14, it is clear that even with cross-validation the solvents are easily discriminated from each other. Therefore the tightly grouped clusters, achieved by this method, and the separation between them is better than that seen in the PCA. This implies that the relative spatial separation is greater, thereby achieving better resolution. Therefore for a known pre-defined system, DFA is superior to PCA for classification purposes.
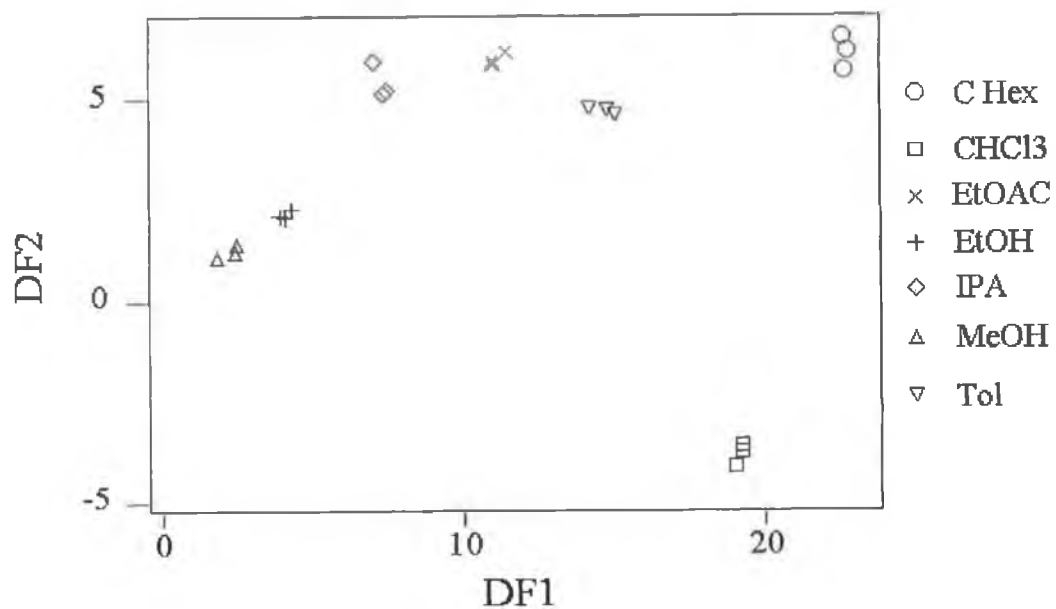
Figure 4-32: DFA plot of solvents
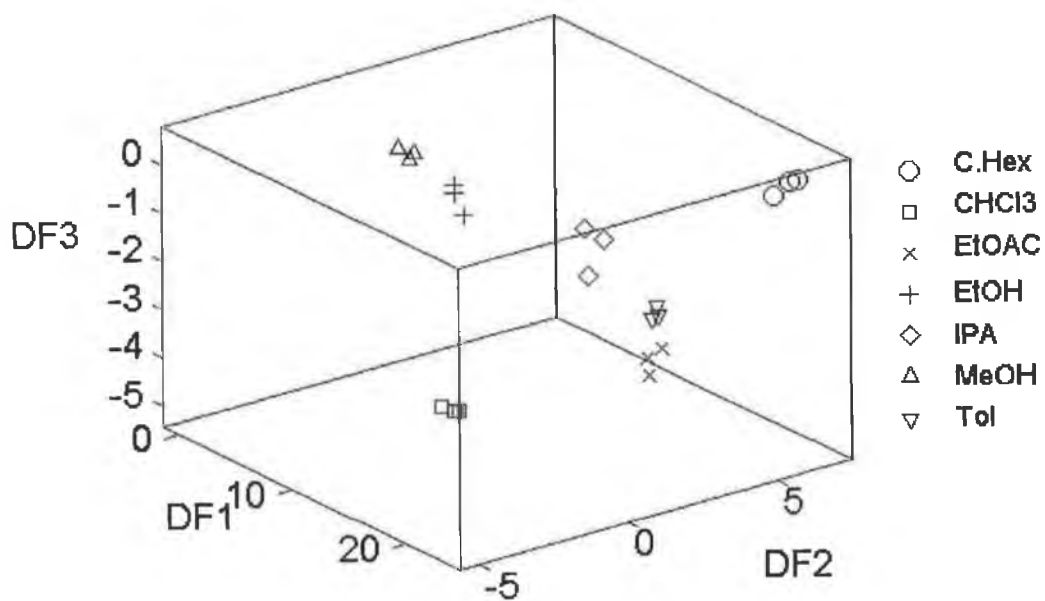
Figure 4-33: 3-D DFA of Solvents

	C_6H_{12}	$CHCl_3$	EtOAc	EtOH	IPA	MeOH	Tol
C_6H_{12}	**4 (4)**	0 (0)	0 (0)	0 (0)	0 (0)	0 (0)	0 (0)
$CHCl_3$	0 (0)	**4 (4)**	0 (0)	0 (0)	0 (0)	0 (0)	0 (0)
EtOAc	0 (0)	0 (0)	**4 (4)**	0 (0)	0 (0)	0 (0)	0 (0)
EtOH	0 (0)	0 (0)	0 (0)	**4 (4)**	0 (0)	0 (0)	0 (0)
IPA	0 (0)	0 (0)	0 (0)	0 (0)	**4 (4)**	0 (0)	0 (0)
MeOH	0 (0)	0 (0)	0 (0)	0 (0)	0 (0)	**4 (4)**	0 (0)
Tol	0 (0)	0 (0)	0 (0)	0 (0)	0 (0)	0 (0)	**4 (4)**
Count	4	4	4	4	4	4	4
N Correct	4	4	4	4	4	4	4
Proportion	1.00	1.00	1.00	1.00	1.00	1.00	1.00

Table 4-14: **Details of Discriminant Function Analysis (with cross-validated entries in parenthesis)**

4.12 Conclusion

GC coatings, with their known chemistries and availability are excellent coating materials for BAW gas sensors. Through careful choice an array of such sensors would be able to discriminate between suitably volatile liquids.

4.13 References

1   W.H. King, Piezoelectric sorption detector, *Anal. Chem.*, **36** (1964) 1735-1739
2   J. Hlavay, G.G. Guilbault, Applications of piezoelectric crystals in analytical chemistry, *Anal. Chem.*, **49** (1977) 1890-1898
3   J.F. Alder, J.J. McCallum, Piezoelectric crystals for mass and chemical measurements, *Analyst*, **108** (1983) 1169-1189
4   C.K. Sullivan, G.G. Guilbault, Commercial quartz crystal microbalances – theory and applications, *Biosensors and Bioelectronics*, **14** (1999) 663-670
5   C. Demathieu, M.M. Chehimi, J.F. Lipskier, Inverse gas chromatographic characterisation of functionalised polysiloxanes. Relevance to sensors technology, *Sensors and Actuators B*, **62** (2000) 1-7
6   B.K. Callihan, D.S. Ballantine, Characterisation of olefininc gas chromatographic stationary phases by linear solvation energy relationships, *J. Chromatogr. A.*, **836** (1999) 261-270
7   CRC Handbook of Physics and Chemistry
8   H. Rotzsche (Eds), Stationary phases in gas chromatography, Journal of Chromatography Library -Vol. 48, Elsevier, Amsterdam, 1991
9   M.H. Abraham, J. Andonian-Haftvan, M.D. Chau, V. Diart, G.S. Whiting, J.W. Grate, R.A. McGill, Hydrogen bonding. Part 29. Characterisation of 14 sorbent coating for chemical microsensors using a new solvation equation, *J. Chem. Soc. Per. Trans.* **2** (1995) 369-378
10   J.W. Grate, M. Abraham, Solubility interactions and the design of chemically selective sorbent coatings for chemical sensors and arrays, *Sensors and Actuators B*, **3** (1991) 85-111
11   F. Patte, M. Etcheto, P. Laffort, *Anal. Chem*, **54** (1982) 2239-2247
12   K. Lau, J. Micklefield, J. Slater, *Sensors and Actuators B*, **50** (1998) 69-79

Chapter 5

5   Polypyrrole Coatings

Abstract:

A study of polypyrroles as sensitive BAW coatings is presented. Using a novel approach, BAW sensors coated with poly(pyrrole) and poly(N-methyl pyrrole) were exposed to various organic vapours. The difference in the chemistries of the two polymers is revealed in the sensor responses to these vapours. The sensors were found to be stable, robust and reproducible, therefore suitable for incorporation into an array with those sensors discussed in Chapter 4.

5.1   Introduction

Pyrrole is a five membered heterocyclic aromatic compound (Figure 5-1). It does not possess the basic properties typical of amines. Instead it mostly undergoes electrophilic substitution, such as nitration, halogenation and Friedal-Crafts acylation. With resonance energies of 100 KJmol^{-1}, pyrrole is said to be aromatic, although not to the same extent as benzene (150 KJmol^{-1}). First discovered in 1834, and characterised in 1870, it is a colourless, slightly hygroscopic liquid. On exposure to air it darkens to a brown resin and so is stored under N_2.
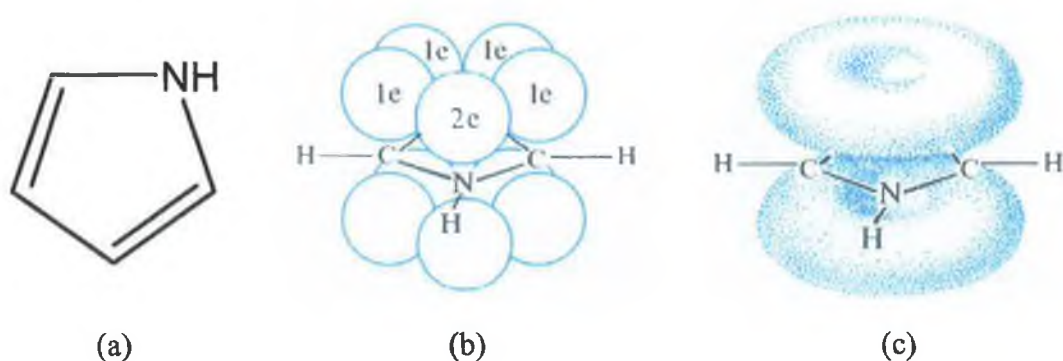
Figure 5-1: (a) Chemical structure of Pyrrole (b) electron distribution in the p-orbitals (c) electon clouds above and below the plane of the ring [Reprinted from 1]

125

With a delocalised π-electron ring pyrrole can best be described using resonance hybrids, which explain its high acidity for an amine (Figure 5-2). Electrophilic substitution tends to occur more readily at the α-position, due to the possible number of resonance structures possible [2].
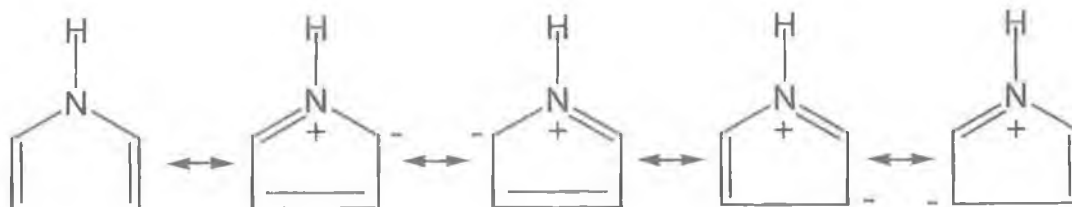
Figure 5-2: Resonant hybrid forms of pyrrole

It was first noted in 1968 that pyrrole could be electrochemically polymerised, and in 1973 it was shown that pyrrole could be chemically polymerised, by a wide range of oxidising agents, to give a black conducting powder. An excellent review of polymerised pyrrole, polypyrrole (PPY), was published recently [3], which details the important progress that has been made in the area of PPY. Since the mid-1980's large amounts of research have been carried out in this area and PPY has found many applications, especially in the area of light emitting devices, light valves, and also conducting gas sensitive layers [4, 5].

Most of such applications make use of the inherently conductive nature of the polypyrrole chain, as electrons can efficiently flow along its length (Figure 5-3). From experimentation it has been found that this is not due to ion-exchange [4], as substitution of triflouromethyl groups in the β-position was found to readily accept any electrons flowing through the chain (Figure 5-4).
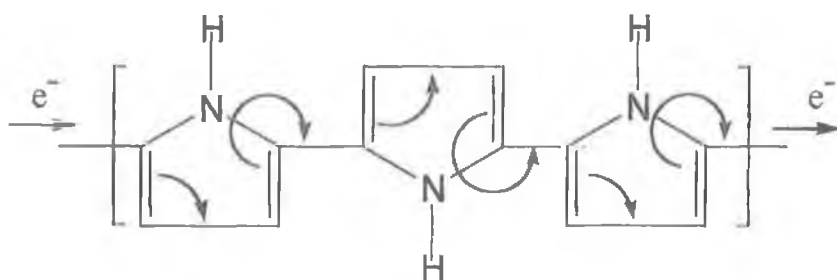
Figure 5-3: Electron flow within a polypyrrole chain
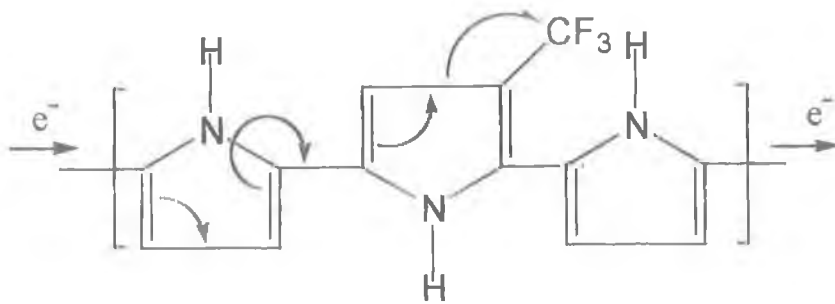
Figure 5-4: Electron flow within a polypyrrole chain terminating at a single triflouromethyl group

When an organic vapour diffuses into a conducting film such as PPY, it causes the film to either swell or shrink. With this change in physical dimensions comes a change in the film resistance. Polymer swelling causes the chains to spread out, increasing the coating volume and surface area, thereby causing a reduction in resistance (Equation 5-1).

$$R = \frac{\rho.l}{A}$$

Equation 5-1

where R is the resistance of a conductor, ρ being the resistivity, l being the conductors length, and A being its cross-sectional area.

Tailoring the conductivity can be achieved through the use of dopants such as chlorides and nitrates. These anions can change the conductive properties of the polymer chain in the presence of certain vapours [5]. This can be easily achieved through the use of relevant oxidising agents, such as salts of transition metals (*eg.* Fe^{3-}, Cr^{6-}, Cu^{2+}, Mn^{7+}) for chemical polymerisations. Hence the general form of PPY formed under such conditions is given in Figure 5-5, where A^- is typically Cl^-, NO_3^-, $Cr_2O_7^{2-}$.
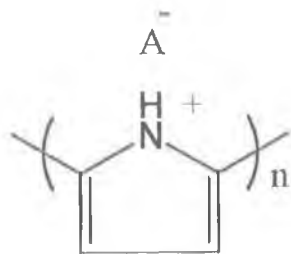
Figure 5-5: General form of PPY with associated anion (A⁻)

It has been reported that poly(N-methyl pyrrole) (PMPY), derived from N-methyl pyrrole (Figure 5-6), has also attracted some interest for applications in solid state devices [6]. Several studies mentioned in this review point out the favourable gas-permeability of PMPY films, as determined in pervaporation studies.
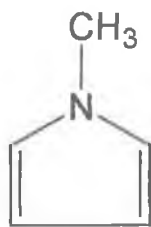
Figure 5-6: Chemical structure of N-methyl pyrrole

Although majority of work with these polymers has been based on their conductivity properties, the work in this study focuses on their characteristics as mass sensitive BAW device coatings.

PPY in its synthetically supplied form is insoluble in most useful solvents and so must be grown on sensitive substrates for useful applications. The two methods most favoured are electrochemical oxidative polymerisation, and chemical oxidative polymerisation. The methods covered in this work deal with the latter method. The former coating method supposedly results in a polymer with a highly crystallised lattice structure [6]. Therefore several methods were examined to derive PPY and PMPY.

5.2 Experimental

5.2.1 Chemicals

Pyrrole and N-methyl pyrrole were purchased from Sigma-Aldrich (Dublin, Ireland), while HCl (conc.) was purchased from Labscan (Dublin). Ferric chloride and potassium dichromate were obtained from chemical stores in the school. Deionised water was obtained using a Milli-Pore system at a resistance of $18M\Omega$.

5.2.2 Formation of Poly(pyrrole) Coatings

5.2.2.1 Direct Deposition

Polypyrrole is supplied as a black powder, but is insoluble in common organic solvents. Therefore to coat BAW's the polymer has to be created *in situ* on the crystal surface. This therefore eliminates spraying, dipping, and smearing as coating methods. The only method that works for this application is drop coating. Therefore the reaction is carried out on a horizontally staged BAW, one side at a time, and then monitored using SEM before testing.

Note: As polypyrrole is insoluble in most solvents it is virtually impossible to remove from the surface of a BAW without damaging the surface. Therefore sensor recycling is impossible, and so several numbers of repetitive tests prove costly, meaning that the conditions are not always optimised.

5.2.2.2 Solvent Choice

Pyrrole is soluble in water and methanol. As the polymerisation is take place on the surface of a BAW, it is desirable to have a solvent that will not evaporate before polymerisation has completed. However it is not just the solubility of pyrrole that is

important, but also the stability of a droplet on the BAW surface. Therefore the contact angle must be favourable also.

(A)   Water

A 4µl aliquot of water was dropped onto the centre of a horizontally staged BAW. Due to the contact angle that it experiences with gold the droplet remained in position, even with slight movement of the crystal.

(B)   MeOH

Methanol (4µl) was dropped onto the centre of a horizontally staged BAW. Immediately the droplet began to move off centre towards the edge, due to the convex nature of the quartz disk (see Chapter 1). Therefore MeOH on its own could not be used as a solvent

(C)   Water-MeOH mixture

Various mixtures of water and methanol were examined as in (A) and (B) above. It was found that as long as the water component was maintained at up to 50% (V/V), the droplet stayed in position satisfactorily.

5.2.2.3   Oxidant Choice

A 4µL aliquot of pyrrole solution (2% (V/V), aq.) was dropped onto the surface of a BAW and left for two hours. No reaction took place and so an oxidant was required to initialise the polymerisation. The most common oxidants available are acids and metal salts.

(a)   Acid as oxidant

(i)   HCl

A 2µL aliquot of pyrrole solution (2% (V/V), aq.) was dropped onto the surface of a BAW, and to this 2µL of HCl (conc., aq) was added. Immediately polymerisation took place, and a thick layer of black polypyrrole (PPY) formed. The concentration was then reduced to 1M and 0.1M and in both cases the same result was achieved.

(ii)   CH₃COOH

A 2μL aliquot of pyrrole solution (2% (V/V), aq.) was dropped onto the surface of a BAW, and to this 2μL of CH₃COOH (1M, aq) was added. No reaction was observed after 30 minutes.

(B)   Metal Salts as Oxidants

(i)   FeCl₃

A 2μL aliquot of pyrrole solution (2% (V/V), aq.) was dropped onto the surface of a BAW, and to this 2μL of FeCl₃ (1M, aq) was added. Within seconds polymerisation took place on the surface, and a thick black crust of PPY resulted. For a technique to produce an even reproducible coating, a longer reaction time was necessary. Subsequent dilution of the ferric solution to 0.1M gave a satisfactory reaction time of 30 minutes. The resulting light outer PPY film was washed to remove any excess chloride, and a grey/brown discolouration on the surface was observed. Analysis by SEM revealed an even coating on the surface (Figure 5-7).

Figure 5-7: PPY formed on BAW surface using 0.1M FeCl₃ as oxidant

(ii)   K₂Cr₂O₇

A 2μL aliquot of pyrrole solution (2% (V/V), aq.) was dropped onto the surface of a BAW, and to this 2μL of K₂Cr₂O₇ (1M, aq) was added. Within 30 seconds polymerisation took place on the surface, and a thick black film of PPY resulted. Subsequent dilution of the chromate solution to 0.1M gave reaction times of in

excess of an hour. After washing a discolouration, similar to that in (i) above, was observed.

5.2.2.4 *Solvent Volumes*

To achieve an optimum loading of approximately 4,000Hz (as explained in Chapter 3), various monomer/oxidant reaction volumes were attempted, and the resulting coating levels are displayed in Figure 5-8. Such an overall loading requires about 2,000 Hz per side. At 1,812 Hz per side, $2\mu L$ of monomer and $2\mu L$ of oxidant (FeCl$_3$) were determined to be satisfactory reaction volumes. Such a loading was found to be typical of these volumes for repeated applications. It could be argued that at lower concentrations that full polymerisation hasn't taken place due to the reduced reaction volumes, hence explained the non-linear nature of the frequency changes.
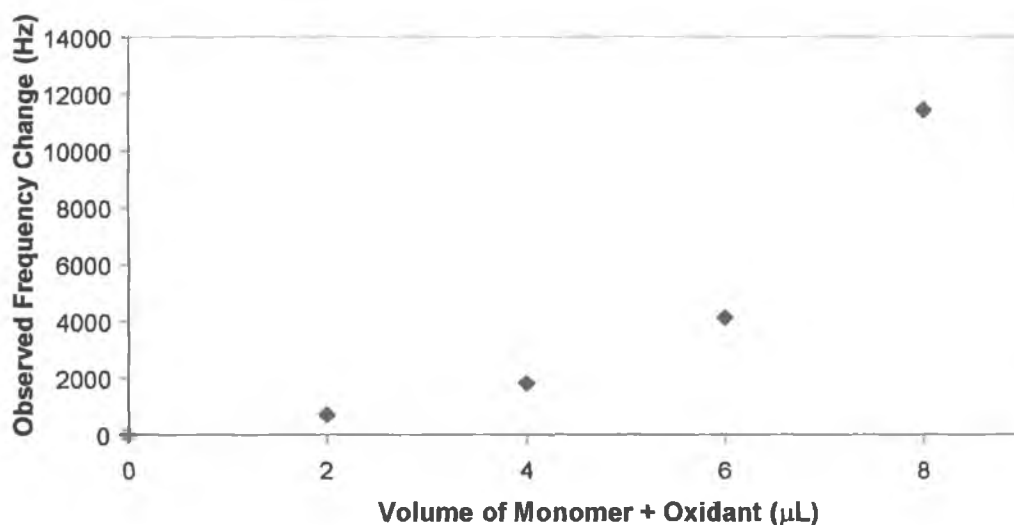
Figure 5-8: PPY mass loading as a function of monomer/oxidant volume

5.2.3 Formation of Poly(N-Methyl Pyrrole) Coatings

N-methyl pyrrole differs from pyrrole by a methylene group on the ring nitrogen. The substitution of this hydrogen with the methyl group, reduces the unusual acidity

of this nitrogen. Consequently the hydrogen bond capabilities of this monomer when polymerised should be different from that of PPY.

5.2.3.1   Solvent Choice

As N-methyl pyrrole cannot hydrogen bond through the N atom, due to the methyl group, its solubility in water is limited. Therefore it was decided to use a 1:1 mixture of water and methanol. This mixture dissolved the N-methyl pyrrole, and formed a stable droplet on the surface of a BAW.

5.2.3.2   Oxidant Choice

Following from the work with pyrrole, $FeCl_3$ dissolved in the water/methanol mix was used as an oxidant. However it was seen that this ferric oxidant was not sufficient to initiate the polymerisation. The same was found with the chromate initiator, even at high concentrations (>1M). Therefore it was decided to investigate ferric solutions in a HCl (1M aq) background. Addition of a 2µL acidified $FeCl_3$ solution (1M HCl, 0.1M $FeCl_3$, 1:1 (V:V) H_2O:MeOH soln) to a 2µL aliquot of N-methyl pyrrole (2% W/V, 1:1 (V/V) H_2O:MeOH soln) resulted in a brown polymer film forming after a few minutes. Washing as before revealed a grey/brown coloured polymer film on the gold surface (Figure 5-9) with a corresponding frequency change of 4,600Hz.
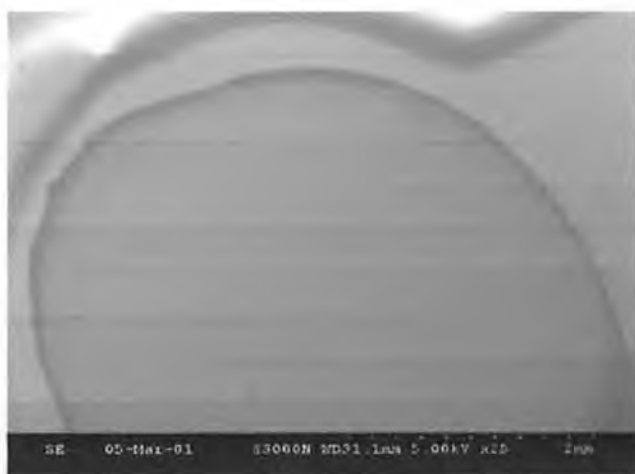
Figure 5-9: PMPY formed on BAW surface using a 1M HCl (aq)/0.1M FeCl₃ solution as oxidant

5.2.3.3   *Vapour Deposition Technique*

As an alternative to the drop coating method, vapour deposition was investigated as a coating technique. In this case the oxidant solution is dropped onto the surface of a horizontally supported BAW, and reacts with the vapour of the volatile monomer (Figure 5-10).
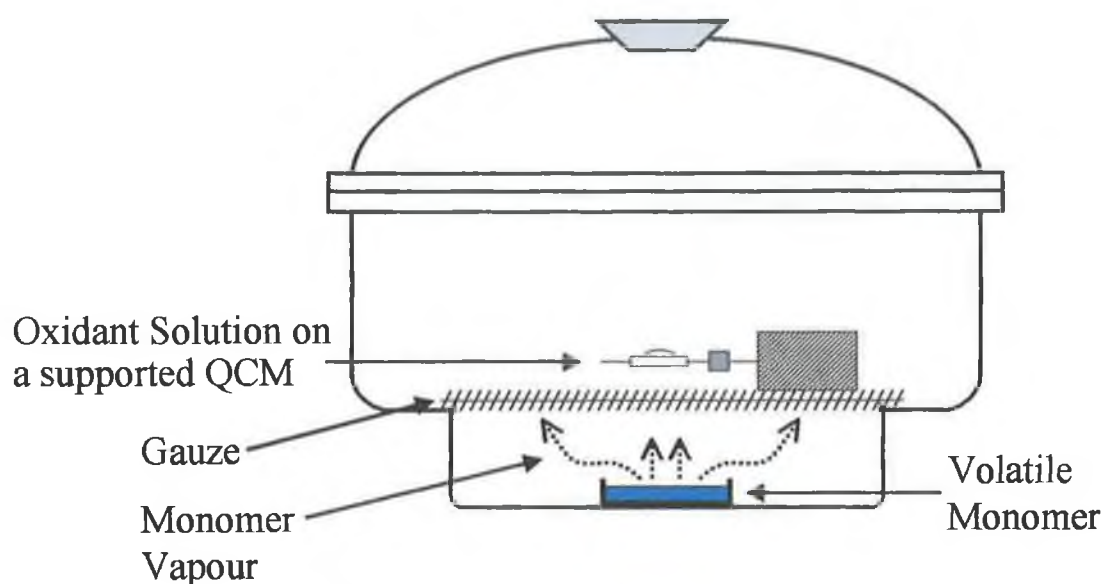
Figure 5-10: Experimental setup for vapour deposition of PPY on BAW's inside a dessicator

4 μL of a FeCl$_3$ solution (0.1M, 1:1 (V/V) H$_2$O:MeOH) was deposited on the BAW surface as a droplet as described previously was sufficient to form the 10μg or so per side. After ten minutes the BAW was removed from the chamber and placed in an oven and allowed to dry. Any loose PPY or remaining salt was then washed off and the sensors were dried again. From the resulting SEM it was seen that the coating wasn't as uniform as with the drop coating method. The level of coating at the edges is greater that at the centre, due to the insoluble PPY flowing to the drop edge, which was in contact with the gold electrode.

134

Figure 5-11: SEM image of PPY coated BAW after vapour deposition

5.3 Results

5.3.1 Polypyrrole

5.3.1.1 Molecular Modelling

MM2 energy minimisations of a 4-unit PPY chain were modelled using Chem3D (Figure 5-12). The polymer chain was found to arrange itself in a flat linear fashion and the acidic hydrogen's were left exposed. The polarisable rings are also very open to any possible π-π interactions.

Acidic Nitrogen

Polarisable Ring

● Nitrogen
● Carbon
● Hydrogen
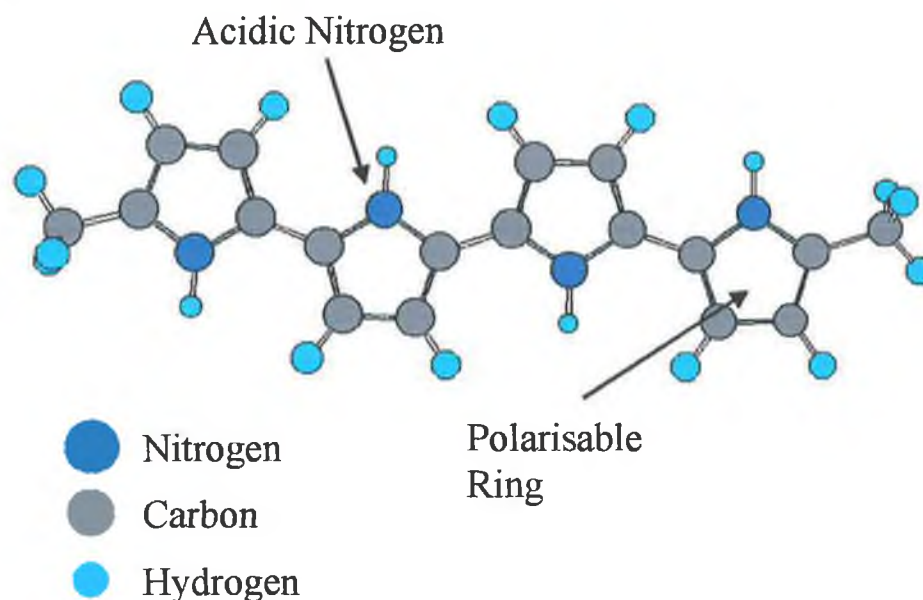
Figure 5-12: MM2 energy minimised model of PPY with functionalities indicated

5.3.1.2 Application Details

BAW's were coated with PPY as detailed in Section 5.2.2, using the drop coating technique, with $FeCl_3$ as the oxidant. The average sensor coating level was ~ 5,000Hz, corresponding to a mass change of 22µg. The responses displayed in Figure 5-14 and Table 5-1 are for a coating of 6,570Hz.

5.3.1.3 *SEM Analysis*

SEM analysis of PPY coated BAW indicated that the polymer coated a high percentage of the gold surface area (Figure 5-11 (a)). Figure 5-11 (b) shows that the coating is quite uniform.

(A)   (B)
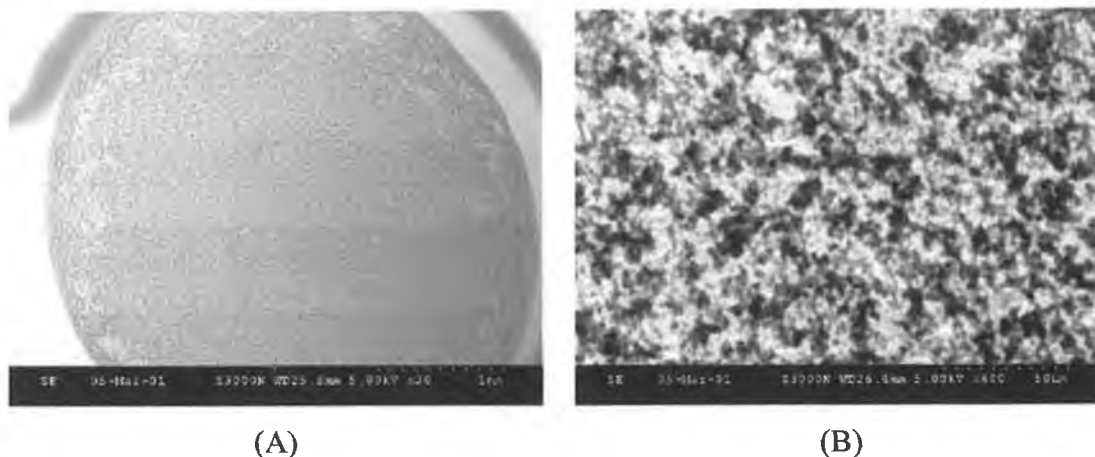
Figure 5-13: SEM images of a PPY coated BAW at a magnification of (A) x30 (B) x600

5.3.1.4 *Sensor Evaluation*

PPY is a hydrophilic acidic polymer due to the hydrogen on the acidic nitrogen. This means that it would find bases attractive. The aromatic nature of the chain means that aromatics would interact strongly with this polymer. From Figure 5-14 and Table 5-1, it can clearly be seen that the overall strength of the solvent interactions are quite low, compared to the GC phases, as would be expected from this insoluble polymer. The largest response is seen for chloroform, which is slow to approach equilibrium. Cyclohexane equilibrates very quickly in comparison. Ethyl acetate being a base appears to have a stronger response than the aromatic toluene. As seen with the results in Chapter 4, when these responses are changed into sensitivities the picture changes quite dramatically. The order of response is now **Tol > IPA > MeOH > C.Hex > EtOAc > CHCl₃**. A normalised plot of the solvents (relative to the most sensitive, toluene) is presented in Figure 5-15. The chain appears to be aromatic, capable of hydrogen bonding and not strongly hydrophilic as would be expected. The low responses (<200Hz) of some vapours indicate that the

interactions through the bulk of the coating are low. Comparison of these responses to those of PMPY in the next section could prove useful, in understanding the interactions of the N hydrogen in bonding with vapour molecules.
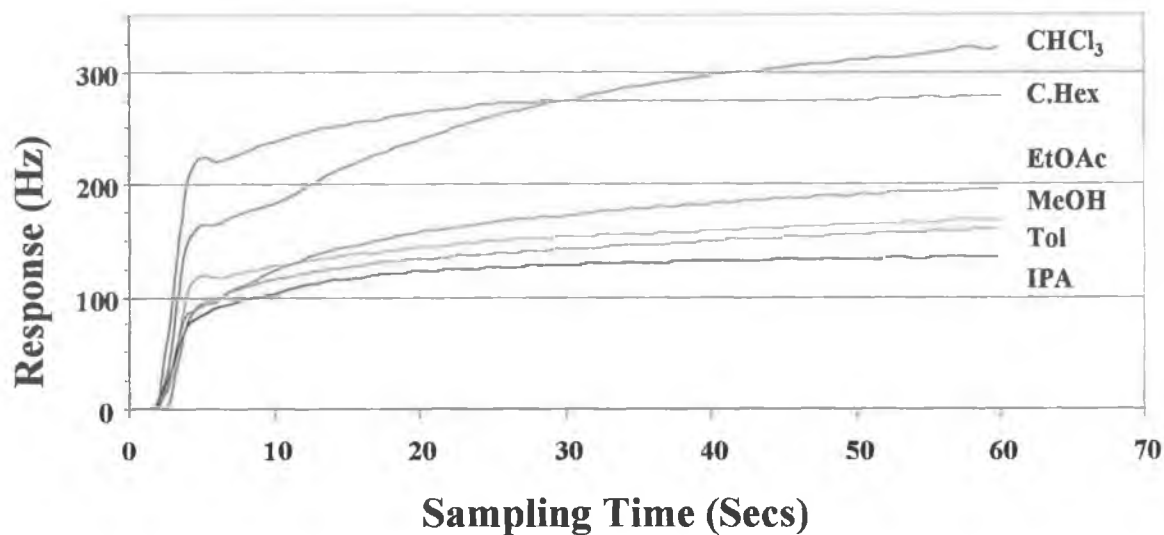
Figure 5-14: Average frequency response of PPY-coated BAW to solvents

Solvents	Response (Hz) @45s	Solubility Factor, K	RSD
Chloroform (CHCl₃)	321	1.00	2.6%
Cyclohexane (C.Hex)	278	2.48	12.2%
Ethyl Acetate (EtOAc)	196	1.72	2.5%
Methanol (MeOH)	168	3.02	1.4%
Toluene (Tol)	153	4.27	9.2%
Isopropyl Alcohol (IPA)	136	3.66	3.8%

Table 5-1: Table of average frequency response of PPY-coated BAW to solvents

The response to some vapours in Figure 5-14 could be described as being 2-stage processes, where the initial adsorption is quite fast, and the subsequent absorption is relatively slower, due to the nature of the PPY coating.

Figure 5-15: Normalised sensitivities of PPY to various solvents (relative to toluene) with standard deviations represented as error bars (n = 3)

5.3.2 Poly(N-methyl pyrrole)

5.3.2.1 Molecular Modelling

Molecular modelling of PMPY indicated that the introduction of the relatively bulky methyl substituent causes the chain to twist out of plane compared to the much more planar PPY. This could mean that there would be more opportunities for vapours to interact with the polymer backbone, compared to that of PPY.

Methyl Group

Nitrogen

Carbon

Hydrogen

Polarisable Ring
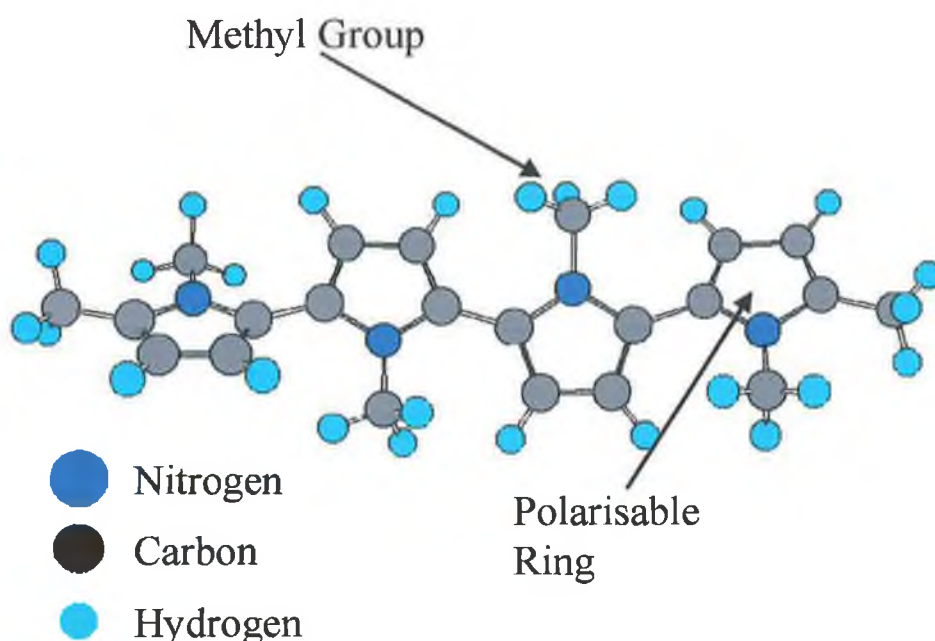
Figure 5-16: MM2 energy minimised model of PMPY with some functionalities indicated

5.3.2.2 Application Details

BAW's were coated with PMPY as detailed in Section 5.2.3 using the drop coating technique, with the acidified $FeCl_3$ solution as the oxidant. The average coating was ~ 5,000Hz, corresponding to a mass change of 22μg. The responses displayed in Figure 5-17 and Table 5-2 are for a coating of 5,410Hz.

140

5.3.2.3   Sensor Evaluation

Compared to PPY, PMPY is expected to be a more hydrophobic polymer with similar aromaticity. The N-methyl group in PMPY cannot interact in hydrogen bonding, and dispersion interactions will tend to dominate.

The response of PMPY is displayed in Figure 5-17 and Table 5-2. In general the magnitude of the PMPY response is much greater than that of PPY. The response to cyclohexane is so great that it overloads the sensor, indicating the hydrophobic nature of the coating. As the sensor has a coating of 5,400 Hz, this would mean that the response of cyclohexane would at least be of the order of 2,000 Hz to cause such overloading. The low response to IPA and MeOH further indicates the reduced hydrogen bonding capability of PMPY. When the sensitivity of PMPY is examined (Figure 5-18) it is immediately clear that sensor is most sensitive to Toluene (or possibly cyclohexane!). For the cyclohexane sensitivity to be greater than toluene, the response would have to be ~ 4,000 Hz. Therefore it is clear that PMPY is an excellent aromatic sensor with possibilities for dispersion interactions. Sampling was carried out 4 times, and as could be expected the solvents with the lowest responses had the greatest RSD values.
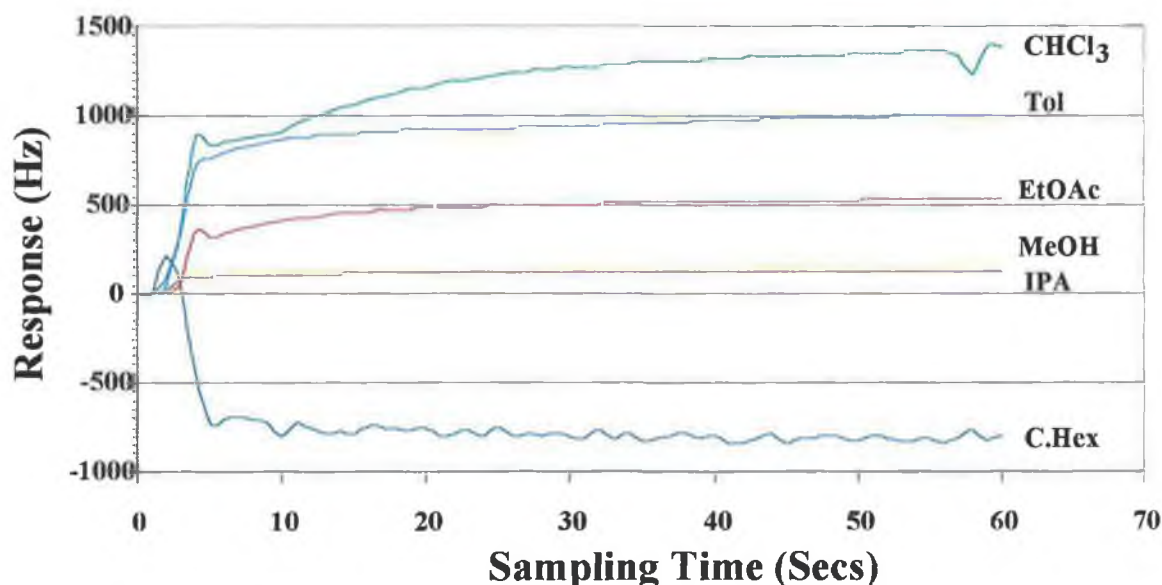
Figure 5-17: Average frequency response of PMPY-coated BAW to solvents

141

Solvents	Response (Hz) @45s	Solubility Factor, K	RSD
Chloroform (CF)	1375	1.73	2.3%
Toluene (Tol)	1005	11.30	5.8%
Ethyl Acetate (EtAc)	526	1.86	3.7%
Methanol (MeOH)	138	1.00	22.1%
Isopropyl Alcohol (IPA)	121	1.31	10.2%
Cyclohexane (Hex)	-803*	N/A	10.1%

Table 5-2: Table of average frequency response of PMPY-coated BAW to solvents
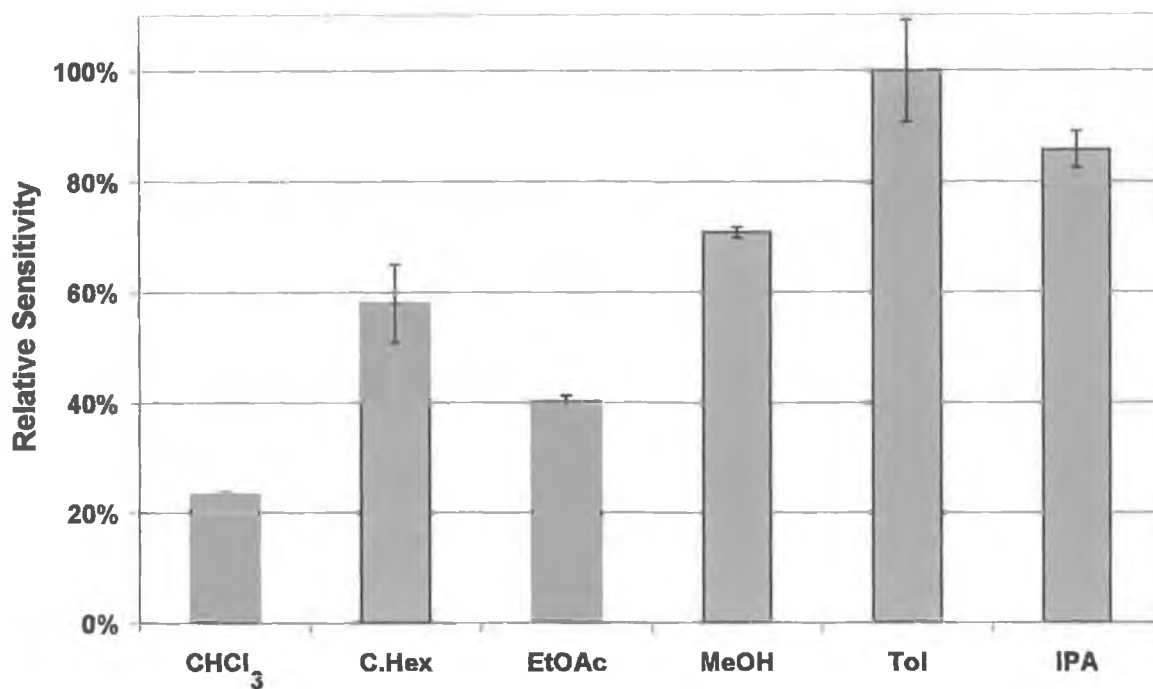
(* - Sensor overloaded)
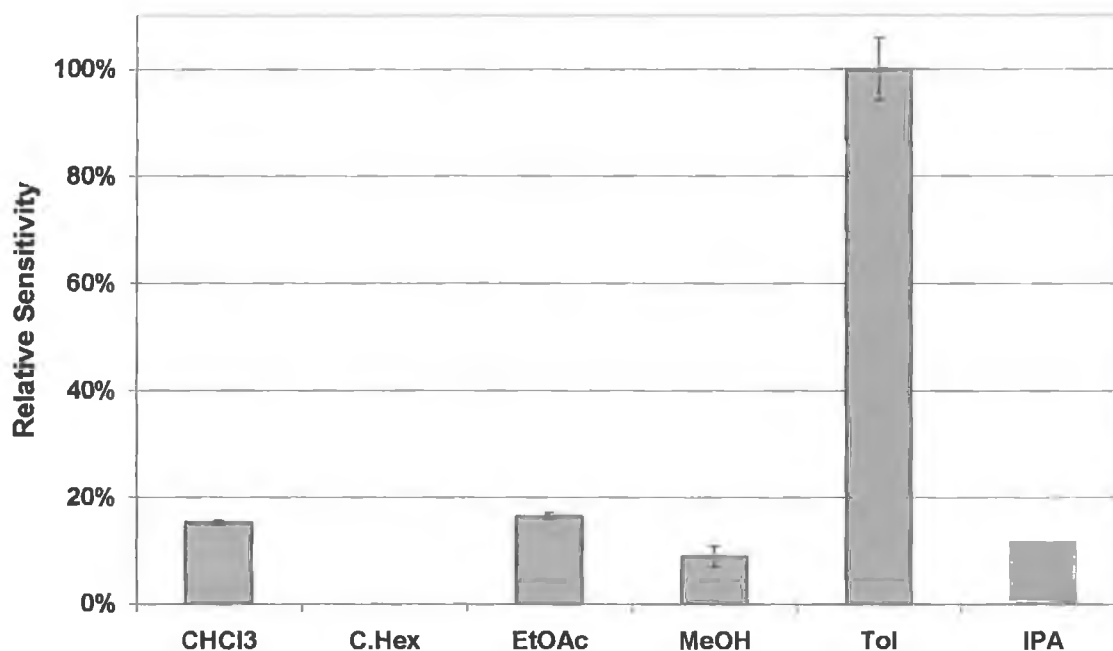
Figure 5-18: Normalised sensitivities of PMPY to various solvents (relative to toluene) with standard deviations represented as error bars (n = 4)

5.3.3 Solvent Detection and Classification

An array of three PPY sensors and three PMPY sensors were incorporated into an array with a blank as a reference. The sensors were exposed to the headspace of seven vapours for sixty seconds, for four repeats (each in a different order). The values of the responses at 60 seconds were then imported into Minitab via MS Excel.

Analysis of the data using PCA would be not be beneficial due to the fact that there are only two types of sensors being employed. Therefore the raw responses of the PPY sensors were plotted against those of PMPY, resulting in six plots. Of these six plots four were found to be similar, and easily separated the vapours into distinct groups. One of the PPY sensors did not perform as well as the other two and meant two plots were unclear. Figure 5-19 is typical of the four plots mentioned.
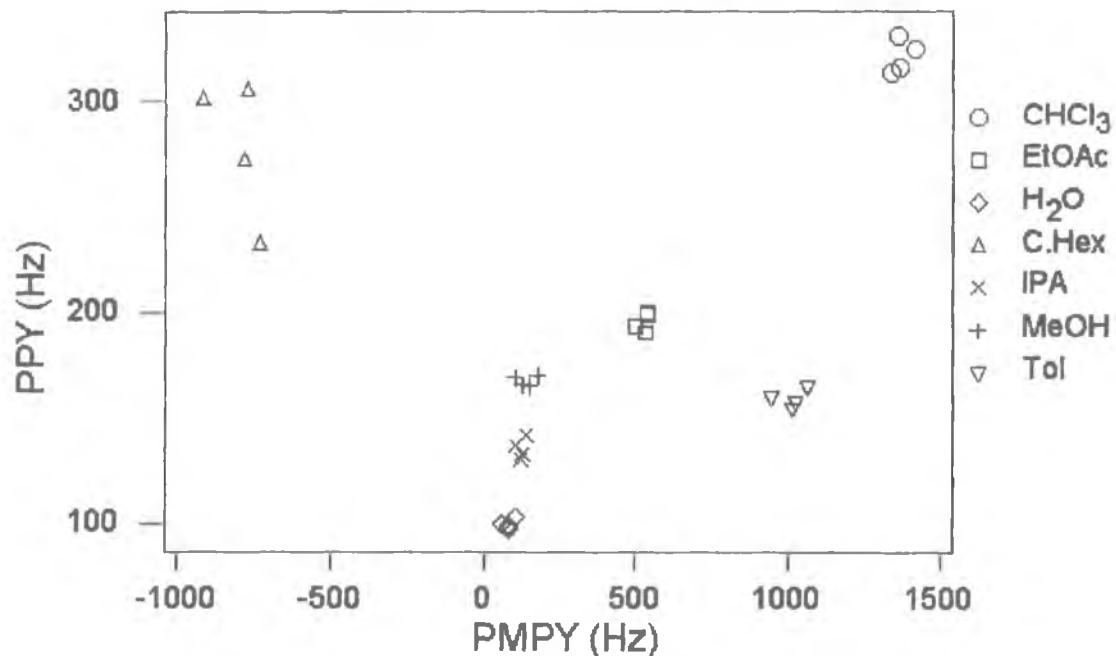
Figure 5-19: 2-D plot of a PMPY sensor response versus that of a PPY sensor

Graphically each vapour is well separated, with the negative responses of cyclohexane due to overloading of the PMPY sensors. PMPY clearly does not see

much difference between water and the alcohols, highlighting it's reduced ability to form hydrogen bonds compared to PPY. However the PMPY sensor responds quiet differently to the polarisable ethyl acetate and toluene.

5.3.3.1   CA

Cluster analysis was carried out on the raw data generated from the six sensors. Clearly a dendrogram based on the data, as presented in Figure 5-19 above, would perfectly classify the vapours. However all the data, including that of the poorly performing PPY sensor, was included in the cluster analysis. Using a single linkage method and a Euclidean distance measure a dendrogram was produced (Figure 5-20). Chloroform and cyclohexane are classed as being totally different to the other solvents. Toluene and ethyl acetate are classed as being similar, as would be expected from the strong polarisabilities. Using the complete data set (6 sensors) meant that the alcohols were the only vapours not clearly discriminated.
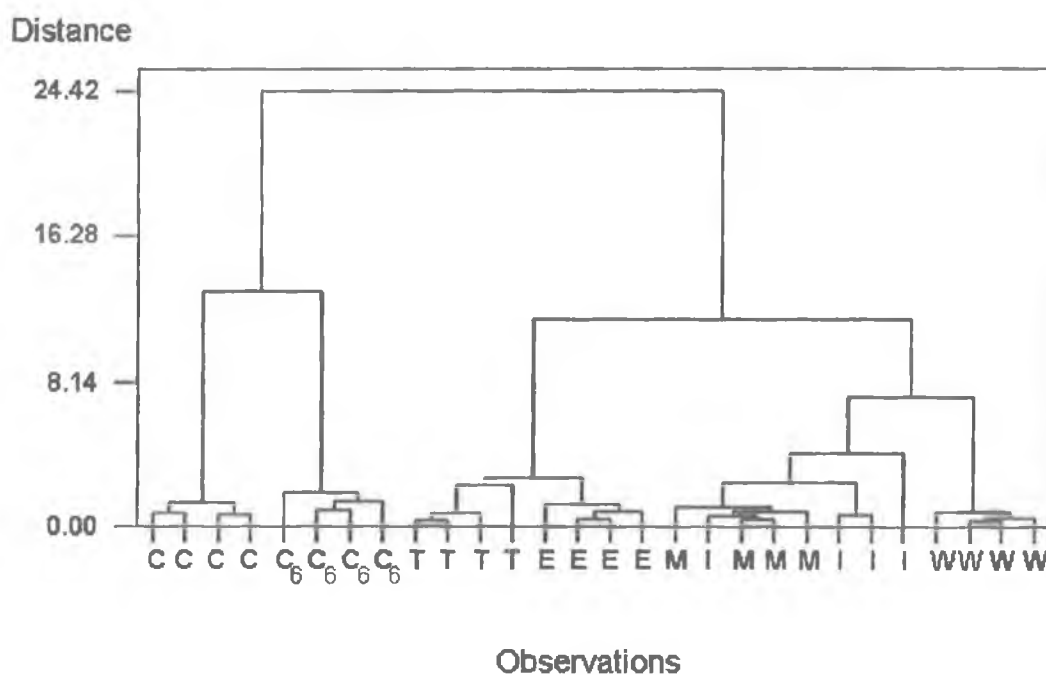
Figure 5-20: Dendrogram of Solvents, based on raw data, using Single Linkage method with Euclidean Distances (C = Chloroform, C₆ = Cyclohexane, T = Toluene, E = Ethyl Acetate, M = Methanol, I = propan-1-ol, W = Water)

5.3.3.2   DFA

Discriminant function analysis is a technique that requires information about the identity of the data so as to generate a rule, which will classify future additions to the data set. Therefore it will use a cross validation technique to authenticate its findings. Table 5-3 details the results of the analysis with cross-validated points included (in parenthesis). The technique set up a rule that will classify any future data, with a 100% success rate.

	C.Hex	CHCl$_3$	EtOAc	Tol	IPA	MeOH
C.Hex	4 (4)	0 (0)	0 (0)	0 (0)	0 (0)	0 (0)
CHCl$_3$	0 (0)	4 (4)	0 (0)	0 (0)	0 (0)	0 (0)
EtOAc	0 (0)	0 (0)	4 (4)	0 (0)	0 (0)	0 (0)
Tol	0 (0)	0 (0)	0 (0)	4 (4)	0 (0)	0 (0)
IPA	0 (0)	0 (0)	0 (0)	0 (0)	4 (4)	0 (0)
MeOH	0 (0)	0 (0)	0 (0)	0 (0)	0 (0)	4 (4)
Count	4	4	4	4	4	4
N Correct	4 (4)	4 (4)	4 (4)	4 (4)	4 (4)	4 (4)
Proportion	1.00	1.00	1.00	1.00	1.00	1.00

Table 5-3: Details of Discriminant Function Analysis (with cross-validated entries in parenthesis)

As an example the first set of 7 samples, usually the least accurate, were treated as unknowns and were submitted for testing. Figure 5-21 shows that these unknowns were successfully classified. A dendrogram was generated, using CA techniques as described above **(B)**, based on the derived factors (Figure 5-22). The unknowns, indicated using an asterisk, were successfully discriminated for each solvent examined.

145
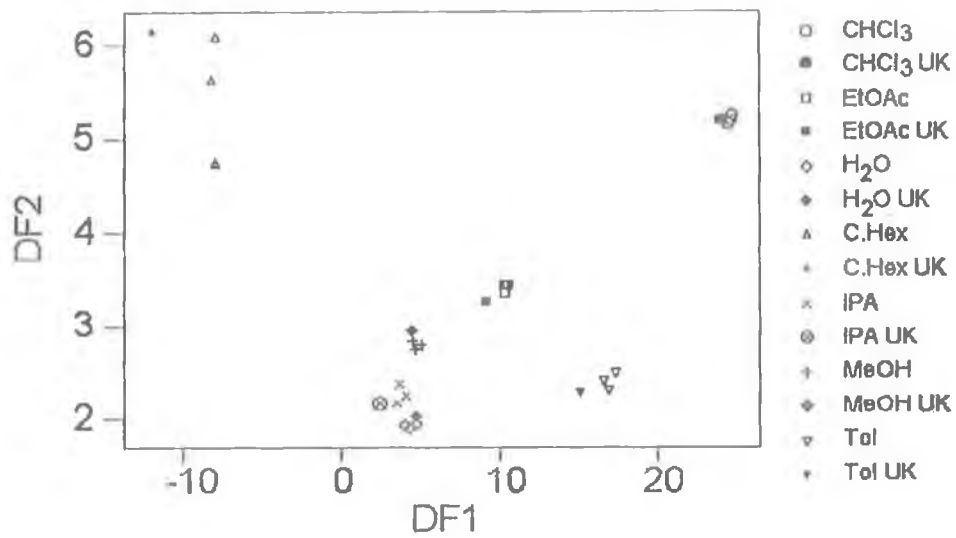
Figure 5-21: DFA plot of solvent classification (Unknown test samples are denoted by UK)
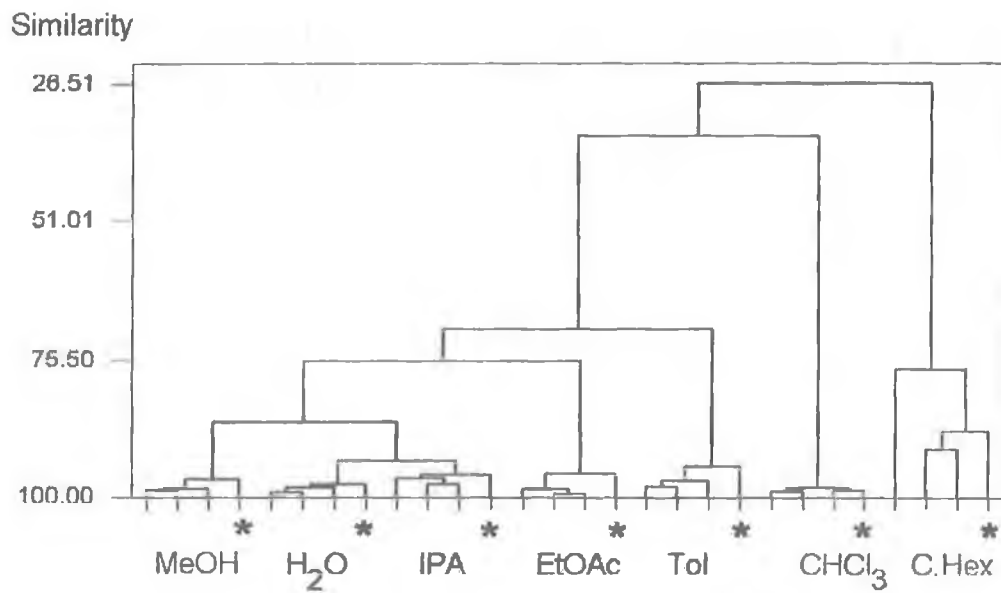
Figure 5-22: CA plot of solvent classification based on Discriminant Factors 1 & 2 (Unknown test samples are denoted by *)

5.4 Conclusion

The sensors have worked very well and succeeded in discriminating the solvents used.

The bulk of the work carried out, made use of only two salts for the initiation of the polymer. However there are several others that may be used, *e.g.* sulphates, nitrates, and phosphates *etc.* The only problem that has to be taken into consideration is the cost that would be involved, as sensors cannot be recycled after use. Initial work into ferric sulphates, nitrates, and phosphates has been carried out but no comparative conclusions can yet be drawn.

Polypyrroles have proven to be an interesting type of gas sensor with PMPY being particularly suitable as a possible aromatic sensor. Incorporation of these sensors into an array, with the likes of PIB, PEG, OV17 *etc.*, would be very attractive for future applications.

5.5 References

1   Morrison & Boyd (Ed.), Organic Chemistry (6th Edn.), Prentice-Hall International, NJ (USA). 1992
2   R.A. Jones in A.R. Katrizky and A.J. Boulton, eds., *Advances in Heterocyclic Chemistry*, Vol. 11. Academic Press, Inc., NY (USA), 1970, P.386
3   A.G. MacDiarmid. Polyaniline and Polypyrrole: where are we headed?, *Synthetic Metals*, **84** (1997) 27-34
4   D. Hodgins, The development of an electronic nose for industrial applications, *Sensors and Actuators B*, **26-27** (1995) 255-258
5   J.E.G. de Souza, B.B. Neto, F.L. de Santos, C.P. de Melo, M.S. Santos, T.B. Ludermir, Polypyrrole based aroma sensors, *Synthetic Metals*, **102** (1999) 1296-1299
6   L.X. Wang, X.G. Li, Y.L. Yang. Preparation, properties and applications of polypyrroles, *Reactive and Functional Polymers*, **47** (2001) 125-139

Chapter 6

6 Calixarenes as BAW Sensor Coatings

Abstract:

A study of Calixarenes as sensitive coatings for BAW's is presented. Calixarenes of varying upper and lower rim substituents were examined as possible coating materials, to compliment established gas chromatography stationary phase coatings. The calixarene sensors prove to be excellent sensors for aromatic compounds due to their high phenyl content, and display excellent stability. Incorporated as part of an array they can be used to successfully distinguish between various organic solvents, using multivariate techniques such as principal component analysis and discriminant function analysis.

6.1 Introduction

Calixarenes are a class of cyclooligomers formed via phenol-formaldehyde reactions [1]. Each calixarene contains at least four repeating phenolic units linked via methylene bridges. The calixarenes possess a vaselike cavity defined by an upper rim, lower rim and central annulus (Figure 6-1). With these well-defined cavities and potential wide variation of polarity of the upper and lower rims, calixarenes can form inclusion complexes with a wide range of guest molecules [2].
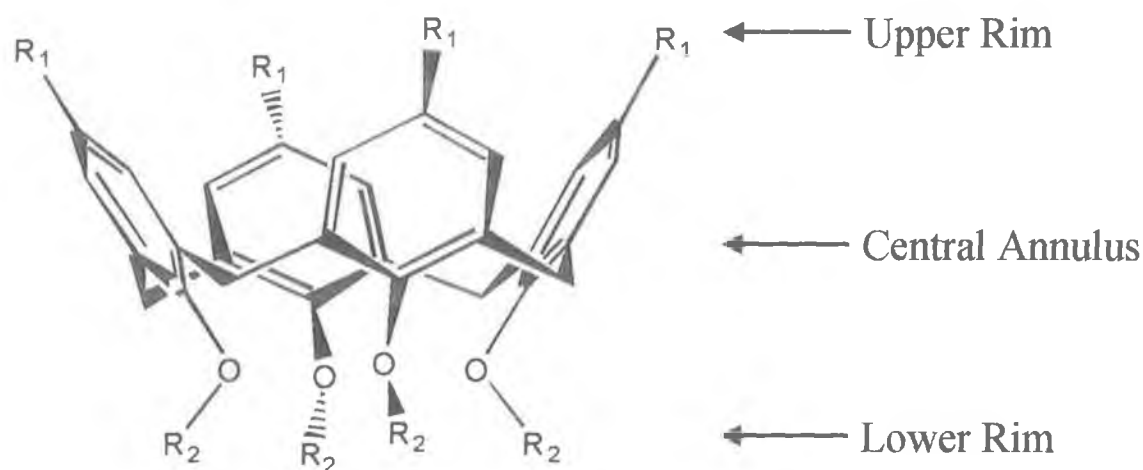
Figure 6-1: Generic Structure of a Calix[4]arene

148

Calixarenes, together with cyclodextrins and paracyclophanes, have been identified as possible supramolecular receptors in gas sensing materials [3]. Due to their superior steric flexibility, and aforementioned polarisable cavities, calixarenes are seen as an ideal sensing material for aromatic molecules. However, up to now this family of sensing materials is better known for liquid phase sensing [4, 5, 6, 7]. In particular, large ring calixarenes, such as Calix[8]arenes have been examined, in conjunction with butadiene, as sensors for water insoluble chemicals, possibly released into the environment from marine accidents [8]. In a more recent study the same authors claimed t-butyl calix[8]arene to be more sensitive for organic solvents (PER, CHCl$_3$, Toluene *etc*.) in aqueous media, than other functionalised calix[8]arenes [9]. Thiolated calixarene monolayers were examined as a selective BAW sensing material for various alkylbenzenes [4], and their analyte interactions were reportedly dominated by the upper rim ligands, as the lower rim was strongly bonded to the gold electrode surface.

Calixarenes have also been used on BAW's to investigate host-guest interactions in vapour phase [10]. The results suggest that calixarene derivatives interact strongly with aromatic compounds via π-π interactions. The electron rich aromatic fragments of the calixarene annulus provide an excellent environment for stabilisation of simple aromatic molecules within the cavity. This key and lock model is supported by molecular modelling data, although it assumes a 1:1 host-guest complex.

Gas phase detection using surface acoustic wave (SAW) devices has made use of charged calixarene species as sensitive coatings [11]. These calixarene coatings showed increased selectivity to organic vapours when compared to poly(sodium 4-styrenesulfonate) and poly(diallyl-dimethyl-ammonium chloride).

Studies of calixarenes as GC stationary phase materials have shown that t-butyl calix[4]arenes are sensitive to alkylbenzenes [12]. *p-tert*-Butylcalix[4]arene was used as a coating material in a micropacked GC column, and was found to successfully discriminate between aromatic benzene and aliphatic cyclohexane and n-hexane. This discrimination is attributed to the interaction of the benzene ring with the calixarene cavity. The same study showed similar retention was seen for various alkyl derivatives (toluene, n-butylbenzene, *p*-xylene). However steric

149

hindrance was considered as the reason for comparatively lower retention times of *o*-xylene, *o*-ethyltoluene compared to isopropyl or more bulky substituents on the benzene ring.

In this chapter a series of calixarenes were used to investigate the effects of variations in ring sizes to the host-guest interactions with different gas molecules. The effects of different substituents in upper and lower rim are also examined.

The sensors were evaluated for vapour response in a static mode and a selection of these was incorporated into an array, with established sensors coated with GC stationary phase materials, for dynamic sampling and discrimination of organic solvents.

6.2   Experimental

6.2.1   Materials and Chemicals

For this body of work new 11MHz AT-cut quartz crystal resonators (Hosonic, Taiwan) were used for sensor fabrication. All solvents used were purchased from Labscan (Dublin, Ireland) and were of analytical grade

The calixarenes used are detailed in Table 6-1, with the substituents R_1 and R_2 indicated in Figure 6-1. Calix[4]arene, t-butyl-Calix[4]arene, t-butyl-Calix[6]arene, and t-butyl-Calix[8]arene were purchased from Sigma-Aldrich (Dublin, Ireland), while t-butyl calix[4]arene tetra acid, t-butyl calix[4]arene tetra ester, t-butyl calix[4]arene ethoxy alcohol, t-butyl calix[4]arene tetra phosphine oxide, t-(2-hydroxy ethyl)-calix[4]acid, t-(2-hydroxy ethyl)-calix[4]ester, Allyl calix[4]arene, Calix[4]arene tetra oxy allyl were synthesised in house in accordance with literature [13,14]. PIB, PEG 1540, OV17 and CA were purchased from Sigma-Aldrich (Dublin) and were of general grade.

150

Sensor Number	Compound [] denotes the number of ring units in the compound	Upper Rim R_1	Lower Rim R_2
I	calix[4]arene	H-	-H
II	t-butyl calix[4]arene	$(CH_3)_3C-$	-H
III	t-butyl calix[6]arene	$(CH_3)_3C-$	-H
IV	t-butyl calix[8]arene	$(CH_3)_3C-$	-H
V	t-butyl calix[4]arene tetra acid	$(CH_3)_3C-$	- CH_2COOH
VI	t-butyl calix[4]arene tetra ester	$(CH_3)_3C-$	- CH_2COOEt
VII	t-butyl calix[4]arene ethoxy alcohol	$(CH_3)_3C-$	-$(CH_2)_2OH$
VIII	t-butyl calix[4]arene tetra phosphine oxide	$(CH_3)_3C-$	-$PO(Ph)_2$
IX	t-(2-hydroxy ethyl)-calix[4]acid	$HO(CH_2)_2-$	- CH_2COOH
X	t-(2-hydroxy ethyl)-calix[4]ester	$HO(CH_2)_2-$	- CH_2COOEt
XI	Allyl calix[4]arene	CH_2CHCH_2-	-H

Table 6-1: Formulae of Calixarenes used
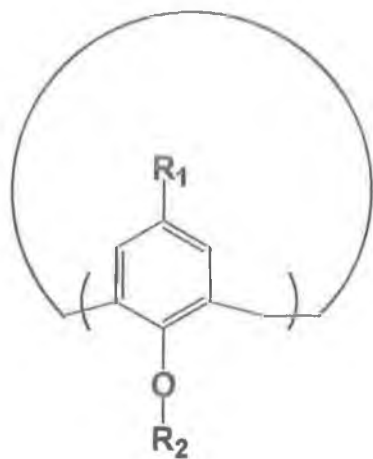
Figure 6-2: Schematic form of a calix[n]arene

6.2.2 Sensor preparation

The BAW's were washed with MeOH and allowed to dry in air. The crystals were then spray-coated with calixarene solutions (0.1% m/v, $CHCl_3$). The calixarene loading was around 3000Hz as measured by the QTS instrument, in real time.

6.2.3 Surface Analysis

Confirmation of the coating success was examined by FT-IR reflectance spectroscopy. A blank crystal was placed in a HATR setup, and a reference spectrum obtained. Then the crystal was coated as described above and its coated reflectance spectrum was compared to the earlier blank spectrum. The resulting difference was compared to an absorbance IR of the calixarene in KBr, to confirm the existence of the coating.

6.2.4 Comparative studies

Calixarenes can be functionalised on the upper and lower rims, or both. A range of calixarenes with varying functionalities were firstly compared in static mode using set volumes of solvent, and then an optimum set were incorporated into an array for dynamic headspace vapour sampling.

6.2.5 Batch Sensor Calibration procedure

The QTS instrument was modified to allow for batch sensor calibration in an airtight sampling chamber of fixed volume as detailed in Chapter 3. Aliquots of volatile analytes, calculated to give 100 ppb when vapourised within the flask, were injected through the septum into the sampling chamber. The stabilised response of the sensor to each injection, considered to be when the baseline variation was $\pm1Hz$ over 30s, was recorded. The system was then purged with N_2 for 2 min or until the sensor response returned to baseline before subsequent injections. Triplicate injections of each sample were made, and the process repeated for 3 sensors of each type. The responses and sensitivities of each calixarene sensor was then compared on the basis of:

    (A)   Cavity Size

    (B)   Upper Rim Substituents

    (C)   Lower Rim Substituents

    (D)   Both Upper and Lower Rim Substituents

6.2.6 Array configuration and dynamic sampling

4 GC stationary phase coated sensors (PIB, PEG 1540, OV17 and Cellulose acetate), 3 chosen calixarene sensors and one uncoated crystal (sampling reference) were incorporated into the array housing as introduced in Chapter 3. The sensors were exposed to vapours as before and the response of the exposed array, relative to the exposed reference, was exported to MS Excel and Minitab for analysis.

6.3 Results and Discussion

6.3.1 FT-IR of sensor surface

To confirm the presence of the calixarenes on the surface, an uncoated crystal was used as a blank for reflectance IR spectra, using the HATR. When this crystal was spray coated with calixarene **V**, a comparative IR was taken (Figure 6-3). The spectrum acquired was then compared to the same calixarene sample in a KBr disk (Figure 6-4). As the level of light being reflected by the gold surface is quite small the strength of signal seen is weaker that that of the transmittance spectrum. However the same peaks can be seen in the 1000cm^{-1} to 1300cm^{-1} region, confirming the calixarene presence on the surface.
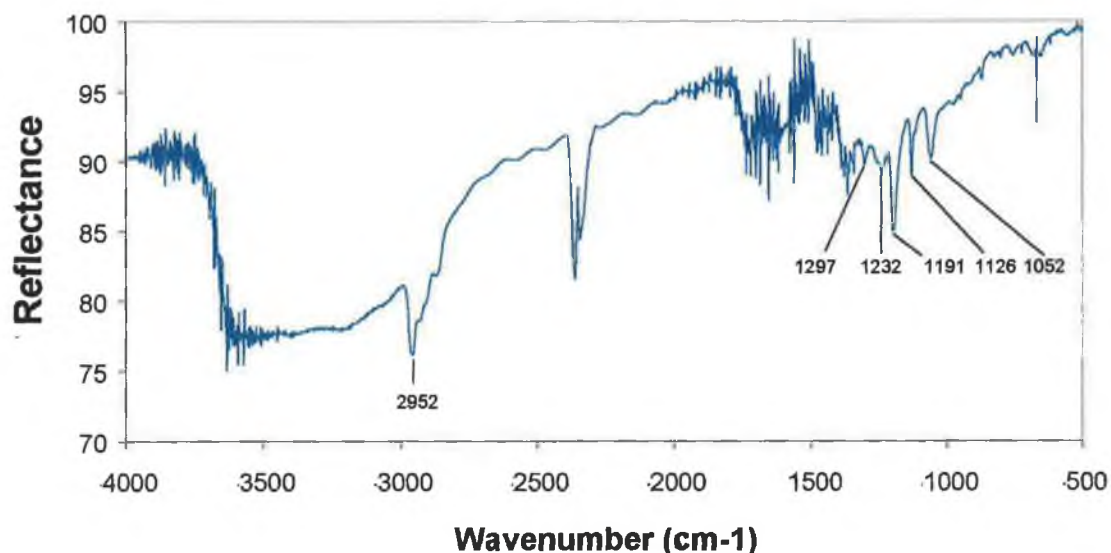
Figure 6-3: FT-IR reflectance spectrum for a Calix V coated BAW

153
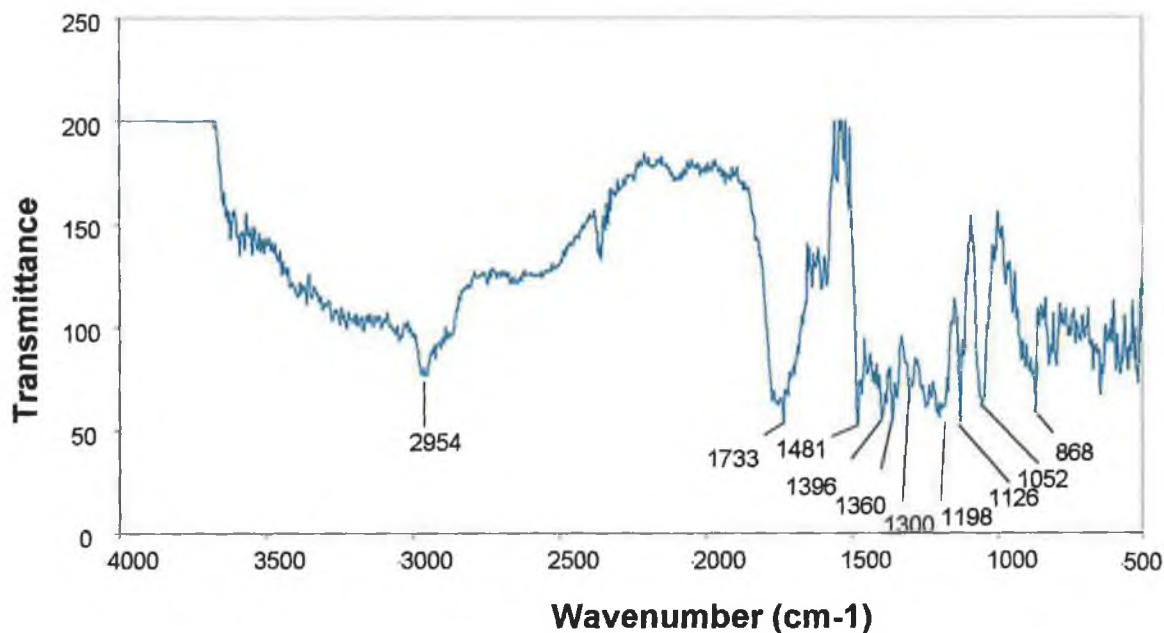
Figure 6-4: FT-IR transmittance spectrum for a Calix V / KBr disk

6.3.2 Batch Calibration of Single Sensors

The combined responses to individual 100 ppb concentrations of seven VOC's (acetone, chloroform, cyclohexane, ethyl acetate, n-hexane, methanol, and toluene) were used to characterise each sensor. All solvents vaporised immediately upon injection into the magnetically stirred environment because of the small sample volume used. When the responses of the sensors to a set of solvents were compared, it was found that the response pattern generated by all the calixarenes were consistent (Table 6-2). The largest typical response came from toluene, followed by chloroform, cyclohexane or ethyl acetate, n-hexane, acetone and finally methanol. As in Chapter 4, the strength of coating-vapour interactions can be discussed using Linear Solvation Energy Relationships (LSER's), and as the response pattern was fairly consistent for all sensors it could be argued that there is no difference between them. To investigate this it is necessary to compare the sensors as outlined in Sec 6.2.5

154

		I (a)	I (b)	I (c)	II (a)	II (b)	II (c)	III (a)	III (b)	III (c)	IV (a)	IV (b)	IV (c)	V (a)	V (b)	V (c)	VI (a)	VI (b)	VI (c)
Cyclohexane	Mean	50.0	36.0	4.7	142.3	129.7	142.7	140.0	129.7	135.0	128.3	122.7	130.3	165.0	126.0	164.0	164.7	92.3	N/A
	±%RSD	22.7	7.3	61.9	6.3	5.8	6.7	6.1	6.6	5.6	1.6	2.5	3.5	2.1	7.9	4.6	2.1	121.5	N/A
n-Hexane	Mean	21.0	27.3	21.3	46.7	52.7	55.0	54.3	53.0	47.0	66.0	60.0	56.3	65.7	52.0	62.3	64.3	59.3	N/A
	±%RSD	4.8	15.2	7.2	5.4	6.7	6.3	9.3	5.0	5.6	10.6	16.9	2.0	7.5	5.1	4.9	3.9	1.9	N/A
Ethyl Acetate	Mean	70.7	52.0	26.7	112.0	105.3	114.0	116.0	95.0	111.3	128.0	112.7	129.0	165.7	137.3	162.3	157.3	139.3	N/A
	±%RSD	32.9	10.2	30.3	2.7	3.6	3.8	4.6	21.0	1.9	0.0	1.8	7.9	8.0	4.4	5.7	1.0	6.2	N/A
Acetone	Mean	38.7	29.7	13.7	37.0	39.7	42.0	43.0	45.0	36.0	49.3	38.3	44.0	60.3	43.3	52.3	63.0	57.3	N/A
	±%RSD	20.9	57.6	125.1	8.1	5.2	4.8	4.0	9.7	4.8	1.2	9.2	7.9	15.4	7.1	2.9	8.2	10.7	N/A
Chloroform	Mean	61.0	50.0	38.3	193.0	177.0	207.0	203.3	179.7	320.3	248.7	281.3	265.7	272.0	211.7	276.7	327.0	381.0	N/A
	±%RSD	1.6	8.7	4.0	1.0	10.2	7.6	8.5	8.4	54.3	2.6	1.1	8.3	1.7	3.5	7.1	3.2	2.7	N/A
Methanol	Mean	32.3	34.0	30.7	15.0	23.3	20.7	18.7	16.3	19.0	38.0	32.3	17.7	48.0	29.0	31.0	27.7	29.7	N/A
	±%RSD	17.0	10.6	13.6	58.1	13.1	19.6	12.4	37.4	19.0	22.8	38.2	76.9	11.0	9.1	14.8	20.6	10.3	N/A
Toluene	Mean	152.7	172.3	201.3	482.0	586.3	497.7	498.7	585.7	485.0	554.3	528.3	715.7	558.7	451.7	519.7	836.3	792.3	N/A
	±%RSD	1.0	3.5	2.5	5.6	0.7	1.3	1.1	0.8	4.7	2.9	4.0	2.6	10.6	5.1	2.8	2.2	4.5	N/A

		VII (a)	VII (b)	VI (c)	VIII (a)	VIII (b)	VIII (c)	IX (a)	IX (b)	IX (c)	X (a)	X (b)	X (c)	XI (a)	XI (b)	XI (c)
Cyclohexane	Mean	122.7	118.0	104.7	122.3	86.7	161.7	182.7	174.0	N/A	101.3	137.7	109.7	82.7	79.0	57.3
	±%RSD	1.7	5.3	1.5	6.7	4.7	3.4	2.6	3.0	N/A	5.4	1.8	7.1	27.0	7.9	11.2
n-Hexane	Mean	82.7	44.3	32.7	53.0	43.0	77.7	69.0	75.0	N/A	149.3	179.3	91.7	14.0	40.3	14.3
	±%RSD	62.2	4.7	1.8	8.2	10.7	2.0	2.9	5.8	N/A	6.6	6.4	59.3	12.4	8.0	4.0
Ethyl Acetate	Mean	133.7	105.7	85.3	94.7	84.3	147.0	55.7	70.7	N/A	118.0	145.7	115.3	51.3	71.7	54.0
	±%RSD	4.3	2.4	4.4	13.5	4.8	3.0	30.8	2.9	N/A	2.5	1.6	1.8	5.6	2.1	3.7
Acetone	Mean	53.3	42.3	30.3	45.0	38.0	70.7	15.3	31.0	N/A	46.7	41.0	34.3	18.7	31.7	25.0
	±%RSD	2.9	3.6	3.8	10.2	0.0	3.6	21.0	9.7	N/A	6.2	18.4	14.4	3.1	7.3	4.0
Chloroform	Mean	187.0	179.3	167.7	223.3	197.7	310.7	73.3	127.0	N/A	168.7	249.3	201.7	96.3	30.3	100.0
	±%RSD	1.6	7.8	3.4	2.5	3.3	4.3	26.8	2.1	N/A	3.4	4.1	2.5	4.7	13.7	2.6
Methanol	Mean	53.3	29.3	26.0	85.0	69.7	125.7	9.3	24.3	N/A	42.0	47.3	48.3	15.3	103.3	20.3
	±%RSD	4.7	2.0	6.7	1.2	4.6	0.5	89.2	8.6	N/A	20.6	14.8	6.0	18.8	4.0	14.2
Toluene	Mean	556.3	517.0	342.3	451.3	318.7	658.0	739.7	496.0	N/A	453.0	480.7	480.0	110.3	338.0	174.0
	±%RSD	2.2	30.8	12.0	3.5	7.7	1.3	2.2	4.7	N/A	2.1	3.7	1.3	6.2	11.4	6.8

Table 6-2: Mean responses and standard deviations obtained from 3 sensors (a, b, c) of each coating (see Table 6-1), in triplicate.

6.3.3 Linear Solvation Energy Relationships

Linear Solvation Energy Relationships have already been introduced in Chapter 4, but the general equation is given again (Equation 6-1), and a summary of the relevant solute parameters is given in Table 6-3.

$$\text{Log } K = c + rR + s\pi^2 + a\Sigma\alpha + b\Sigma\beta + \text{Log}(L^{16})$$

Equation 6-1

Solute	R	π^*	α	β	$\text{Log}(L^{16})$	V.P. (Kpa) (@ 298K)	C_g (ppm)
Toluene	0.601	0.52	0	0.15	3.325	3.79	140.9
Chloroform	0.425	0.49	0.15	0.02	2.48	26.2	1262.4
Cyclohexane	0.305	0.1	0	0	2.964	13.0	441.6
Methanol	0.278	0.44	0.43	0.47	0.97	16.9	218.6
Acetone	0.179	0.7	0.04	0.49	1.696	31.6	739.8
Ethylacetate	0.106	0.62	0	0.45	2.314	12.6	448.0
n-Hexane	0	0	0	0	2.668	20.7	720.0

Table 6-3: Summary of solute parameters

Toluene was expected to give the biggest response because of the potential of the aromatic cage of the calixarenes to form electrostatic interactions with the aromatic analyte, via their delocalised π electron systems, as its R value suggests. However there is also the possibility that binding may occur on the exterior of the cavity aswell as the interior. Cyclohexane is roughly similar in proportion to toluene but lacks the same ability to form electostatic interactions, and the transient dispersion (hydrophobic) interactions were responsible for majority of the sensor response. This resulted in a much smaller response, of only 20-30%, compared to toluene.

The calixarenes responded relatively well to the highly polar hydrophobic chloroform. This polar molecule is much smaller in size than toluene but the highly polarisable aromatic cavity is able to stabilise the strong dipole. n-Hexane being sterically longer than cyclohexane cannot interact with the inside of the cavity like its cyclic counterpart, and hence has a lower response.

The polarisable ethyl acetate and acetone can interact with the calixarenes through hydrophobic and polar components and may have the right size or conformation to fit into the cavity. The sensors responded well to these VOC's. Methanol, being hydrophilic and relatively small, produced the least response with the calixarene based sensors.

6.3.4 Sensor Stability

The stability of the sensors was demonstrated by passing ambient air (160ml/min) over the sensors for over three hours. Very little drift in baseline was observed, with most sensors having a drift of less than 5Hz. For certain sensors, such as **IV** (t-butyl-calix[8]arene), noise was at the bit resolution of the system (1Hz), and a total drift of 2 Hz over a sampling period of 3 hours was observed (Figure 6-5).
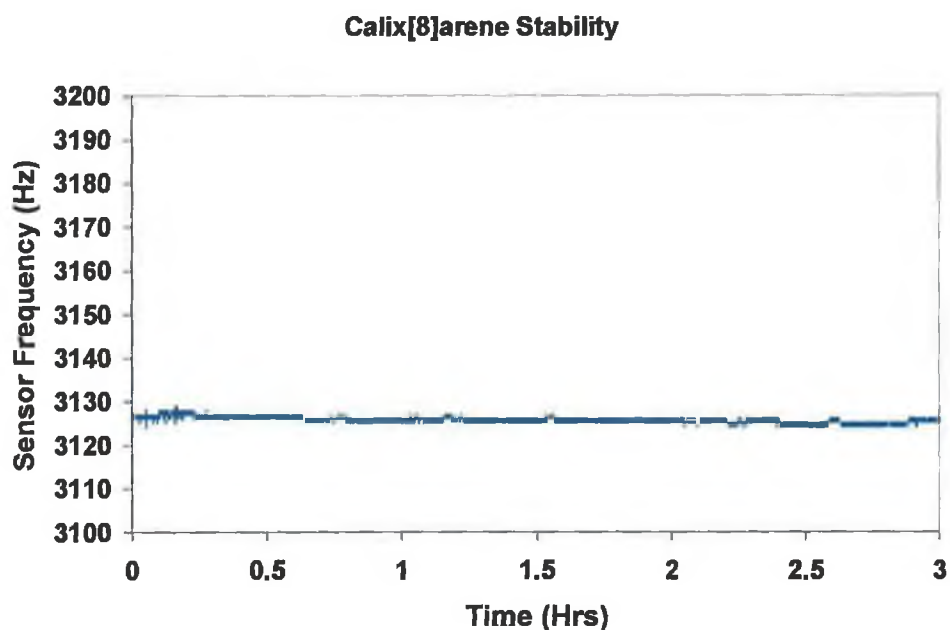
Calix[8]arene Stability

Figure 6-5: Sensor stability over a 3 hr period of ambient air sampling

6.3.5 Cavity Size

A comparative study between calixarenes of increasing cavity size (4-, 6- and 8- ring units) revealed that there was no significant difference in the selectivity to the set of VOCs tested (Figure 6-6). Sensitivity however displayed trends that were expected of the compounds. Essentially, the bigger the cavity size the bigger the response. This trend is true for most solvents except for cyclohexane.

The responses of the calixarene based sensors to toluene, the best-fitted guest molecule, was examined closely. They were evidently size-dependent and decreased with respect to the descending ring unit of 8>6>4 (Figure 6-6). It could be simply explained as the ease with which the guest molecule entered and left the cavity.

The conformation of the cavity may also have contributed to the stability of the host-guest complex. It has been proposed that the most stable conformation for the t-butyl-calix[8]arene is in the alternate (chair) formation (Figure 6-7), which probably best facilitates the guest–cavity interactions as the distances between the 'cavity walls' and the planar guest molecule are shorter in this conformation [3]. This may explain the higher response of cyclohexane to t-butyl-calix[6]arene than the t-butyl-calix-[8]-arene where the elongated cavity is in effect about the same size as t-butyl-calix-[4]-arene and the entrance of the "big" cyclohexane molecule is somewhat restricted.
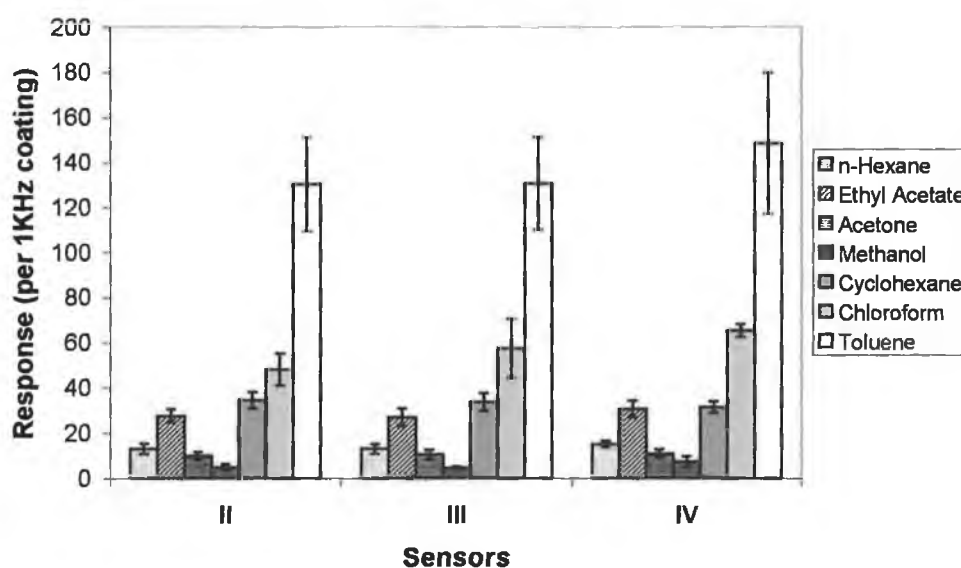
Figure 6-6: Cavity size study showing the mean response of sensors II, III, IV (t-butyl-Calix[m]arene where m=4,6,8) towards 100 ppb concentrations of selected solvents, with standard deviations represented by error bars (n=3).

158
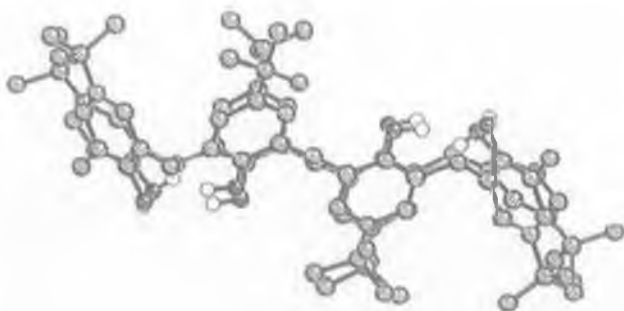
Figure 6-7: Alternate chair conformation of t-butyl Calix[8]arene (Reprinted from [3])

6.3.6 Lower Rim Substitution

An investigation was carried out into the effect of lower rim substitution. The cavity size was fixed to 4 ring units and the 4 upper rim substituents were tertiary butyl ligands. The sensors examined were **II, V, VI, VII, VIII** (Figure 6-8).

Figure 6-8: Lower rim study showing the mean response of sensors II, V, VI, VII, VIII towards 100 ppb concentrations of selected solvents, with standard deviations represented by error bars (n = 3).

The sensors were selective to the aromatic toluene indicating that the substituents were not affecting the prime selectivity of the calixarene based sensors. However, most sensors based on upper rim substituted calixarenes gave higher responses to solvent vapours than the unsubstituted analogue (**II**), with the exception of cyclohexane (Figure 6-8). The results suggested that the presence of ligands might promote the interactions between the host and guest molecules. The mode of this improvement is not clear but one explanation might be that the bulky ligands upset the arrangement of the calixarenes on the surface thus creating some more active binding sites.

While there is little difference in the overall selectivity between the sensors it is important to notice the high response of the phosphine oxide substituted calixarene (**VII**) to methanol. It may be due to the basic phosphine oxide ligands that provided stronger interactions with the protic methanol compared to all other ligands.

6.3.7   Upper Rim Substitution

Calixarenes with bulky alkyl upper rim substituents tend to be more hydrophobic and have larger cavities. Therefore it is more likely that interactions with solvent guests will occur at the upper rim rather than the lower, or outside of the cage altogether. The most stable form of calix[4]arenes is the cone formation, and a variation of the upper rim substituent would clearly result in varying responses. To this end a comparison of I, II, and XI was made (Figure 6-9).

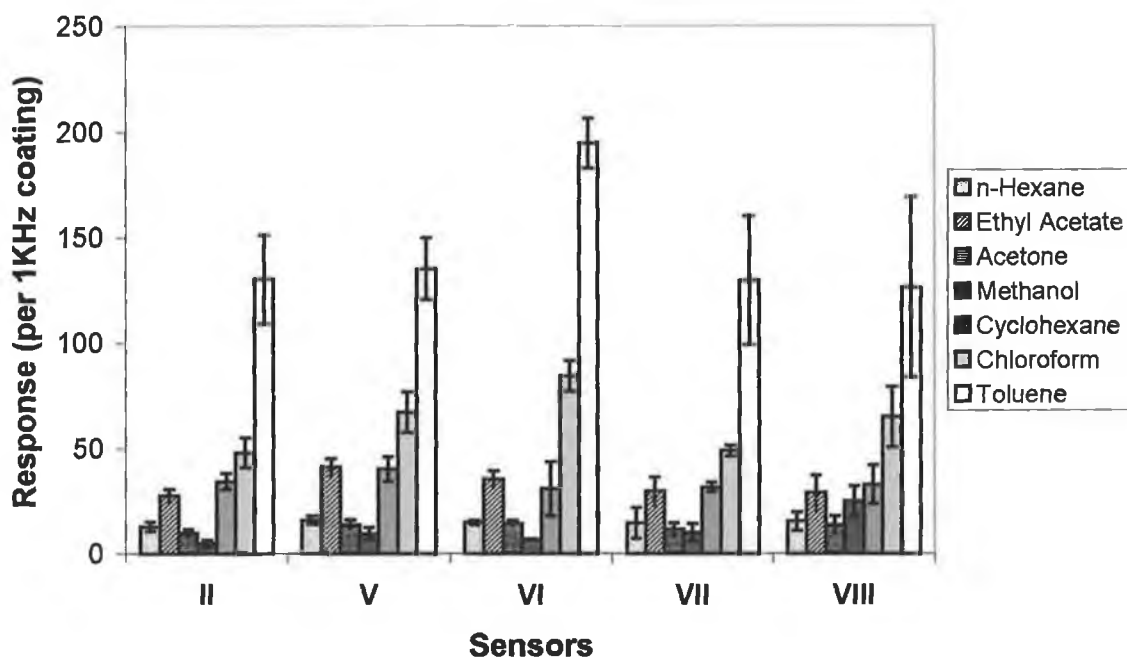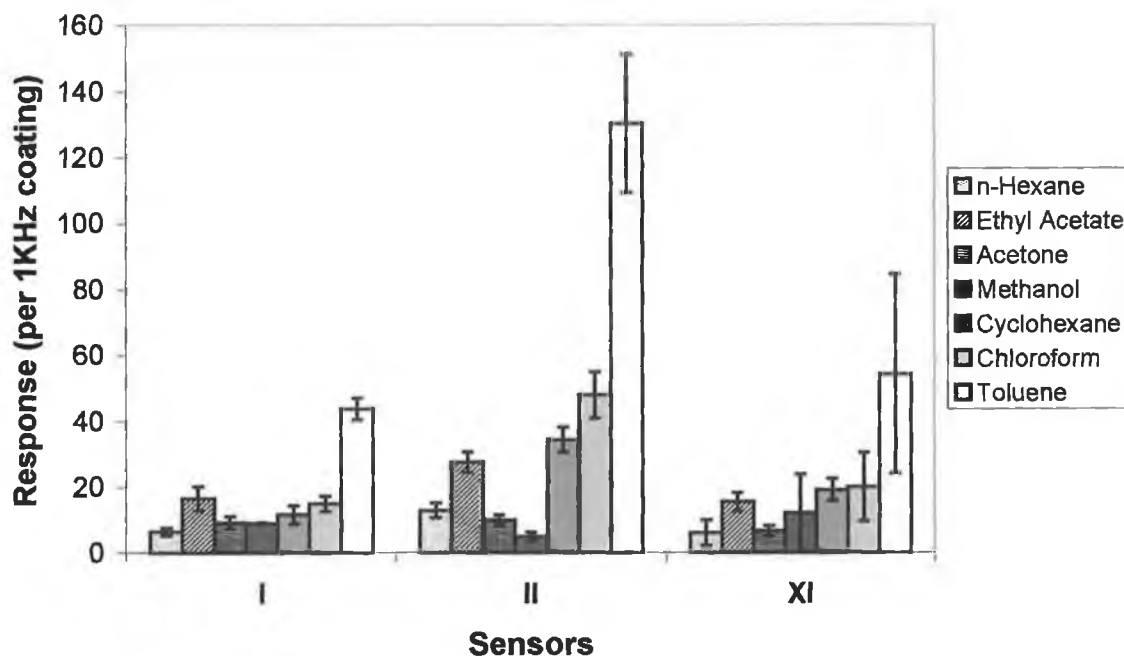**Figure 6-9: Upper rim study showing the mean response of sensors I, II, XI towards 100 ppb concentrations of selected solvents, with standard deviations represented by error bars (n = 3).**

Immediately the effect of upper rim substituents is demonstrated. The sensitivity of **II** is the greatest of this test set, and it can be suggested that as **I** has no upper rim substituents the effective size of its cavity is much less than **II** and **IX**. The upper rim substituent of **II** is a hydrophobic tertiary butyl group with negligible polarisability in comparison to the allyl substituent of **IX**. Initial molecular modelling (Figure 6-10) suggests that the size difference between **II** and **IX** is small but the relative stability of the symmetric tertiary butyl ligands, in comparison to the smaller and more flexible allyl ligands, may explain the difference in their response patterns (Figure 6-9). For instance it easier for the allyl groups to rotate through the annulus than it is for tertiary butyl equivalents.
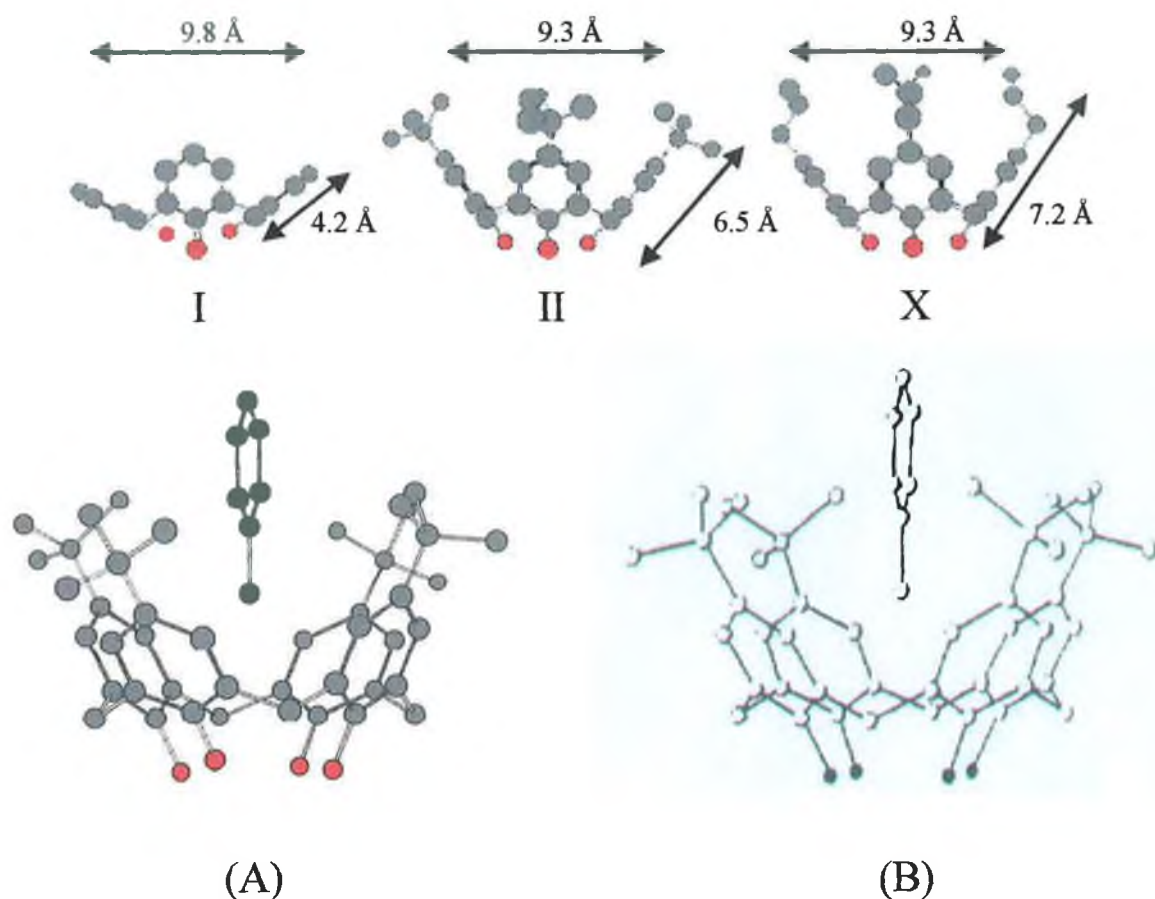
Figure 6-10: Effective Cavity sizes of I, II, and IX with (A) an energy minimised model of II interacting with toluene and (B) an X-ray image of the real solid state form of such a model ((B) is reprinted from [15])

To investigate this interaction with the upper rim, an energy minimised model (MM2) of toluene encapsulated by *p*-t-butyl-calix[4]arene was created (Figure 6-10(A)). This model was compared to X-ray data for the same calixarene recrystallised from toluene [15], and was found to be very similar (Figure 6-10(B)), suggesting that other models of VOC guests in the calixarene cavity could be reasonable representations of the host guest adduct. As can be seen from the X-ray image, toluene does not actually come into the ring and so no π-π stacking occurs. In the gas phase this may not be the case as the host-guest ratio will not be 1:1. π-π stacking or even T-bonding may occur, whereby the methyl component of toluene binds perpendicularly to the electron rich phenyl rings.

6.3.8   Upper and Lower Rim Substitution

Substitution of ethanolic groups on the upper rim for t-butyl groups of **V** and **VI** give rise to slightly different selectivity patterns.   The response to n-hexane was up to three times higher for **IX**, and two times higher for **X** than **II**, **V**, or **VI** (Figure 6-11). Initial modelling of the structures indicates that the hydroxyls on the upper rim are repelled away from the hydrophobic cavity (Figure 6-12).   The equivalent size of the cavity is then similar to the t-butyl-calix[4]arene but sterically hindered, thereby possibly allowing easier access for n-hexane to the cavity. The steric energy of **IX** was also calculated to be lower than **V**, implying a more stable molecule.
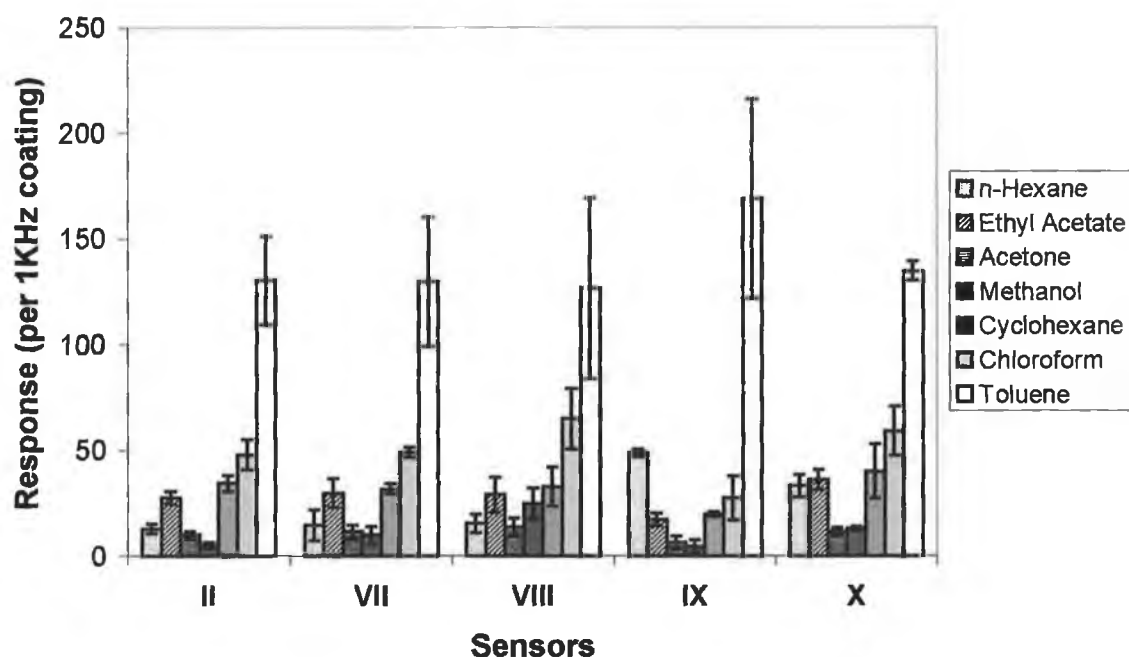

Figure 6-11: Upper and lower rim study showing the mean response of sensors II, VII, VIII, IX, & X towards 100 ppb concentrations of selected solvents, with standard deviations represented by error bars (n = 3).
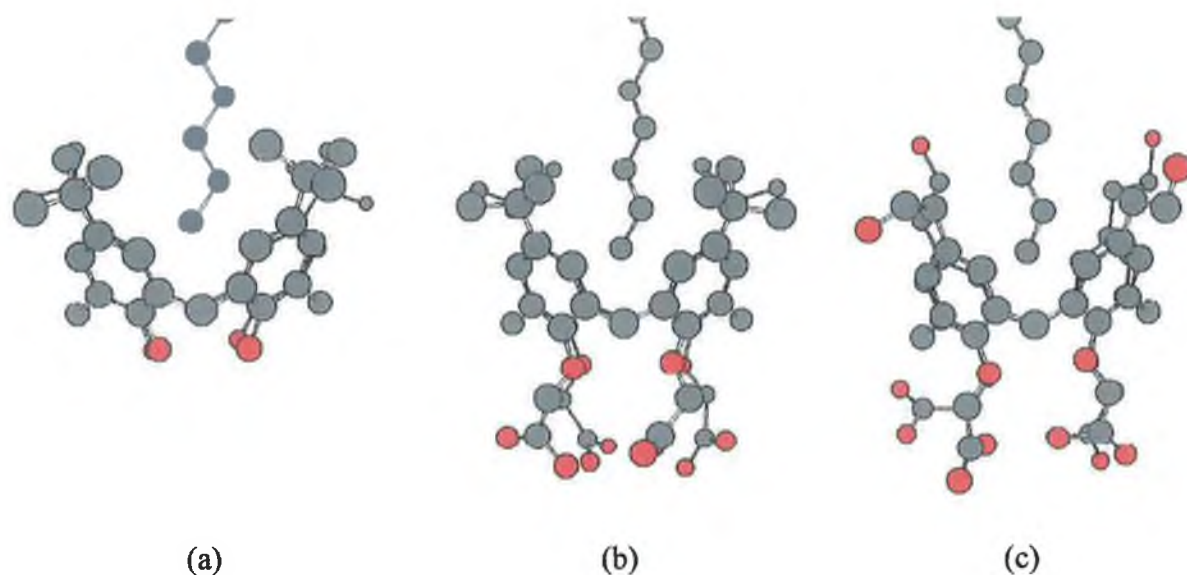
Figure 6-12: Molecular modelling image of 1:1 n-hexane interaction with (a) II (b) V & (c) IX

6.3.9   Comparison of Calixarene and GC stationary phase based sensors

A selection of 3 calixarenes based sensors (sensors **IV**, **V** and **IX**) was chosen on the basis of size (**IV**), lower rim functionality (**V**), and both upper and lower rim functionality (**IX**). These sensors were incorporated into an array with sensors coated with traditional GC phases such as PIB, PEG, OV17, and CA. Using the dynamic sampling system, the two sets of sensors were compared. As this sampling was dynamic, the concentration of 8 VOC's (chloroform, toluene, ethyl acetate, cyclohexane, n-hexane, acetone, methanol and water) in the headspace was dependant on individual vapour pressures. The response of each sensor was normalised, to that of toluene, which happened to realise the highest sensitivity for all sensors (up to 160 Hz / 100 ppm for every KHz of **IV** sensor coating). The sensitivity is expressed as the response (ΔF), per 1 KHz of coating, upon exposure to a specified concentration of the vapour (usually 100 ppm). It is clear that this array of sensors produce distinct response patterns towards VOCs (Figure 6-14). Polyisobutylene (PIB) is an amorphous hydrophobic polymer that responds favourably to aliphatic compounds through transient dispersion interactions. Therefore this sensor responded strongly to the aliphatic cyclohexane. Polyethylene glycol (PEG) is a very popular polar coating that responds strongly to highly volatile polar solvents such as chloroform. OV17 is a siloxane-based polymer with aromatic and aliphatic substitutions, hence the sensor responds well to polar and polarisable compounds.

164

The sensitivity of the typical calixarene to toluene was found to be much higher than that of the GC stationary phases (Figure 6-13). After normalising the data from Figure 6-13, relative to solvent with the maximum response (toluene), the response pattern of the calixarene towards other VOC's is clearly seen to be also different to the other stationary phases (Figure 6-14). The results suggest that the cavitand-based sensors complemented the GC stationary phase based sensors and it is therefore beneficial to incorporate such sensor within an array to increase the diversity of sensors and to promote the discrimination potential of the sensor array.
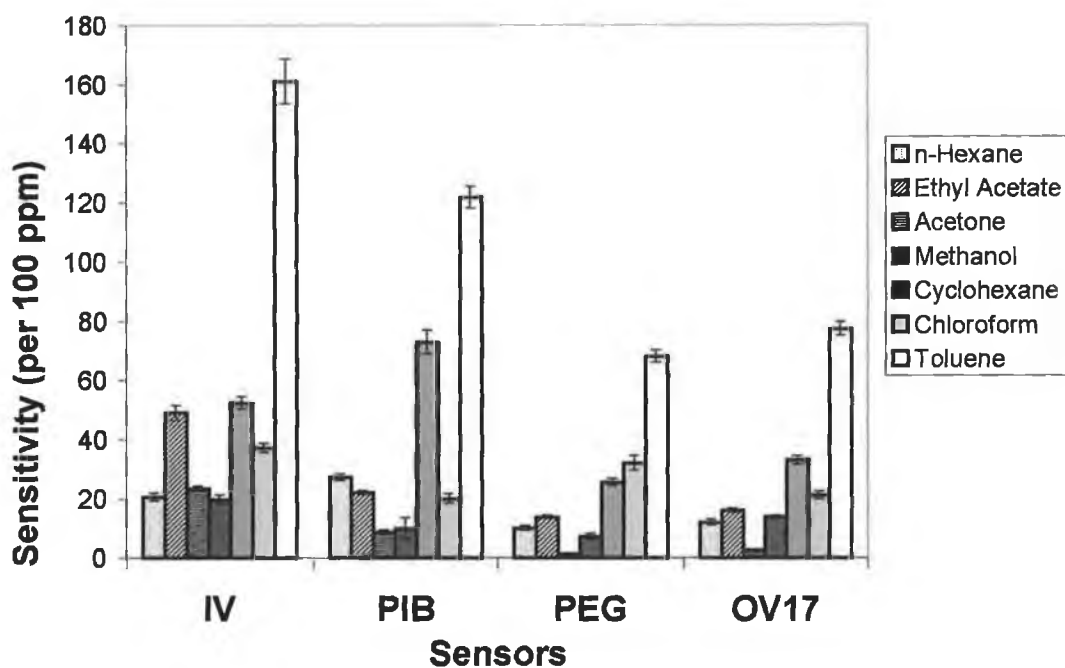
Figure 6-13: Sensitivity plot (ΔF (Hz) per 100 ppm) of a typical calixarene (IV) compared to 3 common GC stationary phases for selected solvents, with standard deviations represented by error bars (n=3).
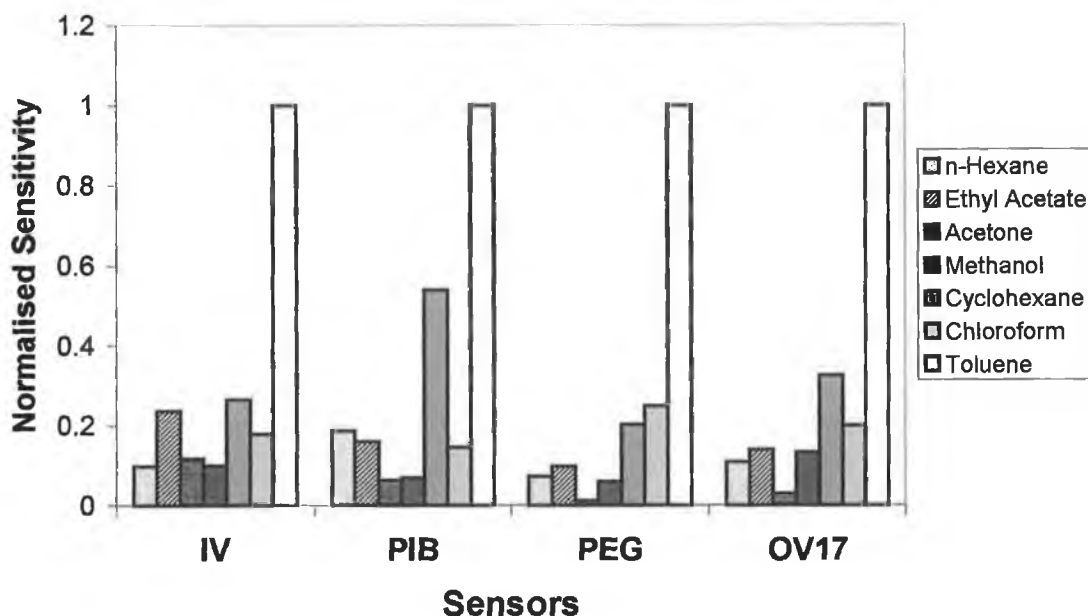
Figure 6-14: Normalised sensitivity (ΔF (Hz) per unit mass of vapour) of a typical calixarene (IV) compared to 3 common GC stationary phases

6.3.10 Correlation of static and dynamic sampling

Gas phase solvent concentrations in the dynamic setup revealed that while ambient concentration of solvents were in excess of 100 ppb, the sensors sensitivity was much higher in the static mode. The sensitivity ($\Delta f\,mol^{-1}$) was typically one order and sometimes almost two orders of magnitude better (in some cases). However even with different sensitivities the responses were consistent between the two methods (Figure 6-15) with a correlation coefficient of R^2 equal to 0.78, which improves to 0.993, if chloroform is ignored.
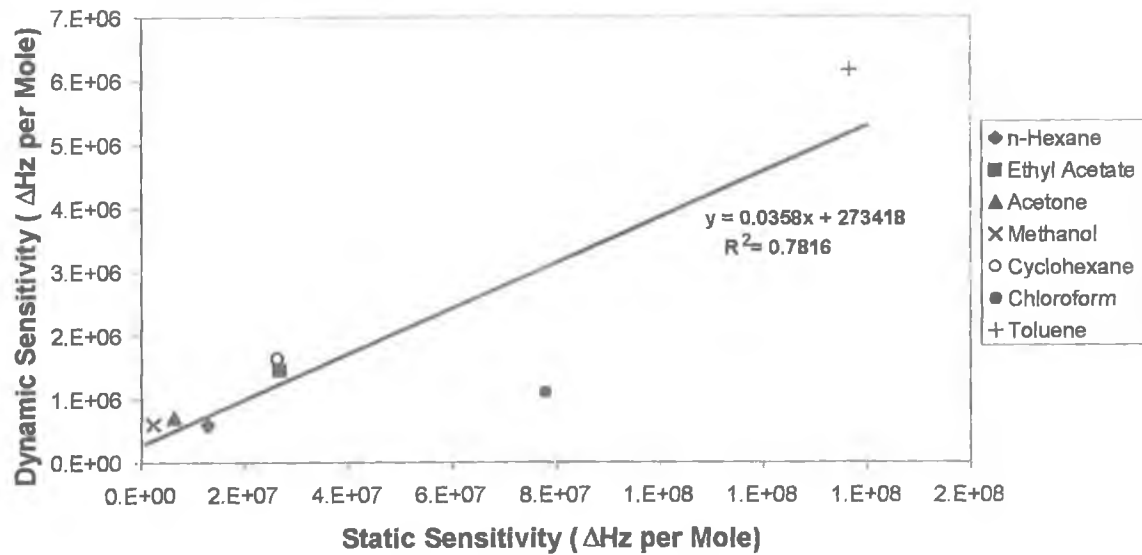
Figure 6-15: Correlation of sensor responses to VOC's in static and dynamic set-ups

6.3.11 Kinetic comparison of sensors

The standard response of an exposed BAW has been generalised in the form
Equation 6-2, as introduced in Chapter 3.

$$\text{Response} = A_0 - A_1(-e^{-K_1 t}) - A_2(-e^{-K_2 t})$$

Equation 6-2

This rate of response to solvents by the BAW sensors was determined using the
SOLVER program (also detailed in Chapter 3). As the interaction between the
sensors and the analyte is a two stage one, SOLVER was used to calculate two
different rate constants. The first constant (k_1) would represent the initial adsorption
of the analyte onto the surface, while the second (k_2) would represent the absorption
into the coating bulk. As it transpired the first rate was often magnitudes greater
than the second but had a very small A_1 value. Consequently its contribution was
often negligible in overall terms. Therefore the model was redefined, by simply
omitting the adsorption component. The rates (k_2) for each of the seven sensors are
given in Table 6-4, and the corresponding A_2 values are given in Table 6-5.

167

	PIB	PEG	OV17	CA	IV	V	IX
Acetone	0.24	2*	2*	0.40	0.23	0.27	0.16
Methanol	0.33	2*	0.26	0.36	0.24	0.26	0.23
Cyclohexane	0.17	0.18	0.20	0.17	0.23	0.21	0.19
Toluene	0.12	0.15	0.18	0.15	0.18	0.16	0.13
Chloroform	0.14	0.16	0.21	0.23	0.24	0.25	0.20
Water	0.07	0.05	0.09	0.14	0.13	0.23	0.16
n-Hexane	0.16	0.16	0.17	0.16	0.19	0.17	0.15
Ethyl Acetate	0.16	0.20	0.36	0.22	0.20	0.19	0.14

Table 6-4: Absorption rate constants for GC and calixarene sensors (* 2 was set as a maximum rate)

	PIB	PEG	OV17	CA	IV	V	IX
Acetone	64.7	12.6	20.9	155.5	170.7	181.8	102.4
Methanol	22.6	19.4	30.2	61.5	41.6	47.9	22.4
Cyclohexane	319.3	111.7	143.1	147.0	226.8	207.6	323.0
Toluene	166.9	92.7	105.2	126.3	221.3	203.5	230.3
Chloroform	242.4	383.7	252.9	276.6	450.3	415.9	380.5
Water	10.0	66.9	11.4	18.5	14.4	13.9	8.6
n-Hexane	198.7	72.9	87.0	99.0	148.2	140.2	181.2
Ethyl acetate	98.3	60.2	70.5	166.5	216.9	233.7	177.6

Table 6-5: Absorption constants for GC and calixarene sensors

Figure 6-16 shows the modelled response of t-butyl calix[4]arene tetra acid (sensor V) on exposure to ethyl acetate. The sharp rise at the start of the model is the initial adsorption, after which the absorption process takes over. From Table 6-4 it is clear that the highest rates appear to be achieved for PEG on interaction with methanol and acetone. However this is likely due to viscoelastic effects, which the model is unable to match. Although this was not observed in Chapter 4, it is not surprising. OV17, the polarisable silicone based polymer, also shows a similar problem with acetone.
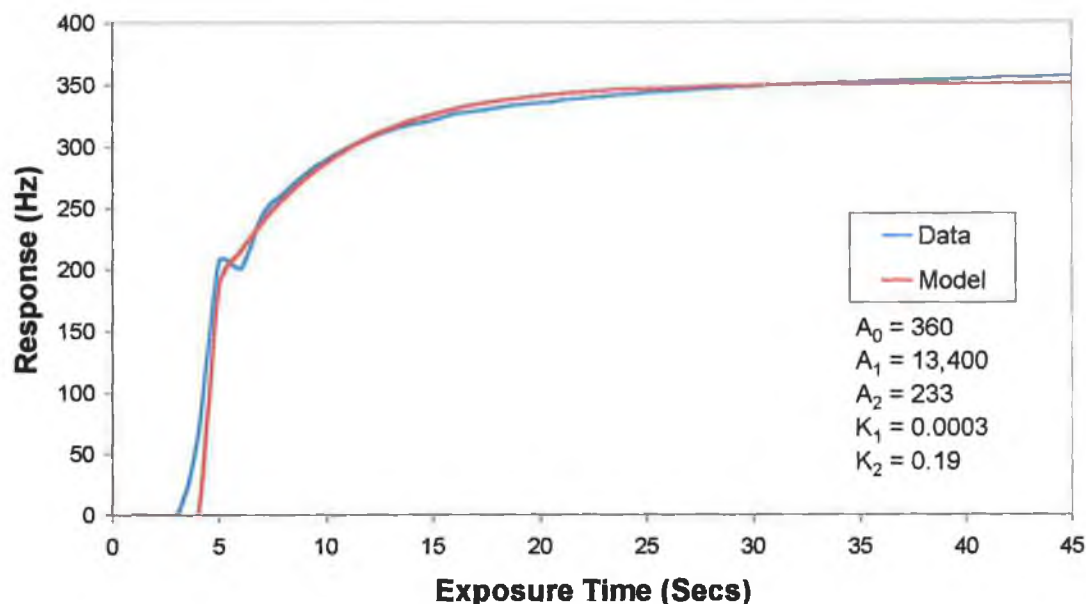
Figure 6-16: Actual and modelled response profile of V on exposure to ethyl acetate

It is also apparent that the absorption of n-hexane is slower than cyclohexane for all sensors. Indeed toluene displays the second slowest response, being only better than water. All this means is that the sensor would have taken 30 seconds to equilibrate instead of 15 or 20 seconds like the others.

Water does not have a high rate constant as would be expected. With the exception of the hydrophilic PEG, it never forms more than a monolayer (~15Hz).

6.3.12 Application in Array Sensing

Using the data generated in Sec. 6.3.9, discrimination of the VOC's was carried out using the multivariate techniques PCA, CA, and DFA as introduced previously.

The equilibrium responses at 45s were used for the multivariate analysis. Equilibrium responses were normally achieved period between 15-30 seconds, so 45 seconds was considered a safe time-slice to use for analysis.

169

6.3.13 PCA

Using a correlation matrix, the first four principal components (PC1 – PC4) were determined. When PC1 was plotted against PC2 a clear clustering into distinct groups for the appropriate samples was achieved (Figure 6-17). The array was successful in discriminating the vapours and the samples with similar functional properties were plotted in feature space that was close to each other. Hence the hydrophilic methanol clustered close to water. The polarisable carbonyl containing acetone and ethyl acetate clustered close together; and the hydrophobic alkanes, n-hexane and cyclohexane, had the highest PC2 values. The hydrophobic aromatic toluene was found between the oxygen containing clusters and the alkane clusters. The chloroform cluster was far apart from all the rest of the vapour samples because of its uniquely high polarisability. Examination of the PC1 eigenvectors showed that **IV** contributed the most towards the discrimination by containing 15.8% of the variance while PIB contributed the least with 11.4%. Significantly PIB contributed to over 57% of the variance in PC2, thus explaining the positive values for the alkanes. By contributing just under 0.5% towards PC2, OV17 was least important. By comparing Figure 6-17 to Figure 6-14, it can be seen that the PC1 component is reflecting the sensitivity of the sensor responses, *i.e.* methanol has the lowest response while chloroform has the highest response. The only exception to this would be PIB, which consequently dominates PC2.
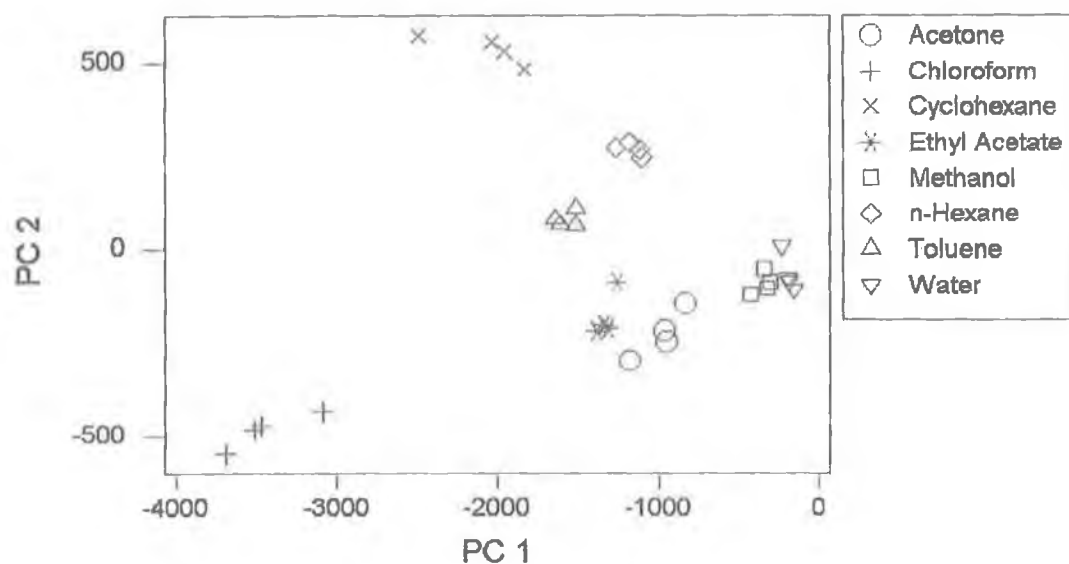
Figure 6-17: Plot of First Two Principal Components

6.3.14 CA

Cluster analysis was carried out on the same data used for PCA above. Using a complete linkage method and Euclidean distances, a dendrogram was produced (Figure 6-18). Chloroform and cyclohexane are immediately classified separate to the other solvents. The hydrophilic water and methanol comprise a second group while the hydrophobic solvents hexane, ethyl acetate, and toluene form a third group. Acetone being hydrophilic, is also polarisable, which explains its position between these two groups.
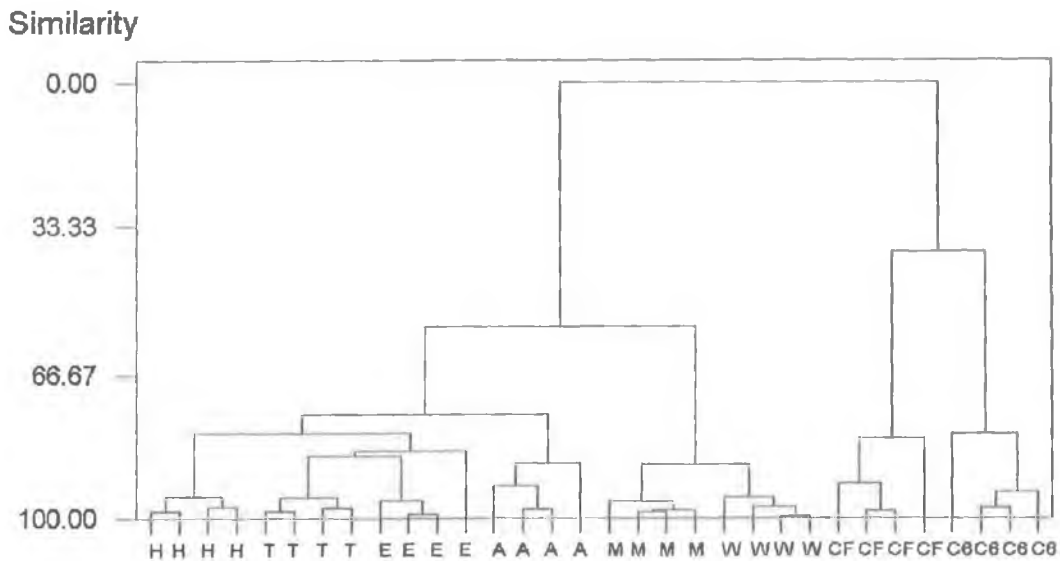
Figure 6-18: Dendrogram of Solvents using a complete linkage method and Euclidean distances (H = Hexane, T = Toluene, E = Ethyl Acetate, A = Acetone, M = Methanol, W = Water, CF = Chloroform, C6 = Cyclohexane)

6.3.15 DFA

The supervised method, DFA, was used for identifying the integrity of the pre-designated groups. The first three discriminant functions were plotted against each other to generate a 3-D graphic (Figure 6-19). Examination of the discrimination scores (Table 6-6) has shown that each solvent is successfully discriminated on cross-validation, therefore giving 100% discrimination. Cross-validation is a "leave-one-out" method, where each object from the data set is removed, one at a time, and tested for membership using a newly devised discrimination rule based on the reduced data set.

172
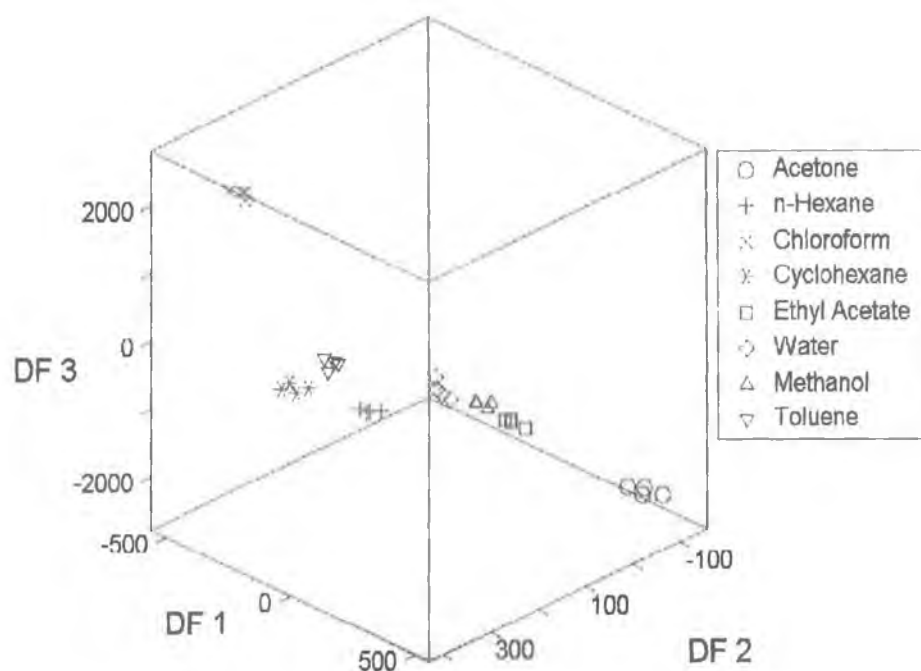
Figure 6-19: Plot of First Three Discriminant Functions

	Acetone	n-Hexane	Chloro-form	Cyclo-hexane	Ethyl Acetate	Water	Methanol	Toluene
Acetone	4 (4)	0 (0)	0 (0)	0 (0)	0 (0)	0 (0)	0 (0)	0 (0)
n-Hexane	0 (0)	4 (4)	0 (0)	0 (0)	0 (0)	0 (0)	0 (0)	0 (0)
Chloroform	0 (0)	0 (0)	4 (4)	0 (0)	0 (0)	0 (0)	0 (0)	0 (0)
Cyclohexane	0 (0)	0 (0)	0 (0)	4 (4)	0 (0)	0 (0)	0 (0)	0 (0)
Ethyl Acetate	0 (0)	0 (0)	0 (0)	0 (0)	4 (4)	0 (0)	0 (0)	0 (0)
Water	0 (0)	0 (0)	0 (0)	0 (0)	0 (0)	4 (4)	0 (0)	0 (0)
Methanol	0 (0)	0 (0)	0 (0)	0 (0)	0 (0)	0 (0)	4 (4)	0 (0)
Toluene	0 (0)	0 (0)	0 (0)	0 (0)	0 (0)	0 (0)	0 (0)	4 (4)
Count	4	4	4	4	4	4	4	4
N Correct	4	4	4	4	4	4	4	4
Proportion	1.00	1.00	1.00	1.00	1.00	1.00	1.00	1.00

Table 6-6: Details of Discriminant Function Analysis (with cross-validated entries in parenthesis)

6.4 Conclusion

Calixarene coated BAW devices were found to be extremely useful sensors for aromatic compounds. The guest-host electrostatic interactions between aromatic toluene and the cavitand were found to be stronger than even H-bonding as evident

by the fact that the cavitands with acidic ligands interact stronger with toluene than with the more volatile methanol. Results from cavity size study suggested that the conformation of the cavity was important for the stability of host-guest complex. Studies were carried out to verify the effects of upper and lower rim substituents. The results suggested that the selectivity towards toluene was enhanced by introduction of upper rim ligands. There is some evidence to suggest introduction of certain substituents to the lower rim can also increase sensitivity.

Application of these calixarene based sensors to array sensing has proved to be successful. Incorporation of calixarene-based sensors into an array that consisted of sensors coated with various GC stationary phases was able to successfully discriminate organic vapours with different chemical functionalities.

6.5 References

1   D. Diamond, K. Nolan, *Anal. Chem.* **73 (1)** (2001) 23A

2   S. Knoblauch, O.M. Falana, J. Nam, D.M. Roundhill, H. Hennig, K. Zeckert, Calix[4]arenes with narrow rim 2-mercaptoethoxy substituents as potential precursor molecules for metallocages and sensors, *Inorganica Chimica Acta*, **300-302** (2000) 328-332

3   F.L. Dickert, R. Sikorski, Supramolecular strategies in Chemical Sensing, *Mat. Sci. and Eng. C*, **10** (1999) 39-46

4   M.T. Cygan, G.E. Collins, T.D. Dunbar, D.L. Allara, C.G. Gibbs, C.D. Gutsche, Calixarene monolayers as quartz crystal microbalance sensing elements in aqueous solution, *Anal. Chem.*, **71** (1999) 142-148

5   R. Mlika, M. Gamoudi, G. Guillaud, M. Charbonnier, M. Romand, J. Davenas, N. Jaffrezic-Renault, R. Lamartine, A. Touhami, Calix[4]arene sensitive thin films for detecting sodium: Surface studies, *Mat. Sci. C*, **11** (2000) 129-136

6   J. Hartmann, J. Auge, R. Lucklum, S. Rösler, P. Hauptmann, B. Alder, E. Dalcanale, Supramolecular interactions on mass sensitive sensors in gas phase and liquids, *Sensors and Actuators B*, **34** (1996) 305-311

7   Francis Cadogan, Paddy Kane, M. Anthony McKervey and Dermot Diamond, Lead-Selective Electrodes based on Calixarene Phosphine Oxide Derivatives, *Anal. Chem.*, **71(24)** (1999) 5544-5550

8   R. Lucklum, S. Rösler, J. Hartmann, P Hauptmann, On-line detection of organic pollutants in water by thickness shear mode resonators, *Sensors and Actuators B*, **36-37** (1996) 103 – 111

9   S. Rösler, R. Lucklum, R. Borngräber, J. Hartmann, P. Hauptmann, Sensor system for detection of organic pollutants in water by thickness shear mode resonators, *Sensors and Actuators B*, **48** (1998) 415-424

10   F.L. Dickert, O. Schuster, Mass sensitive detection of solvent vapours with calix[n]arenes-conformational adaptation to the analyte, *Advanced Materials*, **5(11)** (1993) 826-829

11   X. Yang, S. Johnson, J. Shi, T. Holesinger, B. Swanson, Polyelectrolye and molecular host ion self-assembly to multiplayer thin films; An approach to thin film sensors, *Sensors and Actuators B*, **45** (1997) 87-92

12   P. Mñuk; L. Feltl, Gas chromatographic study of the inclusion properties of calixarenes 1. *p-tert*-butylcalix[4]arene in a micropacked column, *J. Chromatogr. A*, **696** (1995) 101-112

13   J.Org. Chem., **50(26)** (1985), 5802

14   F. Arnaud-Neu, J.K. Browne, D. Byrne, D. J. Marrs, M.A. McKervey, P. O'Hagan, M.J. Schwing-Weill, & A. Walker, Extraction and complexation of alkali, alkaline earth, and F-element cations by calixaryl phosphine oxides, Chem. Eur. J., **5(1)** (1999) 175-186

15   G.D. Andreetti, R. Ungaro, A. Pochini, *J. Chem. Soc. Chem. Commun.*, (1979) 1005

Chapter 7

7   Conclusions and Future Work

Gas Sensor Arrays, often called "Electronic Noses", are becoming increasing popular due to their sampling speed and flexibility. Individual samples can be run in well under a minute allowing for large numbers of samples to be run, usually automatically on a carousel. Commercially such arrays have been applied to a wide range of products such as wines, beers, coffees, perfumes, and other such products that could be considered to have distinct odours. Data generated from these arrays can be analysed with affordable software, by using powerful discrimination techniques, to identify unknowns by comparing them to a pre-determined test set. Such applications have proved robust and fast.

For any array the basic building block will be the sensor itself, which must be reversible, sensitive and possibly selective. As selectivity is difficult to achieve for a single sensor, moderate selectivity through a range of sensors offers a solution. Through careful choice and planning, a set of such sensors can be incorporated into an array, thereby allowing various molecular interactions to be exploited.

Reversibility is essential if the sensor is to be used more than once and a quick return to baseline is very important. A stable response profile for such sensors is essential for any system, and this must be shown consistently over several runs, in conjunction with a low %RSD.

Bulk Acoustic Wave devices (BAW's) are highly sensitive sensors that can be easily coated with a range of sensitive materials. The piezoelectric nature of the quartz means that this additional material on the surface will be seen as a shift in the fundamental frequency of the crystal. Absorption of any analyte into this material will then be seen as an additional frequency change.

Therefore the objectives of this thesis were to:

> ➤ Understand the principles of gas sensing
> ➤ Develop and test a set of suitable BAW sensors coating materials
> ➤ Incorporate these sensors into an array
> ➤ Analyse and identify test organic solvents

To understand the principles of gas sensing it was necessary to identify the components of a gas sensing system, namely the sensitive sorbent layer, the transducer operating mechanism, signal generation and acquisition, and subsequent interpretation.

The system that was supplied was manipulated to allow eight coated sensors to be replaced fully in less than 5 minutes. This allowed for sensors to be quickly examined and rejected if unsuccessful.

To coat BAW's with sensitive materials required a coating method to be decided on. Spray coating was found to be the most practical for most applications, however for selected coatings, poly(pyrrole) (PPY) and poly(N-methylpyrrole) (PMPY), drop coating was found to be more practical, as polymerisation took place on the crystal surface.

Gas chromatography stationary phases were the first polymers to be used as coatings due to their abundance and known chemistries. The polymers investigated were PIB, PEG, OV17, OV225, PECH, PVP, and TDDA. These coating proved to be very successful, as predicted by literature, and discriminated between a selected set of organic solvents.

Pyrroles were the next family of coatings to be examined. Both PPY and PMPY proved to be excellent gas sensors and together were able to discriminate between a selected set of organic solvents. The difference between the two sensors was the ability of PPY to form hydrogen bonds, and PMPY's greater ability to interact through dispersion interactions.

Calixarenes were the final family of chemicals to be investigated as potential BAW sensor coatings. While the response pattern of all calixarenes tended to be similar, they were shown to be excellent aromatic sensors. Results from cavity size study suggested that the conformation of the cavity was important for the stability of host-guest complex. Studies were carried out to verify the effects of upper and lower rim substituents. The results suggested that the selectivity towards toluene was enhanced by introduction of upper rim ligands. There is some evidence to suggest introduction of certain substituents to the lower rim can also increase sensitivity.

All of these candidates, examined as potential sensor coatings, were found to exhibit excellent reversibility and sensitivity, while also displaying different selectivities to the various solvents examined.

The chemometric techniques PCA, CA, and DFA were able to discriminate between the selected analytes, based on the response profiles generated by the BAW sensors. PCA and CA being unsupervised methods proved that there was a clear pattern attainable in the response profiles of the sensors to the selected solvents, while DFA generated rules that would be able to identify possible unknowns that might be examined in the future.

I would see the analysis of food as being the desired target market for gas sensor arrays developed in this thesis. The recommended sensors for such an array would include those that would maximise the following weak interactions:

1. Transient hydrophobic dispersion interactions
2. Polarisable interactions
3. Dipolar interactions
4. Hydrophilic acidic hydrogen bonding
5. Hydrophilic basic hydrogen bonding (minimise dipolarity)
6. Hydrophilic basic hydrogen bonding (maximise dipolarity)

For these interactions I would suggest using the following sensors:

1. PIB/PMPY

2. Calixarenes/OV17
3. PEG
4. PPY
5. TDDA
6. PECH

Such an array would be used to determine the quality of foodstuffs well in advance of any visible discolouration, thus decreasing wastage of materials and time. With advances in current technology soon miniaturised handheld devices could be commonplace.

REFERENCE

Appendix 1

Quantification of Sorption Phenomena seen in QCM Sensors

When a chemical species, X, interacts with a sensor, S, an equilibrium is reached [1]:

$$X + S \underset{k_r}{\overset{k_f}{\Leftrightarrow}} XS \qquad \text{Equation I}$$

The equilibrium constant, K, is expressed in terms of activities and is given by the Equation II,

$$K = \frac{a_{sx}}{a_s a_x} = \frac{k_f}{k_r} \qquad \text{Equation II}$$

where a_{sx} is the activity of the bound species, a_s and a_x are the activities of the species in the sample and the activity of the binding site respectively. The overall rates of the forward (k_f) and reverse (k_r) reactions together with the mass-transport parameters of the species involved in the transduction mechanism determine the response time of the sensor.

By combining Equation II with Equation 2-2, the free energy of interaction is derived:

$$\partial G = 0 = \partial G^\circ = RT \ln \left(\frac{a_{sx}}{a_s a_x} \right) \qquad \text{Equation III}$$

Therefore if there is a change in sample activity, the species will interact with the sensor if the variation in the standard free energy is negative ($\partial G^\circ < 0$). However for sensor applications a high binding constant implies that equilibrium will be reached very quickly, but may cause problems with reversibility and this would be undesirable in a QCM sensor.

The free energy of an open system is a function of temperature, pressure and also composition. If the concentration of a component i (number of moles $= n_i$), changes, the free energy of the system changes and this is known (in molar terms) as the chemical potential of the species, μi.

$$\mu_i = \left(\frac{\partial G}{\partial n_i} \right)_{T,P,j \neq i}$$

Equation IV

Because the standard free energy at equilibrium is equal to zero,

$$dG = \sum_i \mu_i dn_i = 0$$

Equation V

This is the *Gibbs equation*, and is important for phase equilibria. The position of the binding sites is important for the operational characteristics of a sensor. QCM sensors operate on bulk interactions and so their response is a function of a two phase equilibrium.

$$dG = 0 = \left(\mu_i dn_i \right)_{sensor} + \left(\mu_i dn_i \right)_{vapour}$$

Equation VI

At equilibrium the number of moles partitioning into a coating must match that leaving so:

$$\left(dn_i \right)_{sensor} = -\left(dn_i \right)_{vapour}$$

Equation VII

Therefore the chemical potentials of the species in the two phases must be equal:

$$\left(\mu_i \right)_{sensor} = \left(\mu_i \right)_{vapour}$$

Equation VIII

Therefore, the chemical potential in a real gas can be expressed in a hybrid form of the free energy of an ideal solution as Equation IX.

$$\mu_i = \mu_i^o + RT \ln a_i \qquad \qquad \text{Equation IX}$$

Equation IX implies that QCM sensors, being based on absorption, measure activity and their output is usually logarithmic

However the process for a QCM sensor is a 2-stage and for adsorption of a species at a surface, there is an equilibrium constant that applies,

$$X \underset{k_r}{\overset{k_f}{\Longleftrightarrow}} XS \qquad \qquad \text{Equation X}$$

where SX represents the adsorbed species and

$$K = \frac{a_{sx}}{a_x} \qquad \qquad \text{Equation XI}$$

The concentration of the species at the surface is defined as Γ^i (moles per area), which is dependant on the surface activity through an adsorption isotherm. The general form of an adsorption isotherm is

$$\beta a = F(\Gamma) \qquad \qquad \text{Equation XII}$$

where

$$\beta = \exp\left(\frac{-\Delta G_a}{RT}\right) \qquad \qquad \text{Equation XIII}$$

The free energy of adsorption $-\Delta G_a$ depends on the type of substrate-adsorbate and adsorbate-adsorbate interactions. If we take the simplified assumption that activities can be equated with concentrations, then QCM sensors as steady-state devices will give a signal, S, as follows

$$S = \Re\left[\sum_i K_i\left(\frac{dC_i}{dx}\right)\right] \quad or \quad S = \Re\left[\sum_i K_i\left(\frac{dC_i}{dt}\right)\right] \qquad \textbf{Equation XIV}$$

given that the output can be controlled by the concentration gradient (dC/dx) or time variation in concentration (dC/dt).

If the activity equation (Equation XV) is differentiated with respect to time or distance, Equation XVI is obtained, where f is the activity coefficient.

$$a = fC \qquad \textbf{Equation XV}$$

$$\frac{da}{dx} = \frac{df}{dx}C + f\frac{dC}{dx} \quad or \quad \frac{da}{dt} = \frac{df}{dt}C + f\frac{dC}{dt} \qquad \textbf{Equation XVI}$$

As df/dx and df/dt in Equation XVI are almost always equal to or close to zero, they can be neglected. For the most common kinetic case, first order, the activity coefficients cancel and so concentrations and activities can be interposed. Therefore mass-transport sensors can be explained in terms of concentrations rather than activities, while equilibrium sensors depending on partitioning and adsorption rely on activities. QCM sensors as members of both these families rely on both concentration and activity. The number of molecules, i.e. *concentration*, governs transduction while *activities* govern chemical interactions.

---

1 J. Janata, *Principles of Chemical Sensors*, Plenum, NY, 1989